PhD Thesis

May 2018

Mechanism of Growth Failure in Mucopolysaccharidosis VII mice

Zhirui Jiang

BSc (Biotech), BSc (Hons)

Thesis submission for the degree of

Doctor of Philosophy

in

Department of Genetics and Evolution

School of Biological Sciences

Faculty of Sciences

University of Adelaide

Principle supervisor: Dr Sharon Byers

Co-supervisors: Dr Ainslie Derrick-Roberts

Dr Janice Fletcher

Prof Cory Xian

Table of Contents

Summary

Short stature due to progressive growth failure in mucopolysaccharidosis (MPS) does not respond to current treatment. The mechanism behind impaired bone growth in MPS is poorly understood but is crucial to the development of improved strategies to alter bone growth.

Bone length was measured in 5 mouse models of MPS to determine the best model for further analysis. The severe MPS VII mouse model ($Gus^{mps/mps}$ strain) displayed the greatest reduction in bone length and was chosen as the model for studying bone shortening in MPS. Bone formation was delayed in both the primary and secondary ossification centres in MPS VII mice. The growth plate was thickened with enlarged chondrocytes in the resting (RZ) and hypertrophic zones (HZ) but there was a reduced number of chondrocytes in the proliferative zone (PZ) and HZ.

Chondrocytes progress through the cell cycle to proliferate and withdraw from the cell cycle to differentiate. Immunohistochemical analysis of cell cycle regulators in the MPS VII growth plate revealed that fewer chondrocytes progressed to mitotic division for proliferation. Fewer HZ chondrocytes progressed to cell cycle withdrawal for terminal differentiation in MPS VII growth plate. Thus, MPS VII chondrocytes while committed to the cell cycle were unable to progress normally through the different stages.

Circulating GH, T3 and IHH levels in MPS VII mice were not significantly different from normal. However, IGF1 production in MPS VII mice was reduced both in the circulation and in primary hepatocytes culture, suggesting an impaired GH/IGF1 signaling pathway in MPS VII mice, which may limit the proliferation of chondrocytes in the growth plate. This dysfunction of GH/IGF1 signaling was not caused by a deficiency of the hepatic growth hormone receptor but was associated with a reduction in tyrosine phosphorylation of STAT5 in MPS VII liver. Responsiveness of MPS VII chondrocytes to GH was decreased and local

growth plate expression of GHR was reduced, indicating that GHR deficiency may cause the reduced proliferation in MPS VII growth plate.

Proliferation and differentiation of chondrocytes are also regulated by locally expressed factors such as IHH, PTHrP and IGF1. Reduced IHH protein level was observed in MPS VII growth plate and in chondrocyte culture, suggesting a potential relationship between IHH and the reduced number of chondrocytes in the PZ of MPS VII growth plate. Persistent expression of *Pthrpr* and *Sox9* and elevated IGF1 secretion by chondrocytes indicated relationships between altered PTHrP and IGF1 signalling pathways and the delayed hypertrophic transition of chondrocytes in the MPS VII growth plate.

This thesis highlights that the bone phenotype of MPS is established before birth and suggests that the decreased numbers of chondrocytes in the PZ and HZ of MPS VII growth plate are the results of disruptions in the pace of cell cycle progression. Decreased GHR level would also contribute to reduction of chondrocyte proliferation. Although a decrease in circulating IGF1 level and a decrease in IHH expression in the growth plate was observed, a direct relationship between these observations and short stature cannot be established.

Declarations

I, Zhirui Jiang, declare that this piece of writing does not contain any material written by another person, except where due reference has been given in the text, and the work has not been presented previously as a component of any other academic course. In addition, I certify that no part of this work will, in the future, be used in a submission in my name, for any other degree or diploma in any university or other tertiary institution without the prior approval of the University of Adelaide and where applicable, any partner institution responsible for the award of this degree.

I give consent to this copy of my thesis, when deposited in the University Library, being made available for loan and photocopying, subject to the provisions of the Copyright Act 1968. I also give permission for the digital version of my thesis to be made available on the web, via the University's digital research repository, the Library Search and also through web search engines, unless permission has been granted by the University to restrict access for a period of time.

Zhirui Jiang

Bachelor of Science (Honours)

DATE ..04../..07.../..2018

Acknowledgments

I would particularly like to thank my supervisors Dr. Sharon Byers, Dr. Ainslie Derrick Roberts, Dr. Janice Fletcher and Prof. Cory Xian for many fruitful discussions and meetings, for their diligence in ploughing through the many drafts of this thesis and their constant support and assistance throughout the whole project. Acknowledgment must also go to Dr. Gwen Mayo for her advice on microdissection and RNA isolation and Ms. Ruth Williams for her assistance on getting ultrathin sections for transmission electron microscopy (TEM), both from Adelaide Microscopy. I would also like to thank the other members of Matrix Biology Unit, past and present, Dr. Matilda Jackson, Rebecca Lehmann, Claire Reichstein, Charné Rossouw, Dr. Nathan Rout-Pitt, Dr. Carmen Macsai, Daniel Deverson, Neimal Usmani, Srimayee Vaidyanathan, and Hannah Linard for their support, friendship and encouragement. Thank you to the Women's and Children's hospital animal house staff, Ms. Lynn Garrard, Mr. Steven Court and Ms. Lesley Jenkins-White for their excellent care of the mice used in this study. To Ms. Rupal Pradhan and Mr. Andrew Beck for their generous helps on processing paraffin samples used in this study.

To Dr Frank Grutzner, Associate Professor Jeremy Austin and Professor Robert Richards, the postgraduate coordinators of the Department of Genetics, Genomics and Evolution, School of Biological Sciences, Faculty of Science, University of Adelaide, thank you for your support throughout my candidature and for providing a structured and coherent program.

Last but not least, I would like to thank my family and friends, especially my parents, thank you for your unconditional support throughout all my years of study. This would not happen without your love and encouragement.

Abbreviations

BMP	Bone morphogenetic protein
BMT	Bone marrow transplant
CDK	Cyclin-dependent kinase
CKI	Cyclin-dependent kinase inhibitors
CS	Chondroitin sulphate
CycpA	Cyclophilin A
DAPI	4’,6-diamidino-2-phenylindole
DS	Dermatan sulphate
DMEM	Dulbecco’s modified eagle medium
ECM	Extracellular matrix
EO	Endochondral ossification
ERT	Enzyme replacement therapy
FCS	Foetal calf serum
FGF	Fibroblast growth factor
FGFR	Fibroblast growth factor receptor
FITC	Fluorescein isothiocyanate
GAG(s)	Glycosaminoglycan(s)
GH	Growth hormone
GHR (or *Ghr*)	Growth hormone receptor
GLI (or *Gli*)	Glioma-associated oncogene homologue
GT	Gene therapy
GUS	β-Glucuronidase
HCT	Haematopoietic cell transplantation
HS	Heparin sulphate

HA	Hyaluronan
HZ	Hypertrophic zone
IGF1 (or *Igf1*)	Insulin like growth factor 1
IGFR1 (or Igfr1)	Insulin like growth factor receptor, Type I
IGFALS (or *Igfals*)	IGF acid labile subunit
IGFBP (or *Igfbp*)	IGF binding protein
IHH (or *Ihh*)	Indian hedgehog
JAK2	Janus kinase 2
KS	Keratan sulphate
MMP	Matrix metalloproteinase
MPS	Mucopolysaccharidosis
MPS I	Mucopolysaccharidosis type I
MPS IIIA	Mucopolysaccharidosis type IIIA
MPS VII	Mucopolysaccharidosis type VII
MPS IX	Mucopolysaccharidosis type IX
pRb	Retinoblastoma protein
PTC (or *Ptch1*)	Patched
PTHrP (or *Pthrp*)	Parathyroid hormone related peptide
PTHrPR (or *Pthrpr*)	Parathyroid hormone related peptide receptor
PBS	Phosphate buffered saline
POC	Primary ossification centre
PZ	Proliferative zone
RUNX2 (or *Runx2*)	Runt-related transcription factor 2
RZ	Resting zone
SMO (or *Smo*)	Smoothened

SOC	Secondary ossification centre
SOX9 (or *Sox9*)	SRY-Box 9
STAT (or *Stat*)	Signal transducer and activator of transcription
T3	Triiodothyronine
VEGF	Vascular endothelial growth factor
WNT	Wingless-type MMTV integration site

1 Introduction

1.1 Mucopolysaccharidosis

The mucopolysaccharidosis (MPS) are a group of lysosomal storage disorders that result from deficiencies in enzymes catalysing the degradation of glycosaminoglycans (GAGs). Long, unbranched GAG chains are located primarily in the extracellular matrix (ECM) and pericellular matrix and are essential in building bones, cartilage, skin, tendons and many other tissues in the body (Alberts et al. 2008). In the course of normal life, GAGs are continuously renewed and such involves breaking down GAGs by a series of enzymes working in sequence.

The accumulation of undegraded or partially degraded GAGs in MPS cells leads to dysfunction in multiple tissues and organs. Eleven known MPS enzyme deficiencies have been characterised (Table 2.1) (Muenzer 2011; Neufeld & Muenzer 2001). All MPS are inherited in an autosomal recessive manner except for MPS II, which is an X-linked recessive disease. MPS patients display various symptoms depending on MPS type and severity, but patients commonly present with hepatosplenomegaly, corneal clouding, upper airway disease, cardiac defects, central nervous system deterioration, skeletal dysplasia, decreased joint mobility, short stature and abnormal facies (Neufeld & Muenzer 2001).

Table 2.1 Classifications of MPS.

Disorder	**Enzyme deficiency**	**GAG affected**	**Genetic inheritance**
MPS I	α-L-iduronidase	DS, HS	Autosomal recessive
MPS II	Iduronate-2-sulphatase	DS, HS	X-linked recessive
MPS III	A: heparan *N*-sulphatase	HS	Autosomal recessive
	B: α-*N*-acetylglucosaminidase		Autosomal recessive
	C: acetyl-CoA: α-glucosaminide acetyltramsferase		Autosomal recessive
	D: N-acetylglucosamine 6-sulphatase		Autosomal recessive
MPS IV	A: galactose 6-sulphatase	A: KS, CS	Autosomal recessive
	B: β-galactosidase	B: KS	Autosomal recessive
MPS VI	Arylsulphatase B	DS, CS	Autosomal recessive
MPS VII	β-Glucuronidase	DS, HS,CS	Autosomal recessive
MPS IX	Hyaluronidase	HA	Autosomal recessive

Note: DS=dermatan sulphate; HS=heparan sulphate; KS=keratan sulphate; CS=chondroitin sulphate; HA=hyaluronan

Adapted from (Muenzer 2011)

1.2 Short stature

Short stature is observed in MPS I, MPS II, MPS IV, MPS VI, and MPS VII patients (Melbouci et al. 2018; Neufeld & Muenzer 2001). Growth and final height are significantly reduced (Table 2.2; (Neufeld & Muenzer 2001), with the final height -3 to -6 standard deviations below that of normal children of the same age and gender (Polgreen & Miller 2010). While affected children may be at a normal length at birth, growth failure becomes progressively worse with age. Growth velocity of severely affected children declines significantly after 1 year of age, and their growth effectively stops around the age of 2-6 years (Kubaski et al. 2016; Montano et al. 2016; Montaño et al. 2008; Patel, Suzuki, Maeda, et al. 2014; Quartel et al. 2015; Rozdzynska-Swiatkowska et al. 2015). Such extreme short stature has a significant, negative influence on daily life, education and career choices of affected patients (Polgreen & Miller 2010; Ross et al. 2004; Zimet et al. 1997). Short stature can be attributed to a combination of a primary failure of growth plate transition into bone, joint contractures, skeletal deformities including spine curvatures, genu valgum and hip dysplasia, as well as endocrine and nutrient deficiencies (Field et al. 1994; Polgreen et al. 2008). The role of each mechanism in affecting MPS bone growth is still poorly understood. This thesis describes a series of experiments aimed at elucidating the cause of poor bone growth using MPS murine models.

Table 2.2 Final height of MPS patients

MPS type	Final height (cm)
MPS I	~110 (Neufeld & Meunzer 2001)
MPS II	~151 (Rozdzynska et al. 2011)
MPS IVA	113 (F)/122 (M) (Montaño et al. 2008)
MPS VI	110-140 (Neufeld & Meunzer 2001)
MPS VII	96~159 (Montano et al. 2016; Sly et al. 1973)
MPS IX	145.5 (F, 14yr) (Natowicz et al. 1996) 161 (F)/177 (M) (Imundo et al. 2011)

Average normal adult female (F) and male (M) height is 164.5cm and 178.4cm, respectively (Australian Bureanu of Statistics, 1995).

1.3 MPS therapies

Treatments, including hematopoietic cell transplantation (HCT) and enzyme replacement (ERT), are currently available for select patients with MPS I, II, IVA, VI and VII (Chinen et al. 2014; Decker et al. 2010; Fox et al. 2015; Furujo, Kosuga & Okuyama 2017; Harmatz et al. 2017; Herskhovitz et al. 1999; Hobbs et al. 1981; Jones, SA et al. 2013; Kakkis et al. 2001; McGill et al. 2010; Muenzer et al. 2006; Patel, Suzuki, Tanaka, et al. 2014; Polgreen et al. 2009; Polgreen et al. 2008; Sands & Birkenmeier 1993; Schulze-Frenking et al. 2011; Sifuentes et al. 2007; Sohn et al. 2013; Vellodi et al. 1997; Yamada et al. 1998). HCT (either bone marrow or stem cell transplantation), and ERT have significantly diminished some symptoms of MPS including respiratory diseases, cardiovascular dysfunction, joint mobility, liver and spleen pathology, and coarse facial features (Cox-Brinkman et al. 2006; Herskhovitz et al. 1999; McGill et al. 2010). However, not all symptoms respond equally to these therapies. Musculoskeletal and joint abnormalities seem to have no or short-lived response to the current treatments (Arora et al. 2007; Chinen et al. 2014; Field et al. 1994;

Furujo, Kosuga & Okuyama 2017; Harmatz et al. 2017; Herskhovitz et al. 1999; Horovitz et al. 2013; Polgreen et al. 2008; Tylki-Szymanska et al. 2010; Zuber et al. 2014). Both therapies require early and accurate diagnosis to obtain the best outcome due to the irreversible nature of some symptoms (Prasad & Kurtzberg 2010).

A small improvement in growth was observed in children with MPS I post-HCT, however, these patients were still significantly shorter than normal (Gardner et al. 2011). In a 15 years follow-up study, the linear growth of MPS I patients after HCT at 20 months of age continued for some years, but gradually decreased with time (Vellodi et al. 1997). Furthermore, the conditioning regimen used in HCT has itself been associated with adverse effect on growth due to one or more of the following reasons; growth hormone (GH) deficiencies, abnormal gonadal and thyroid functions, and damage to the epiphyseal growth plate, pituitary gland and hypothalamus by radiation and chemotherapy (Brennan & Shalet 2002; Frisk et al. 2004; Giorgiani et al. 1995; Huma et al. 1995; Legault & Bonny 1999; Polgreen et al. 2008; Ranke et al. 2005; Shalitin et al. 2006). For example, the prevalence of growth failure in children with MPS I after HCT who had no total body irradiation (TBI) exposure is 32% less than those who had TBI exposure. Therefore, HCT as treatment for skeletal defects of MPS is of limited efficacy.

While some studies report a continuing decline in height such that MPS children on ERT regimens are not different to untreated patients (Arora et al. 2007; Tylki-Szymanska et al. 2010), other studies report an increase in growth velocity after ERT (Decker et al. 2010; Jones, SA et al. 2013; Kakkis et al. 2001; Pineda et al. 2016; Schulze-Frenking et al. 2011; Sifuentes et al. 2007). However, in no case did the height of treated MPS patients approached normal values (Fox et al. 2015; Furujo, Kosuga & Okuyama 2017; Harmatz et al. 2017; Horovitz et al. 2013; Sohn et al. 2012; Zuber et al. 2014). Response to ERT was greatest in prepubertal children (27% improvement of growth velocity) as compared to

pubertal children (0.5% improvement) (Sifuentes et al. 2007). Therefore, the age of MPS children at which the ERT starts thus defines the capacity for further growth. As age is a crucial factor in the response to the therapy, this may explain the conflicting results observed in different studies.

Studies in animal models also show mixed results. Improvement of bone length was not observed in MPS animals after HCT or ERT (Birkenmeier et al. 1991; Byers et al. 1997; Crawley et al. 1997; Pievani et al. 2014; Rowan et al. 2012; Sands et al. 1993; Sands et al. 1994; Vogler et al. 1996). A single study that used a chemically modified form of GUS for prolonged circulation in MPS VII mice showed improvements in tibia length (Rowan et al. 2012). However, the efficacy of this treatment with modified form of GUS on MPS patient has not been reported.

Trials using gene therapy (GT) in MPS affected animals showed improvement of bone length when normal or sub-normal level of circulating enzyme are achieved (Daly et al. 2001; Elliger et al. 2002; Mango et al. 2004). A level of 50% of normal circulating enzyme is suggested as the minimum level to rescue the defects of longitudinal bone growth (Cotugno et al. 2010). However, not all bones respond to treatment. The radius and tibia of MPS VII mice treated with gene therapy were longer than those of untreated MPS VII mice (Donsante et al. 2007), while femur length was not different to untreated mice(Daly et al. 2001; Derrick-Roberts et al. 2014; Elliger et al. 2002; Macsai et al. 2012). Thus, the efficiency of gene therapy on bone correction is dependent on the differences in growth rate. Overall, applications of BMT, ERT and GT have limited efficacy for improving bone growth in MPS animal models. To maximize the effectiveness and to translate beneficial results of these approaches from animals to human patients, a better understanding of the pathology of growth retardation in MPS is required.

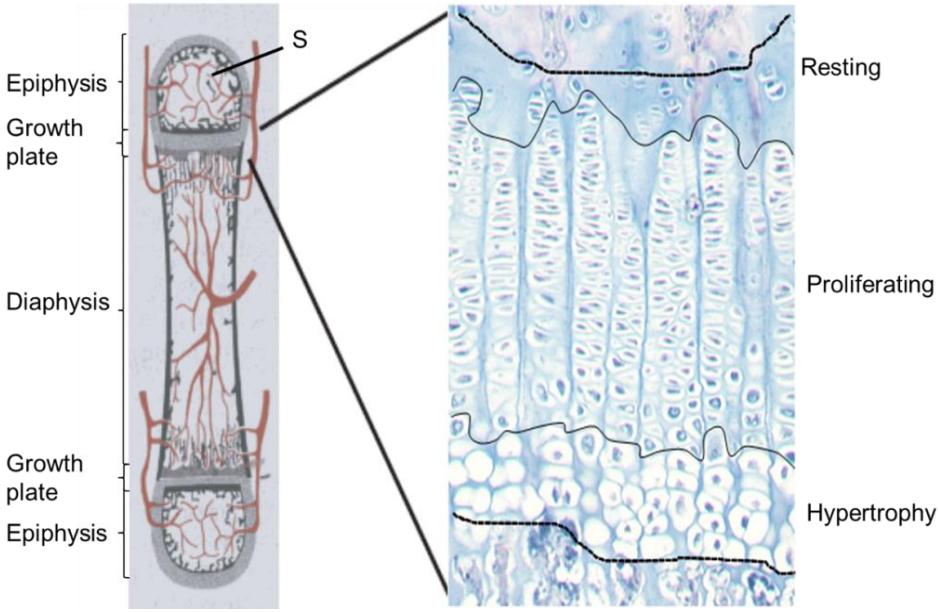

Figure 1.1 Histology of a long bone and its growth plate. Endochondral ossification of long bone during childhood (Left, modified from the Primer on the Metabolic Bone Diseases and Disorders of Mineral Metabolism, Chapter 1, Figure 9 (Yang, Yingzi 2009). The growth plate is located at each end of a long bone. Alcian blue stained mouse proximal tibial growth plate (right, derived from Matrix Biology Unit, SA Pathology), showing the resting, proliferating and hypertrophic zones. S-secondary ossification centre.

1.4 Mechanism of longitudinal bone growth

While the mechanism behind poor bone growth in MPS is poorly understood, the mechanism of normal bone growth is better characterised. Bones continually change in size and shape, from foetal development until maturity. The growth plate, a mesoderm-derived cartilage template, is the tissue responsible for bone growth via endochondral ossification (EO), whereby rapidly growing cartilage is replaced by bone.

1.4.1 Growth plate and endochondral ossification

During bone formation, the primary ossification centre (POC) is formed at the middle of cartilage template, and the secondary ossification centre (SOC) is formed at each end of the developing bone, leaving the cartilaginous growth plates between the POC and SOC (Figure 1.1) (Yang, Yingzi 2009). Eventually, the growth plates vanish as the ossification centres meet at maturity and bone growth ceases (Mackie et al. 2008).

During formation of the POC, chondrocytes differentiate to hypertrophic chondrocytes from the middle of diaphysis in mice. Hypertrophic chondrocytes secrete ECM and enzymes including matrix metalloproteinase (MMP) 13 and MMP 14 that degrade Type II collagen and aggrecan (Holmbeck et al. 1999; Inada et al. 2004; Mitchell et al. 1996). The surrounding ECM is then mineralised through the deposition of hydroxyapatite that consists of calcium and phosphate (Gerber et al. 1999; Hunziker 1994). Vascular endothelial growth factors (VEGF) are also expressed by hypertrophic chondrocytes, which allows rapid invasion of vascular endothelial cells from the bone collar through pre-existing cartilage canals, into the calcified matrix in the future POC site (Burkus, Ganey & Ogden 1993; Carlevaro, M.F. et al. 2000; Maes, C. et al. 2004). Blood vessels are also formed for transporting of hematopoietic and osteogenic cells for marrow and bone deposition (Maes, Christa & Kronenberg 2016). MMP 9 expressed by osteoclasts and endothelial cells

degrades cartilaginous matrix and releases VEGF from ECM (Gerber et al. 1999; Vu et al. 1998). The latter triggers the sprouting of new vessels at metaphysis, which is also facilitated by fibroblast growth factors (FGFs) and connective tissue growth factors (CTGFs) (Baron et al. 1994; Ivkovic et al. 2003; Nishida et al. 2009; Seghezzi et al. 1998; Shimo, T. et al. 1998).

Chondrocytes in the growth plate arrange themselves into morphologically distinct zones, which reflect their different lifespan (Figure 1.1). Chondrocytes in the resting zone (RZ) are irregularly arranged and rarely divide, and occupy the region nearest to the epiphysis. RZ chondrocytes are believed to replenish the adjacent proliferative zone (PZ) (Abad et al. 2002). Chondrocytes undergo division in the PZ, appearing as flattened cells which are arranged in columns parallel to the long axis of the bone (Abad et al. 2002). After replication, the cells gradually enter the hypertrophic stage, enlarging their volume about 6 to 10-fold, increasing alkaline phosphatase enzyme activity, and secreting type X collagen (Cooper et al. 2013; Farnum et al. 2002). Hypertrophic chondrocytes eventually die either through apoptosis or autophagic cell death (Ahmed et al. 2007; Shapiro et al. 2005). Removal of the transverse septa of the cartilage ECM allows invasion of the ossification front, including blood vessels, osteoclasts, and bone marrow cells and osteoblast precursors. Osteoclasts erode the mineralised ECM, and osteoblasts continuously deposit bone matrix (Hall & Miyake 1995).

Vascularization and formation of the SOC are slightly different to those of the POC. Shortly after birth, hypertrophic chondrocytes in the middle of the epiphysis secret MMP14, which clears a path for the formation of cartilage canals that contains blood vessel and perivascular cells. MMP13 and A Disintegrin and Metalloproteinase with Thrombospondin Motifs (ADAMTS) 5 (Hurskainen et al. 1999; Makihira et al. 2003; Stanton et al. 2005) expressed by the hypertrophic chondrocytes degrades both type II collagen and aggrecan.

Hypertrophic chondrocytes in the future SOC site forms a hypoxic and avascular tissue. Secretion of VEGFs by chondrocytes surrounding cartilage canals in the hypoxic site is induced by hypoxia inducible factor (HIF) (Lin, X 2004; Maes, C. 2017), stimulating blood vessel invasion in the epiphysis of long bones (Allerstorfer et al. 2010). Transportation of osteoclasts, osteoblasts and hematopoietic cells through blood vessels thus initiates formation of the SOC in the epiphysis (Maes, Christa & Kronenberg 2016).

Thus, the key regulatory points in EO are:

(i) entry into the cell cycle (proliferation);

(ii) exit from the cell cycle and initiation of hypertrophy;

(iii) blood vessel invasion from the metaphysis of long bones

The behaviour of chondrocytes during EO is highly regulated by a group of endocrine and paracrine factors and components of the cartilage ECM.

1.4.2 Regulation of endochondral ossification

Sequential proliferation, ECM secretion and hypertrophy of growth plate chondrocytes are required for proper skeletogenesis, and are regulated by a number of systemic factors, including GH, thyroid hormone, glucocorticoids, estrogen and testosterone (Clarke, BL & Khosla 2009; Fernandez-Cancio et al. 2008; Goldring, Tsuchimochi & Ijiri 2006; van der Eerden, Karperien & Wit 2003), paracrine/autocrine factors such as insulin like growth factors (IGF), indian hedgehog (IHH), and parathyroid hormone-related peptide (PTHrP), their downstream transcription factors, as well as by GAGs and other components of ECM (Figure 1.2).

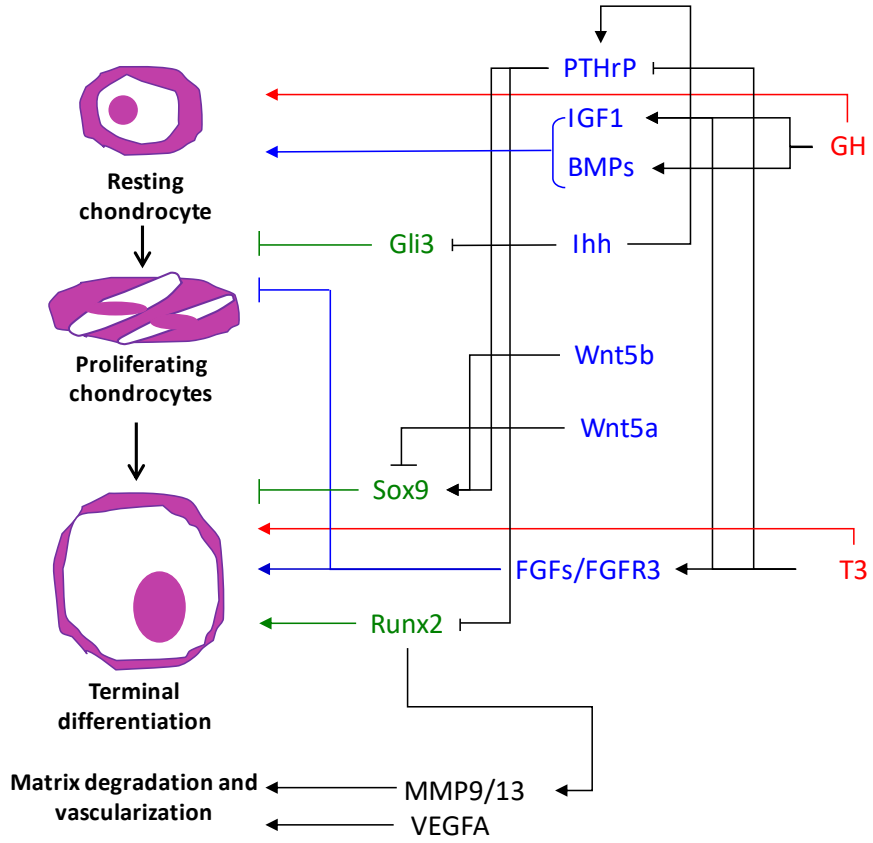

Figure 1.2 Regulation of growth plate chondrocyte proliferation and hypertrophy during EO. Systemic factors (red), paracrine/autocrine factors (blue), transcription factors (green) and other factors (black) are involved. Arrows indicate stimulatory pathways, and crossed lines indicate inhibitory pathways. Based on Mackie *et al.* (2008). GH, growth hormone. T3, triiodothyronine. IGF1, insulin growth factor 1. PTHrP, parathyroid hormone related peptide. BMPs, bone morphogenetic proteins. Ihh, indian hedgehog. Gli3, glioma-associated oncogene homologue. Wnt, wingless-type mouse mammary tumor virus integration site. Sox9, SRY-Box 9. Runx2, Runt-related transcription factor 2. FGF, Fibroblast growth factor. FGFR, fibroblast growth factor receptor. MMP, Matrix metalloproteinase. VEGFA, vascular endothelial growth factor A.

1.4.2.1 Systemic factors

1.4.2.1.1 1. Growth hormone and liver-derived IGF1

GH is secreted by the anterior pituitary gland (Veldhuis & Bowers 2003) in a basal and a pulsatile pattern under the regulation of GH-releasing hormone (GHRH) and somatostatin from the hypothalamus. GH is released into the bloodstream and primarily acts on the liver where it stimulates the production of endocrine form of IGF1(Butler & Le Roith 2001). It is also an important stimulator of chondrocyte proliferation in the growth plate where it induces resting cells to enter the proliferative cycle (Baker et al. 1993; Hunziker, Wagner & Zapf 1994; Isaksson, Jansson & Gause 1982). GH functions through the growth hormone receptor (GHR), which is expressed systemically by hepatocytes and locally by chondrocytes in all layers of the growth plate (Gevers et al. 2002; Ram et al. 1996). Pituitary secretion of GH is both age- and sex-dependent. The level of free GH is normally high after birth and decreases slightly until puberty. At puberty, it reaches a peak and then continuously decreases with age during adulthood. Females normally have a higher level of GH than males. Excess GH due to pituitary adenomas results in gigantism (Nilsson, O et al. 2005), while a shortage of GH due to mutations in GHRs or defects in GH signalling pathways causes impaired postnatal growth (Wit, Kamp & Rikken 1996).

Acceleration of longitudinal growth in GH-injected tibial growth plates of rats was observed when compared to saline-injected growth plates, supporting the theory that GH directly stimulates chondrocyte proliferation (Isaksson, Jansson & Gause 1982). However, the effects of GH on chondrocytes *in vitro* reported by various research groups are conflicting. In some cases, no response was observed with GH alone (Jones, KL, Villela & Lewis 1986; Trippel et al. 1989), while in combination with IGF1, GH stimulated DNA and matrix synthesis (Smith, Kuniyoshi & Talamantes 1989). It is not clear what causes the discrepancy, but variations in experimental conditions, including the initial cell density,

time of cell culture and the existence of serum in the medium may all contribute (Isaksson et al. 1990).

IGF1 is the primary mediator of GH. GH binds to the dimerized transmembrane GHR, triggering the activation of Janus kinase 2 / signal transducer and activator of transcription 5 (JAK2/STAT5) signalling cascade (Figure1.3) (Piwien-Pilipuk, Huo & Schwartz 2002; Teglund et al. 1998). Upon phosphorylation and dimerization, STAT5 translocates to the nucleus and binds onto the promoter of the target gene induces hepatic IGF1 synthesis (Rotwein 2012; Woelfle, Billiard & Rotwein 2003), as well as IGF binding protein (IGFBP3) and the acid labile subunit (IGFALS) (Baxter, Martin & Beniac 1989). These proteins form a protective ternary complex, which prolongs the half-life of IGF1 in the circulation and regulates the bioavailability of IGF1 to bones. Liver-derived IGF1 contributes 75% of IGF1 in the circulating pool (Sjogren et al. 1999; Yakar et al. 1999). IGF1 is then released to bone and bound by bone/cartilage-derived IGFR1 to regulate EO. While bone growth is mainly regulated by GH-independent IGF2 before birth (Baker et al. 1993; DeChiara, Efstratiadis & Robertsen 1990), IGF1 stimulate linear bone growth during postnatal life (Schlegel et al. 2010; Yakar et al. 2002). Yakar et al. (2002) reported that reduction in IGF1 levels leads to decreased linear bone growth, while circulating IGF1 treatment was able to resuce longitudinal bone growth in both human and mice with GHR mutations (Guevara-Aguirre et al. 1997; Sims et al. 2000). IGFR1 is an essential mediator of IGF1, and mice with a deficiency of IGFR1 display more severe growth retardation than those without IGF1 itself (Baker et al. 1993).

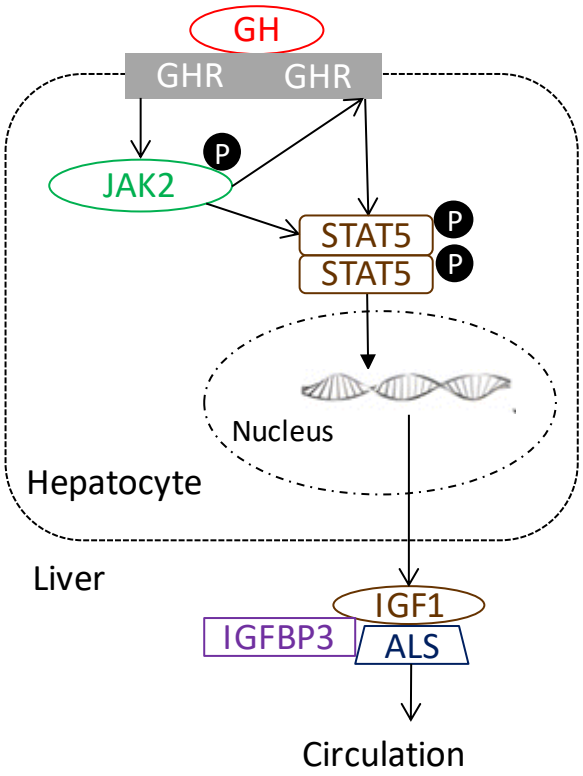

Figure 1.3 GH mediated IGF1 production in liver. Binding of growth hormone (GH) triggers dimerization of the cell surface growth hormone receptor (GHR), which activates Janus kinase 2 (JAK2) through phosphorylation. Activated JAK2 lead to phosphorylation of the GHR and subsequently cytoplasmic transcription factors including signal transducer and activator of transcription 5 (STAT5). Phosphorylated STATs dimerize and translocate to the nucleus, where they bind onto the promoter of target genes (insulin like growth factor 1 (*Igf1), IGF binding protein 3 (Igfbp3) and IGF acid labile subunit (Igfals*)). Secreted IGF1, IGFALS and IGFBP3 form protective ternary complex, which is released to the circulation.

1.4.2.1.2 Thyroid hormone

Thyroid hormone is important in supporting cell hypertrophy at the expense of proliferation. In humans, hyperthyroidism accelerates longitudinal bone growth and EO, while hypothyroidism slows these processes by attenuating the growth plate and impairing chondrocyte hypertrophy (Buckler, Willgerodt & Keller 1986; Leger & Czernichow 1989). Thyroid hormone level is the highest in the first month after birth, and subsequently decreases with age before adulthood (Kapelari et al. 2008).

Two primary thyroid hormones, triiodothyronine (T3) and thyroxine (T4) are produced by the thyroid gland. T4 is the precursor of T3 and must be converted to T3 to function (Leonard & Kohrle 1996). T3 stimulates morphological hypertrophy, expression of collagen type X as well as alkaline phosphatase activity, and diminishes proliferation *in vitro* (Ballock & Reddi 1994; Burch & Lebovitz 1982; Robson et al. 2000). Two thyroid hormone receptors, TR-α and TR-β, are expressed in growth plate chondrocytes (Ballock et al. 1999). TR-α is the major mediator of T3 action on mouse growth plate cartilage (Forrest et al. 1996; Gauthier et al. 1999; Kaneshige et al. 2001), while both receptors may be important in humans (Takeda et al. 1992). In addition, GHR and IGF type I receptor (IGFR1) are T3-responsive, indicating that T3 may also act through the GH/IGF1 axis. (O'Shea et al. 2005).

1.4.2.2 Locally secreted factors & transcription factors

1.4.2.2.1 IGF1

Local secretion of IGF1 in the growth plate is also promoted by GH (Isgaard et al. 1988; Nilsson, A et al. 1990). It is produced by RZ and PZ chondrocytes and acts as an autocrine/paracrine factor to promote growth plate chondrogenesis (Isgaard et al. 1988; Parker et al. 2007; Schlegel et al. 2010). Cartilage-specific IGF1 (Wang, Y et al. 2006) and IGFR1 (Wang, Y et al. 2011) null mice exhibit apparent growth retardation.

1.4.2.2.2 IHH & GLI3

IHH is secreted by pre-hypertrophic (pre-HZ) and early hypertrophic chondrocytes and it regulates chondrocyte proliferation and hypertrophy (Koyama et al. 1996; Maeda et al. 2007; St-Jacques, Hammerschmidt & McMahon 1999; Vortkamp et al. 1996). *Ihh-null* mice display reduced chondrocyte proliferation, inappropriate chondrocyte maturation, and complete loss of osteoblasts (St-Jacques, Hammerschmidt & McMahon 1999). Although the secretion of IHH by chondrocytes is stimulated by IGF1 (Wang, Y et al. 2006; Yang, ZQ et al. 2017) and both IHH and IGF1 signalling pathways are involved in promoting chondrocyte proliferation in cartilage, the two pathways are thought to operate independently (Long et al. 2006). IHH binds the 12-pass transmembrane receptor, patched (PTC), and signals through the 7-pass transmembrane G-protein coupled receptor, smoothened (SMO), to mediate downstream IHH signalling (Zhang, XM, Ramalho-Santos & McMahon 2001). IHH signalling is mediated by the glioma-associated oncogene homologue (GLI) family of transcription factors (Hilton et al. 2005) (Figure 1.4). IHH stimulates chondrocyte proliferation through inactivation of the repressor function of GLI3 in a PTHrP-independent manner, as demonstrated by the restoration of chondrocyte proliferation and reactivation of PTHrP expression in *Ihh-/-Gli3-/-* double mutant mice. IHH also inhibits chondrocyte hypertrophy via induction of PTHrP expression (Hilton et al. 2005; Koziel et al. 2005).

It is unclear what controls the expression of IHH in cartilage development; however, several studies have identified factors that may induce production of IHH. Treatment with T3 in *Thsr-/-* mice rescued expression of *Ihh* in the growth plate; and incubation of T3 also increased expression of *Ihh* in tibia rudiment culture (Xing et al. 2014). Addition of bone morphogenetic protein 2 (BMP2) leads an increase of *Ihh* expression in mouse limb explants, but it is not clear whether this is a direct or secondary consequence of BMP

regulation of *Ihh* expression (Minina et al. 2001). ATF4 directly binds to the *Ihh* promoter and regulates *Ihh* transcription in chondrocytes (Wang, W et al. 2009). Runt-related transcription factor 2 (RUNX2) directly induces *Ihh* expression, coordinating chondrocyte proliferation and differentiation (Yoshida et al. 2004). A recent study demonstrated that core binding factor beta (CBFβ) upregulates *Ihh* expression, as well as IHH target genes including *CyclinD1* and *Patched* (*Ptch1).* CBFβ also downregulates the PTH/PTHrP receptor (*Pthrpr*) expression, thereby regulating chondrocyte proliferation and maturation (Tian et al. 2014).

1.4.2.2.3 PTHrP, SOX9 and RUNX2

PTHrP is expressed by perichondrial cells, resting and early proliferating chondrocytes, and is directly upregulated by IHH (St-Jacques, Hammerschmidt & McMahon 1999; Vortkamp et al. 1996). PTHrP maintains chondrocytes in a proliferative state and inhibits hypertrophic differentiation. It diffuses to PTHrPR that is expressed by late PZ and pre-HZ chondrocytes and acts directly on proliferating chondrocytes. The prevention of hypertrophy regulated by PTHrP is driven via activation of transcription factor SRY-Box 9 (SOX9) that delays chondrocyte hypertrophy, and/or via inhibiting expression of transcription factor RUNX2, which stimulates chondrocyte differentiation (Dy et al. 2012; Guo et al. 2006; Huang, W et al. 2001). RUNX2 is also directly repressed by SOX9, which is consistent with their opposite functions on chondrocyte hypertrophy (Zhou, G et al. 2006). IHH and PTHrP form a negative feedback loop together with other factors including RUNX2 and SOX9 (Figure 1.4). As previously mentioned, pre-HZ chondrocytes secrete IHH which induces production of PTHrP. By inhibiting hypertrophic differentiation through RUNX2 and SOX9, PTHrP limits the production of IHH-expressing chondrocytes, and thus regulates its own expression (Guo et al. 2006; Zhou, G et al. 2006). Increased PTHrP expression in hypothyroid rats and

suppression of PTHrPR expression in thyrotoxic rats suggest that T3 might regulate hypertrophy by inhibiting PTH/PTHrP signalling through PTHrPR (Stevens et al. 2000).

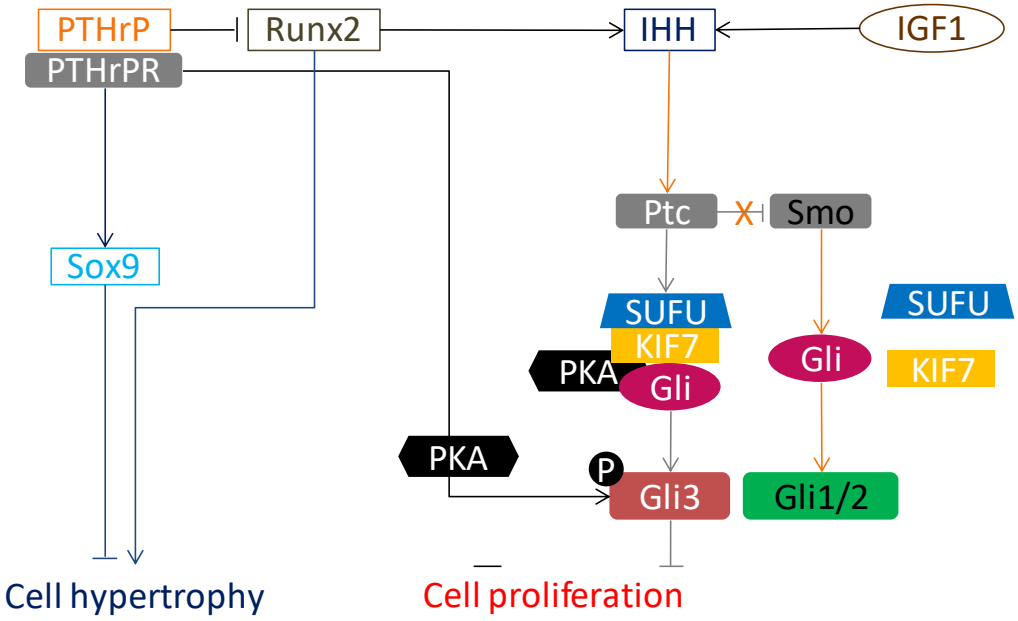

Figure 1.4 Interaction of growth factors and IHH/PTHrP signalling in growth plate. Parathyroid hormone-related peptide (PTHrP) is expressed by perichondrial chondrocytes. Indian hegehog (IHH) is synthesized by pre-hypertrophic chondrocytes. Arrows indicate stimulatory pathways, while crossed lines indicate inhibitory pathways. IGF1, insulin-like growth factor 1. Ptc, patched. Smo, smoothened. SUFU, suppressor of fused homologue. KIF7, kinesin family member 7. Gli, glioma-associated oncogene homologue. PTHrPR, parathyroid hormone related peptide receptor. Sox9, SRY-Box 9. Runx2, runt-related transcription factor 2. PKA, protein kinase A. P, phosphorylation.

1.4.2.2.4 BMPs, FGFs and WNT family

Other groups of locally secreted factors, including bone morphogenetic proteins (BMPs), wingless-type mouse mammary tumor virus integration site (WNT) family proteins, and FGFs, also regulate growth plate chondrocytes and EO in a paracrine/autocrine pattern (Minina et al. 2002; Minina et al. 2001; Yoon et al. 2006). Activation of BMP signalling promotes proliferation of chondrocyte in the growth plate, induces IHH expression, and is involved in chondrocytes hypertrophy (Minina et al. 2001; Yoon et al. 2006). A recent study also suggested a role of GH in induction of BMP2 expression in growth plate chondrocytes (Wu, S et al. 2011). Such findings suggest that BMP and IHH/PTHrP signalling operate downstream to GH and interact with each other to coordinate chondrocyte proliferation and differentiation (Figure 1.2). FGFs function through fibroblast growth factor receptor 3 (FGFR3), suppressing chondrocyte proliferation and inducing hypertrophic differentiation (Minina et al. 2002; Naski et al. 1998). FGF signalling has also been demonstrated to downregulate IHH/PTHrP signalling; however, its inhibition of proliferation is independent of IHH (Minina et al. 2002). The WNT family of secreted proteins is essential for proliferation, hypertrophy, survival and migration of chondrocytes during embryonic development and postnatal development (Akiyama et al. 2004; Yang, Y. et al. 2003). Target disruption of *Wnt5a* in mice revealed its role in preventing chondrocytes from entering proliferation, while WNT5b promotes cell proliferation (Yang, Y. et al. 2003). In addition, Hartmann and Tabin (2000) also found that WNT5a delays chondrocyte differentiation, whereas WNT4 expression promotes chondrocyte differentiation through β-catenin.

During EO, many local signalling pathways, which act as a complex network through transcription factors, link circulating hormones and endocrine/paracrine factors together to regulate proliferation and differentiation of growth plate chondrocytes cells during both embryonic and postnatal growth. The GH/IGF1 system seems to be the most essential

pathway in regulating the proliferation of cartilage, whereas IHH, functioning in parallel to the GH/IGF1 axis, controls the balance between proliferation and hypertrophy either through PTHrP-independent or PTHrP-dependent pathways.

1.4.2.3 GAGs and components of ECM

Growth plate chondrocytes are also influenced by components of the ECM that comprises structural proteins such as proteoglycans and collagens and ECM-remodelling enzymes such as MMP13, MMP14 and MMP9 (Holmbeck et al. 1999; Inada et al. 2004; Mitchell et al. 1996; van der Eerden, Karperien & Wit 2003). Aggrecan, type II and type X collagens are the major ECM proteins expressed in the PZ and hypertrophic zone (HZ) of the growth plate, respectively (van der Eerden, Karperien & Wit 2003). A peptide secreted by type II collagen degradation induces chondrocyte hypertrophy and MMP13 and MMP14 production, which is crucial for matrix remodelling and degradation (Tchetina et al. 2007).

Several signalling pathways discussed above interact with GAGs and cartilage ECM. IHH directly interacts with chondroitin sulphate (CS) chains, binding to the major cartilage proteoglycan aggrecan, and the degree of sulfation of aggrecan modulates IHH signalling in the developing growth plate (Cortes, Baria & Schwartz 2009; Domowicz et al. 2009; Lin, X 2004). Heparan sulphate proteoglycans can interact with several BMPs, negatively regulating BMP signalling to interfere with cartilage differentiation during limb chondrogenesis (Fisher et al. 2006). Accumulation of GAGs in MPS may therefore contribute to the deregulation of such signalling pathways, and lead to disrupted EO and longitudinal bone growth.

1.4.2.4 Factors involved in cell division cycle and apoptosis

Chondrocytes rapidly proliferate under the guidance of certain signalling pathways such as IGF1, IHH, PTHrP, BMPs, FGFs and WNTs. Similar to other tissues and cells, proliferation

in chondrocytes requires strict control of the cell cycle by specific complexes that consist of cyclin-dependent kinase (CDK) and regulatory subunit cyclin, as well as cyclin-dependent kinase inhibitors (CKIs) (LuValle & Beier 2000) (Figure 1.5). CyclinD1 triggers the exit from G0 phase and allow chondrocytes to enter the G1 phase, where they spend the greatest proportion of time. Cyclin D1 is highly expressed in cartilage, and is regulated by numerous growth factors and hormones, including WNT5a, WNT5b, IHH and PTHrP (Goodrich et al. 1991; Ito et al. 2014; Yang, Y. et al. 2003). CyclinD1 forms complexes with CDK4 and CDK6 that phosphorylate the pocket proteins (Retinoblastoma protein (pRb) and the closely related p107 and p130 proteins) (Calbó et al. 2002). The pocket proteins dissociate from a E2F complex, releasing E2F1, E2F2 and E2F3a, which serve as transcriptional activators and induce transcription of target genes that promote DNA replication (S phase), G2 phase and mitosis (M phase). S phase is the second longest phase of the cell cycle, in which the DNA replication of chondrocytes occurs.

Activation of CyclinB-CDK1 complex is essential for entry to mitosis (Lindqvist, Rodríguez-Bravo & Medema 2009), during which chromatins condense into chromosomes. Phosphorylation of histone H3 is required for initiation of chromatin condensation, whereas at the end of mitosis, histone H3 is rapidly dephosphorylated (Hendzel et al. 1997). After several rounds of proliferation, chondrocytes receive anti-mitogenic signals during G1 phase. Dephosphorylation of pocket proteins allows their association with E2F3b, E2F4 and E2F5, which forms complexes that function as transcription repressors that recruit histone deacetylases to promoters of target genes to inhibit their transcription (Gaubatz et al. 2000; Polgreen & Miller 2010). Inhibition of CDK activity by CKIs is then required for cell cycle exit upon onset of hypertrophic differentiation. Members of the CIP/KIP family (p27 and p57) are common CKIs expressed in the chondrocytes (Kiyokawa et al. 1996; Yan et al. 1997).

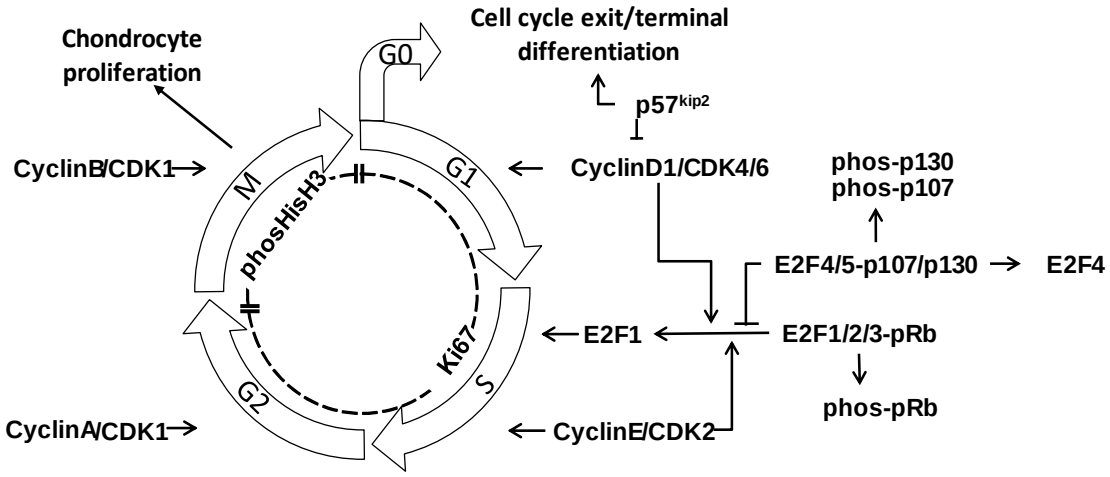

Figure 1.5 Control of cell cycle progression. Progression of cartilage cells through the cell cycle is controlled by the activity of cyclins, cyclin-dependent kinases (CDKs) and CDK inhibitors (CKIs, such as $p57^{kip2}$). Phosphorylation of pocket proteins regulated by CyclinD1/CDK4/6 complexes release E2F1 for entry into S phase. CyclinB1/CDK1 complexes and phosphorylation of histoneH3 are essential for entry to mitosis and chromatin condensation, respectively. Cell cycle withdrawal for terminal differentiation is regulated by the balance of activator and repressor E2F proteins, which is under the control of CKIs, CyclinD1 and CDKs.

After the termination of chondrocyte hypertrophy, cells in the growth plate undergo cell death. Apoptosis has been proposed as one of the cell death mechanisms during EO (Lewinson & Silbermann 1992). Proteins involved in apoptotic activity include cysteine-aspartic acid protease 3 (Caspase 3), anti-apoptotic gene B cell leukemia/lymphoma 2 (BCL2), pro-apoptotic protein BCL2-associated X protein (BAX), TNF receptor superfamily member 6 (FASR) and FAS ligand (FASL). The activation of *Caspase 3* is induced by the maturation of chondrocyte hypertrophy and results in cell death (Oltvai, Milliman & Korsmeyer 1993). The *Bax/Bcl2* ratio determines cell survival or death after an apoptotic stimulus. *Bcl2* expression is known to be regulated by PTHrP (Amling et al. 1997). Apoptosis is also triggered by activation of the FASR in FAS-expressing cells by the binding of the FASL (Ju et al. 1995). However, one study reported that FASL was absent in chondrocytes (Hashimoto et al. 1997).

1.5 Growth plate dysfunction in MPS

Investigation into growth plate dysfunction in MPS patients is limited to histological description at autopsy. Enlarged, vacuole-filled chondrocytes and a disorganised columnar structure have been observed in both MPS I and MPS IVA growth plates (McClure et al. 1986; Silveri et al. 1991).

Abreu *et al.*(1995) and Nuttall *et al*. (1999) found clusters of enlarged, GAG-containing cells in the growth plate, increased growth plate height with a poorly organized proliferating zone, loss of column formation in HZ, and an irregular number of osteoclasts in the cat MPS VI model. An increase in chondrocyte proliferation rate was observed in MPS VII dog growth plate (up to 5-fold faster than normal); however, most of the newly formed cells were immature and unable to mineralize into bone (Simonaro et al. 2005). A single study using MPS VII mice showed shortened bones, accumulation of the major GAG chondroitin-4-sulfate (C4S), depletion of proliferating cell numbers, and reduction of chondrocyte

proliferation in cartilage growth plates (Metcalf et al. 2009). This study also found reduced phosphorylation of STAT3 (a pro-proliferative factor), reduced expression of activators for STAT3 phosphorylation and reduced expression of pro-proliferative gene *Ihh*, which may underly the reduced chondrocyte proliferation and shortened bones in MPS.

To date, growth plate abnormalities that have been commonly observed in either patients or animal models are irregular growth plate structure, ballooned, vacuolated chondrocytes, and loss of columnar arrangement of chondrocytes in the PZ and HZ.

1.6 Endocrine function and current GH therapy in MPS

Although factors like GH, IGF1, T3 and IHH have been demonstrated to function in EO in linear bone growth, little information is known of their levels in MPS patients. Low serum IGF1 levels were detected in 3 untreated MPS II brothers (Toledo et al. 1991). Also, relatively low serum IGF1 levels were observed in 13 out of 22 MPS I patients post HCT (Gardner et al. 2011).

Recombinant human GH has been used to treat short stature in children with various diseases (GH deficiency, idiopathic short stature, Turner syndrome and Prader-Willi syndrome) (Hardin 2008), with beneficial effects on skeletal and bone development. GH therapy has been used in post-HCT/ERT MPS children with conflicting results. hGH treatment (one year treatment) in MPSII and MPS VI patients with ERT and untreated MPS IV patients was initially shown to result in some improvement in growth velocity, spine correction, total body height and IGF1 level (Polgreen & Miller 2010). However, the study found no improvement of growth velocity in MPS IH (Hurler, severe form) or MPS II children with longer term GH treatment (two year treatment) (Polgreen et al. 2014). GH treatment for patients with GH deficiency (GHD) responded better than those without GHD.

In another study, minimal response to GH treatment was observed and treatment discontinued in 4 MPS IH children (Gardner et al. 2011).

Hypothyroidism has also been reported in a case of MPS I patient with short stature (Mohanalakshmi, V. & S. 2014). Thyroid hormone substitution in the short stature of hypothyroidism has been applied for decades; however, there are currently no available reports of clinical trials of such therapy in MPS (Hermosa & Sobel 1972; Smith, RN, Taylor & Massey 1970).

1.7 MPS VII mouse model

Naturally occurring animal models of MPS are found in domestic, agricultural and wild species (Birkenmeier et al. 1989; Cowell et al. 1976; Haskins et al. 1984; Haskins et al. 1979; Lorincz 1964; Spellacy et al. 1983; Thompson, JN et al. 1992). The development of naturally occurring animal models is similar to human MPS. However, not all types of MPS have corresponding naturally occurring animal models. Thus, transgenic and knockout models have been created to mimic specific mutations for which there is no spontaneous form (Clarke, LA et al. 1997; Evers et al. 1996; Garcia et al. 2007; Martin et al. 2008; Russell et al. 1998; Tomatsu et al. 2014; Tomatsu et al. 2003). However, although these models are genetically or biochemically similar to human MPS, some phenotypes such as skeletal deformities and short stature are mild or absent in transgenic and knockout animal modes (Clarke, LA et al. 1997; Garcia et al. 2007; Tomatsu et al. 2003).

Mouse models are of great value in studying MPS as they are well-characterized inbred strains, many with a good representation of the pathology and clinical features of human MPS including skeletal deformities (Birkenmeier et al. 1989; Evers et al. 1996; Haskins et al. 1984). Murine models used in this study are MPS I mice (Clarke, LA et al. 1997), MPS IIIA mice (Roberts et al. 2009), attenuated form of MPS VII mice ($Gus^{tm(L175F)Sly}$) (Tomatsu

et al. 2002), and MPS IX mice (Martin et al. 2008). In addition, the naturally occurring murine MPS VII (*Gus*$^{mps/mps}$) model is also employed (Birkenmeier et al. 1989). MPS I mice have sclerosis, thickened facial and long bones and joint diseases (Clarke, LA et al. 1997; de Oliveira et al. 2013; Russell et al. 1998). MPS IIIA mice have milder defects including thickened calvarium and vertebral deformation (Bhattacharyya et al. 2001; Bhaumik et al. 1999). While MPS IX mice do not have obvious skeletal deformities except for altered matrix components in articular cartilage and in the growth plate (Martin et al. 2008). While these mouse models are normally used for investigating efficacy of therapies on lysosomal storage in brain and other organs, attenuated form of MPS VII mice (*Gus*$^{tm(L175F)Sly}$) and MPS VII (*Gus*$^{mps/mps}$) model have been used to develop therapies for skeletal diseases (Derrick-Roberts et al. 2016; Derrick-Roberts et al. 2014; Macsai et al. 2012)

The majority of this study utilises the severe strain MPS VII (*Gus*$^{mps/mps}$). The MPS VII (*Gus*$^{mps/mps}$) mouse mutation maps to the distal half of chromosome 5, the region homologous to human chromosome 7 (Schwartz et al. 1991). A 1bp deletion in exon 10 results in the formation of a premature stop codon, leading to the complete lack of β-glucuronidase activity and accumulation of the DS, HS, C4S and C6S (Sands & Birkenmeier 1993). MPS VII (*Gus*$^{mps/mps}$) mice are physically distinguishable from normal littermates by 7 days of age by their smaller body size, shorter limbs, shorter and thicker tail and facial dysmorphism (Figure 1.6) (Birkenmeier et al. 1989). Lifespan is reduced and affected mice die by 6-7 months of age.

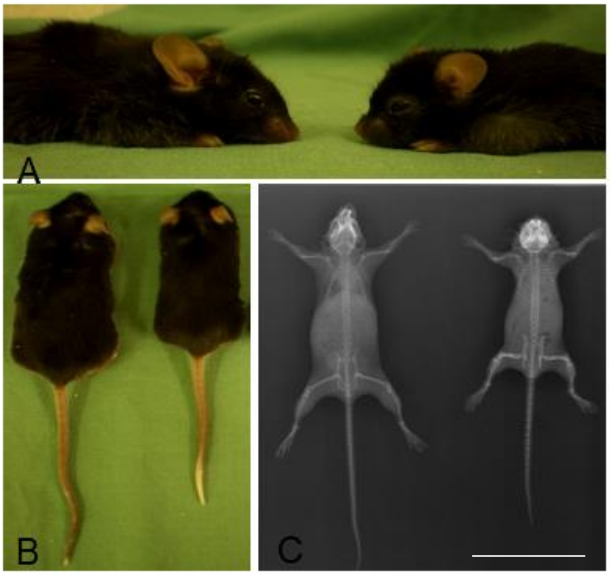

Figure 1.6 Six-month-old normal mouse (left) and MPS VII (*Gus*$^{mps/mps}$) mouse (right). (A) Visual facies; (B) visual bodies and (C) X-ray of mouse models. Figures are derived from Matrix Biology Unit, SA pathology. Scale bar=5cm.

1.8 Aims

Growth plate dysfunction has been identified as the most likely cause of bone shortening in MPS. Growth plate cartilage cells of normal children respond to circulating hormones such as GH and T3. These factors either directly act on chondrocytes, or triggers activation/inhibition of downstream paracrine/autocrine factors and transcription factors as well as cell cycle regulators that promotes proliferation and differentiation of chondrocytes in the growth plate. While the regulations of chondrocyte proliferation and differentiation involve a complex network, it is possible that the reduced proliferation in the MPS VII growth plate results from multiple impaired signalling pathway.

This study therefore aims to characterise bone development and growth plate maturation and to determine potential pathways that are affected in MPS during these processes using a naturally occurring MPS VII murine model. With an improved understaning the underlying mechanism, potential intervention point(s) for therapy could be highlighted to improve growth in MPS.

The specific aims are:

1. To characterise the development of bone growth in different MPS mouse models (MPS I, IIIA, VII ($Gus^{mps/mps}$ and $Gus^{tm(L175F)Sly}$ and IX)
2. To investigate the regulation of EO through cell cycle in MPS VII mice
3. To investigate the regulation of bone growth at endocrine level in MPS VII mice
4. To investigate the relationship between local signalling pathways and growth plate dysfunctions in MPS VII mice

2 Materials and Methods

2.1 Materials

Materials used are listed in the Appendix A.

2.2 Animal husbandry and genotyping

All experimental procedures were approved by the Womens and Childrens Health Network and the University of Adelaide Animal Ethics Committees. Founder animals for MPS I, MPS IIIA, MPS VII (*Gus*$^{mps/mps}$ strain) and attenuated MPS VII (*Gus*$^{tm(L175F)Sly}$ strain) were obtained from Jackson Labs while MPS IX founder mice were obtained from Mutant mouse resource & research centers (MMRRC). MPS and normal mice were bred from heterozygous parents with the same background in each case. Homozygous normal mice from were used as normal control. Mice were housed in a 14/10 light/dark cycle with food and water *ad libitum.*

Genomic DNA was extracted from tissue by lysis in Viagen lysis buffer containing 0.4 mg/mL proteinase K as per the manufacturer's instruction (Viagen Biotech Inc., USA). A polymerase chain reaction (PCR) based genotyping protocol was performed on genomic DNA as previously described (Clarke, LA et al. 1997; Derrick-Roberts et al. 2014; Macsai et al. 2012; Martin et al. 2008; Roberts et al. 2009).

2.2.1 Mouse sacrifice and tissue harvest

Mice were humanely killed at experimental end points by carbon dioxide asphyxiation followed by cervical dislocation before blood was collected via cardiac puncture or retriobital bleed. Blood was stored at 4°C overnight before serum was separated by centrifugation at 800 x *g* for 10 minutes and stored at -80°C for future analysis. Liver tissue was collected and fixed in 10% neutral buffered formalin and embedded in paraffin for immunohistochemical analysis or stored at - 80°C for real-time PCR analysis. Hindlimbs

and L4-L6 vertebrae were removed and fixed in 10% buffered formalin overnight and then stored in 70% ethanol for radiography. Hindlimbs were embedded in paraffin for histological, histomorphometrical and immunohistochemical analysis. The proximal tibia growth plates from 14 days old (P14) normal and MPS VII mice were isolated, snap frozen and then stored at -80°C for later real-time PCR analysis, or snap frozen in optimal cutting temperature compound (OCT) and then stored at - 80°C for microdissection.

2.3 Bone and growth plate histomorphometric measurement*Radiography and bone length measurements*

Femurs, tibiae and L4-L6 vertebrae were harvested from 6-month old normal and MPS mice and X-rayed as previously described to compare bone length of 5 mouse models at maturity (Derrick-Roberts et al. 2014). Additional radiographs of femurs from MPS I, MPS VII (*Gus*$^{mps/mps}$ strain) and attenuated MPS VII (*Gus*$^{tm(L175F)Sly}$ strain) mice along with normal littermates were taken at P14, 1 month, 2 months and 3 months of age to determine the natural history of linear bone growth in MPS. X-ray films were scanned, converted to digital data using the GE healthcare radiograph system Discovery XR656 (GE healthcare, Australia). Digital radiographs were calibrated and femur, tibia and L5 vertebrae lengths were measured from the most proximal point to the most distal points of articular surface of the bones using Olympus analySIS® LS Research Olympus Soft Imaging Solutions version 3.1 (Olympus Australia Pty. Ltd., Gulfview Heights, SA). The number of mice of each genotype and age are presented in Table B.1 of Appendix B.

2.3.2 Proximal tibia morphology

Knee joints were removed from normal and MPS mice and fixed in 10% neutral buffered formalin for 24 hours and then decalcified in Immunocal^{Tm} between one day (E17.5 and E18.5 samples) and 4 weeks (postnatal samples) prior to routine processing and embedding

in paraffin blocks. Five microns sections were cut using a Leica RM2235 microtome (Leica Microsystems Pty Ltd, NSW, Australia) and stained with a modified safranin-O/ fast-green protocol (Rosenberg 1971). Consecutive sections deparaffinized using Solv21C (United Bioscience, VIC, Australia), 100% ethanol, 70% ethanol and dH_2O and then stained for 5 min in 0.07% fast-green stain. Sections were rinsed with 1% acetic acid then stained in 0.07% safranin-O. Sections were dehydrated in 70% ethanol, 100% ethanol and subsequently in xylene. Stained samples were mounted using Leica CV Mounting Media.

2.3.3 Quantification analysis of area occupied by secondary ossification centre growth plate zone height, and chondrocyte number and size.

Sections collected from each animal that have the largest area occupied by the SOC was considered as the midsagittal plane. Sections were stained with safranin-O/fast green. The area occupied by the SOC contains marrow elements and bones (stained green by Fast Green) and is defined as Figure 2.1. The area occupied by the SOC and total area of the proximal epiphysis were measured using an Olympus BX51 microscope (Olympus Australia Pty. Ltd., Gulfview Heights, SA). and Olympus analySIS® LS Research Olympus Soft Imaging Solutions (version 3.1) software and results of area occupied by the SOC were represented as percentage of total epiphysis area.

Individual growth plate zones were defined using morphological criteria as previously described (Nuttall et al. 1999). The RZ consisted of round, single chondrocytes; the proliferating zone adjacent to the RZ was characterized by flattened cells arranged into multicellular clusters to form columns of chondrocytes perpendicular to the growth axis. The HZ was considered to start at the point at which chondrocyte size had doubled and terminated at the metaphysis. Zone height was measured at 100 μm intervals across the growth plate for a total of 8 measurements in P14 mice and 16 measurements in 1 and 2 months old mice. Measurements were averaged to yield a single value for each zone for

each animal. The total height of the proximal tibial growth plate was determined by summing the heights of the RZ, PZ and HZ. Distinct zones were difficult to define in 6-month old mice and thus individual zone heights were not measured. The total growth plate height in 6 months old mice was taken as the distance between the epiphysis and metaphysis, with 16 measurements taken at 100 µm intervals across the growth plate and averaged for each animal. Eight, sixteen and eight 50 µm x 50 µm squares were randomly selected in the RZ, PZ and HZ respectively of each animal. The number of chondrocytes within each square was measured. Chondrocyte number in each square of each zone was averaged to give the final value per animal. Since lacunae are presumed to represent expanded cell size (Orkin et al. 1977), the horizontal diameter of each chondrocyte lacuna within each square was measured to determine the size of chondrocytes and was averaged per animal.

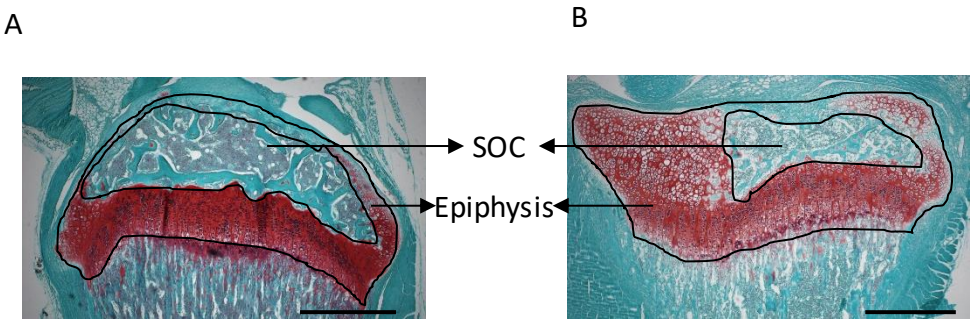

Figure 2.1 Histologic structure of the proximal end of normal and MPS VII mice tibia at 1 month of age. Safranin O/fast green stained proximal tibia section of normal (A) and MPS VII (B) mice. The region from the edge of articular surface to the last cells of the hypertrophic zone of the growth plate represents the epiphysis. The region within the epiphysis represents the developing SOC, which was measured as the area occupied by SOC. Scale bar = 500µm.

2.4 Transmission electron microscopy (TEM)

Tibia from normal and MPS VII mice aged P14 were fixed in Karnovsky's fixative supplemented with 0.7% (v/v) safranin O (Wilson, R et al. 2010) for 2 hours and then decalcified for 7 days in 14% EDTA (pH 7.4) with 0.1% glutaraldehyde. Tibia were post fixed in 2% osmium tetroxide, processed and embedded in Araldite-Procure resin (Pelco BioWave; Pelco International) (Derrick-Roberts et al. 2014; Kopecki et al. 2009; Macsai et al. 2012). Semi-thin (1 µm) sections were stained with 1% toluidine blue in 1% borax for orientation. Ultrathin (80 nm) sections were cut on a Leica UltraCut S Ultramicrotome (Leica system, Germany) with an ultra-diamond knife. The sections were mounted on copper grids and stained with uranyl acetate and lead citrate for 7 minutes. The ultrathin sections were examined with a Tecnai G2 Spirit transmission electron microscope (FEI, Eindhoven, the Netherlands) equipped with a VELETA CCD camera (Olympus SIS, Münster, Germany) at Adelaide Microscopy (Adelaide, Australia) and EDS system comprising an Apollo XLT SDD running EDAX's TEAM software were used. The chondrocytes in the RZ, PZ and HZ of tibia growth plate were assessed using TEM in both normal and MPS VII mice.

2.5 Measurement of circulating hormones

Blood was collected from mice at P14, 1, 2 and 6 months of age via cardiac puncture. Serum was prepared as described in section 2.2.1 and stored at -80°C. Measurement of circulating levels of GH, IGF1, IGFALS, IGFBP3, T3 and IHH in normal and MPS VII serum was performed using ELISA kits according to manufacturer's instruction (Appendix A).

2.6 GH production

Normal and MPS VII mice (1, 2 and 4 months of age) were anaesthetized with ketamine (75 µg/gm body weight) and dormitor (1 µg/gm body weight) combination. GH secretion

was stimulated by the intraperitoneal injection of ghrelin at 10 μg/animal. Control mice received saline instead of ghrelin. Blood was collected by retro-orbital bleeding at 0, 5 and 15 minutes after injection. Serum was prepared as described in section 2.2.1 and stored at -80°C prior to GH level determination by ELISA as above. GH level of serum collected at 0 minutes after injection was considered as baseline level. GH release at 5 and 15 minutes after ghrelin injection was compared to baseline level to assess the stimulatory effect of ghrelin

2.7 IGF1 production

2.7.1 Isolation and in vitro culture of primary hepatocytes

Seven-week old normal and MPS VII mice were anesthetized as described in section 2.2.1. and the peritoneal cavity was opened. The liver was perfused with pre-warmed perfusion medium I (PBS containing 1M HEPES, 5%(w/v) KCl, 1M glucose, 200 mM EDTA, pH 7.4), and then with perfusion medium II (PBS containing 1M HEPES, 5%(w/v) KCl, 1M glucose, 500 mM $CaCl_2$, pH 7.4 containing 0.8 mg/ml collagenase type I). Digested liver was removed and rinsed with perfusion medium II and then gently teased with forceps and scissors until cells were released in solution. The cells were filtered through a sterile 70 μm nylon cell strainer (Corning Inc, Durham, USA) to remove excess tissue. The cells were then washed and centrifuged for 5 minutes at 50 x g in perfusion medium II three times using Beckman Coulter optima L-100K ultracentrifuge and SW60 rotor. Cell pellet was resuspended in Williams E medium containing 1% 5,000 U/mL penicillin and 5,000 μg/mL streptomycin (P/S), 1% 200mM L-glutamine, 1% nonessential amino acids and 10% heat-inactivated FCS. The yield and viability of hepatocytes was determined using the Countess® automated cell counter and 0.4% trypan blue (Invitrogen, Life Technologies, Australia). and the yield of hepatocytes ranged between 100-400 million cells per animal,

with a viability at 85-95% for all experiments. A 24-well plate was coated with Geltrex LDEV-Free hESC-qualified reduced growth factor basement membrane matrix at a concentration of 1:10 in Williams E medium containing 1% P/S, 1% 200 mM L-glutamine, 1% nonessential amino acids and 10% heat-inactivated FCS. Each well was seeded with $1x10^5$ hepatocytes and incubated at 37°C, 5% CO_2. After 24h, non-adherent cells were removed by aspiration and Williams E medium containing 1% P/S, 0.5mg/ml gentamycin, 0.04% fungizone, 20mM L-glutamine and 1% nonessential amino acids was added.

2.7.2 Production of IGF1 in response to stimulation

Triplicate wells were incubated with recombinant GH at a final concentration of 0 ng/ml, 10 ng/ml, 50 ng/ml, 100 ng/ml, 500 ng/ml and 1000 ng/ml. Medium was collected and stored at -20°C for later IGF1 measurement by ELISA as described in section 2.6.2. The cell layer was harvested for enzyme activity assay (Section 2.7.3) by 0.25% trypsin/EDTA and cell lysed by freeze-thaw in 0.1% Triton X100. Total protein was measured using Bradford assay according to manufacturer's instruction.

2.7.3 β-glucuronidase production and administration to MPS VII hepatocytes

A lentiviral vector was constructed to encode mouse β-D-glucuronidase (pHIV-EF1αmmGUS) as previously described (Jackson et al. 2015). β-glucuronidase was produced in CHO-K1 cells. Briefly, CHO-K1 cells were seeded in Hams F12+10%FCS at $5.5x10^4$ cells/cm^2 and transfected 3 h later with the addition of 0.75 μg/ml p24 protein of pHIV-EF1αmmGUS in the presence of 8ng/ml polybrene and 100ng/ml gentamycin. After 24h the media was removed and replaced with Hams F12 medium containing 1% P/S and 1% 200mM L-glutamine. Medium collected was pooled and concentrated by centrifugation on a YM-30 Centricon filter (Amicon,USA). β-glucuronidase enzyme activity from concentrated medium was determined using the fluorogenic substrate 4-

methylumbelliferyl-b-D-glucuronide (Derrick-Roberts et al. 2014; Macsai et al. 2012) on a LS 50B luminescence spectrometer using an AS 91 auto-sampler (Perkin Elmer, Waltham, Massachusetts, USA) at excitation and emission wavelength of 366nm and 446nm, respectively.

Hepatocytes isolated from MPS VII mice were incubated in Williams E medium containing 1% P/S, 0.5 mg/mL gentamycin, 0.04% fungizone, 1% 200mM L-glutamine and 1% nonessential amino acids alone (control) or in the medium containing 0.04 nmol/min β-glucuronidase, while hepatocytes isolated from normal mice were incubated in Williams E medium containing 1% P/S, 0.5% gentamycin (10mg/mL), 0.04% fungizone, 1% 200 mM L-glutamine and 1% nonessential amino acids alone at 37°C, 5% CO_2 for 24 h. 500 ng/mL recombinant mouse GH was added to primary hepatocyte culture (section 2.6.1.2). Hepatocytes were cultured for additional 24 h at 37°C, 5% CO_2. Medium was collected and stored at -20°C for later IGF1 measurement by ELISA as described in section 2.6.2. β-glucuronidase enzyme activity from cells was determined using the fluorogenic substrate 4-methylumbelliferyl-b-D-glucuronide (Derrick-Roberts et al. 2014; Macsai et al. 2012).

2.8 Response of chondrocytes to systemic or local factors

2.8.1 Isolation and in vitro culture of primary chondrocytes

The proximal tibia growth plate was dissected out from P14 normal and MPS VII mice (Figure2.1) free of perichondrium, POC and SOC. Growth plate was collected into Hams F-12 medium and the incubated in Hams F-12 containing 1% (w/v) pronase and 1% P/S at 37ºC for 1 hour. Tissue was washed with PBS to remove pronase and incubated in Hams F-12 containing 0.08% (w/v) collagenase, 5% FCS and 1% P/S at 37ºC for at least 15 h. Cells were filtered through a 50μm nylon filter and collected by centrifugation at 1500 rpm for 5

min. Cell number was determined using the Countess® automated cell counter and 0.4% trypan blue.

2.8.2 Cell proliferation assay

To determine cell proliferation, chondrocytes were seeded at $6.25x10^4$ cells/cm^2 in a 96-well plate and maintained in Dulbecco's Modified Eagle Medium (DMEM) containing 1% P/S, 1% FCS. The dose to GH, T3, IGF1 and IHH was determined in normal chondrocytes on day 2 of culture. Recombinant mouse GH reconstituted in dH_2O at 1 mg/ml and added to chondrocyte cultures to give a final concentration of 50 ng/mL, 100 ng/mL, 200 ng/mL, 250 ng/mL, 500 ng/mL, and 1000 ng/mL. Recombinant mouse IGF1 and recombinant human/mouse were reconstituted in dH_2O at 100 µg/ml and added to chondrocyte cultures to give a final concentration of 25 ng/mL, 50 ng/mL, 100 ng/mL, 200 ng/mL, 250 ng/mL and 500 ng/mL. T3 was dissolved in 1M NaOH at 1mg/mL and added to chondrocyte cultures to give a final concentration of 1 ng/ml, 10 ng/ml, 50 ng/ml, 100 ng/ml, 250 ng/ml, 500 ng/ml. The CyQUANT® Direct Cell Proliferation Assay Kit was used for assessment of cell proliferation. Cells were lysed according to manufacturer's instruction, and total cellular nucleic acid was measured using florescence (485nm excitation, 535nm emission, 0.1sec) on a $VICTOR^2$ plate reader (Perkin Elmer). Dose-response results are shown in Figure 2.2 and the following concentrations used in subsequent experiments: 250 ng/mL GH, 500 ng/mL IGF1, 25 ng/mL IHH and 10 ng/mL T3. Normal and MPS VII chondrocytes were cultured in DMEM containing 1% P/S, 1% FCS, with the presence of 250 ng/mL GH, 500 ng/mL IGF1, 10 ng/mL T3 or 25 ng/mL IHH. On day 0, 2, 4, and 6, cell proliferation was assessed. The negative control consisted of cells incubated in DMEM containing 1% P/S plus 1% FCS. The positive control consisted of cells incubated in DMEM containing 1% P/S plus 10% FCS.

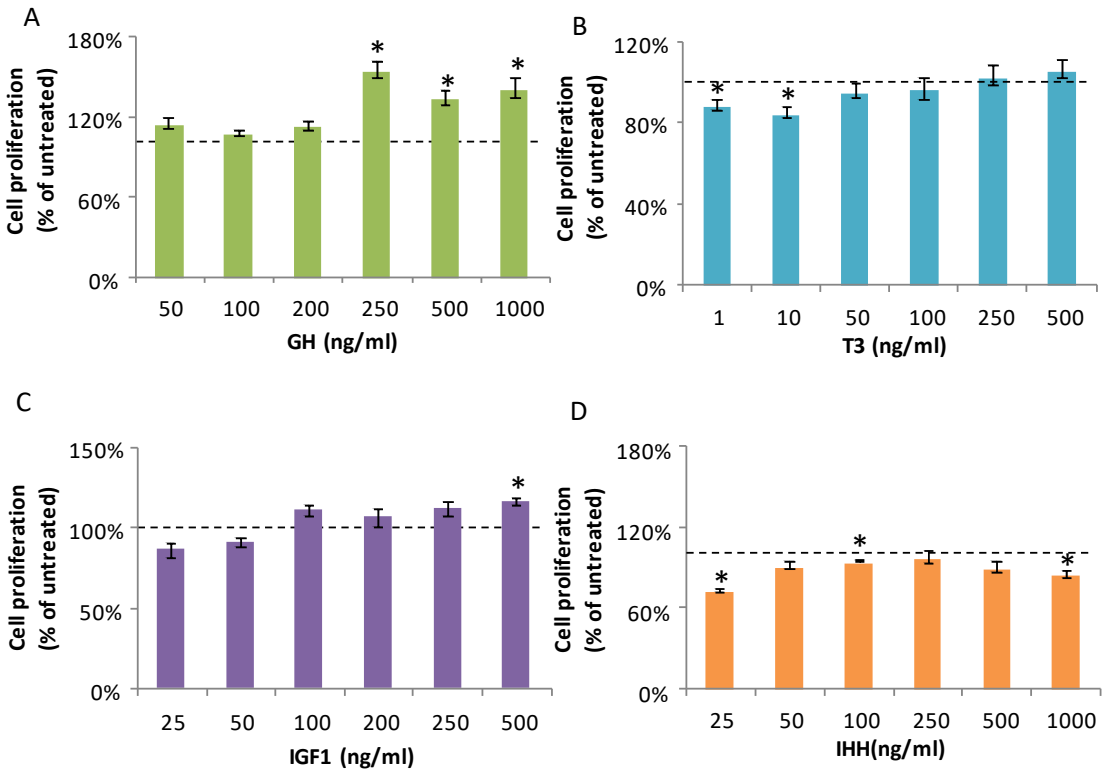

Figure 2.2 Dose-response effects of hormones on normal chondrocytes. Cell proliferation of triplicate samples was measured 2 days after addition of A) GH, (B) T3, (C) IGF1 and (D) IHH.

* denotes a $p<0.05$ significant difference between GH, T3, IGF1 or IHH treated and untreated chondrocytes, student's t-test.

2.8.3 IHH secretion by chondrocytes

To assess the secretion of IHH by chondrocytes, cells were seeded at a density of $1x10^5$ cells/cm^2 on 24-well plates and maintained in DMEM containing 1% P/S and 1% FCS for 48h and 96h. Medium were collected and assayed for IHH expression using commercially available ELISA kits as above (Section 2.5).

2.9 Gene expression analysis

Liver from 14 days old normal and MPS VII mice was dissected. The proximal tibia growth plate from 14 days old normal and MPS VII mice was dissected clear of bone and surrounding perichondrium. For gene expression analysis in the liver and whole growth plate, samples were snap-frozen in liquid nitrogen and stored at -80 ºC until RNA isolation. Liver tissues were homogenized using a Potter-Elvehjem test pestle (Sigma, NSW, Australia) in Trizol reagent and RNA isolated according to manufacturer's instruction. Whole growth plates were finely ground in liquid nitrogen, homogenized by passage over a QIAshredder column (Qiagen, Maryland, USA) and RNA isolated using the RNaqueous® Micro Kit including a DNaseI digestion. The PZ was also manually microdissected from the proximal tibia growth plate of D14 mice using a method from (Belluoccio et al. 2008) with modification from zone specific analysis. Briefly, whole growth plates were snap frozen in OCT compound using pre-cooled isopentane in liquid nitrogen and stored at -80°C. Twenty microns longitudinal sections were cut using a Leica CM1800 Cryostat (Leica Microsystems Pty Ltd, NSW, Australia), pre-cooled to -22°C (maintained between -20 and 23°C) and mounted on RNase-free Superfrost Plus glass slides (Lomb Scientific Pty Ltd, NSW, Australia). Slides were fixed in 70% EtOH in diethylpyrocarbonate (DEPC) treated water for five minutes with regular agitation and dehydrated through serial ethanol wash and dried on 50°C hot plate for 5 seconds. Slides were then immobilized on Nikon SMZ25 stereo microscope and the PZ dissected using an ophthalmic knife (MVR20, Mani

Inc., Tochigi, Japan). The tissue was harvested into an RNase-free tube and total RNA was isolated using TRIzol reagent according to the manufacturer's instruction. The concentration of RNA isolated by either procedure was determined using a Thermo Scientific NanoDrop 1000 and its operating software, version 3.8.1 (Thermo Scientific, VIC, Australia).

Approximate 200 ng of the isolated RNA was reverse transcribed into cDNA using the QuantiTect® Reverse Transcription Kit. Quantitative real-time PCR was performed on an ABI 7300 real-time PCR system (Applied Biosystems, Life Technologies, California, USA) using SYBR® Green Master Mix. Primers used were listed in Appendix B Table B5. The thermal cycling conditions comprised the initial steps at 50 ºC for 2 minutes, and 95ºC for 10 minutes. Amplification of cDNA consisted of a denaturation step at 95ºC for 15 seconds, and an extension step at 60ºC for 1 minute. A dissociation stage consisting of a cycle of 15 seconds at 95ºC, 30 seconds at 60ºC, and 15seconds at 95ºC was added. Data were normalized to cyclophilinA (*CycA*) and the fold change was calculated using the ΔΔCt method (Livak & Schmittgen 2001). For samples collected from the manual microdissection of the PZ, markers of the RZ (*Pthrp)* and HZ (*Mmp13)* were analyzed to check for the accuracy of isolation of PZ chondrocytes.

2.10 Immunohistochemistry

P14 normal, MPS VII and MPS IIIA proximal tibiae (n=3 per genotype, except for detection of phosphor Ser10 histone H3 (phos-hisH3), n=5 MPS VII tibiae were used) were fixed in 10% neutral buffered formalin, decalcified in Immunocal^{Tm} and embedded in paraffin. Livers from P14 normal and MPS VII (n=5 per genotype) were fixed in 10% neutral buffered formalin and embedded in paraffin. Testis from 2m normal mice were fixed in 10% neutral buffered formalin and embedded in paraffin. Five-micron sections were collected from each tissue sample. Immunohistochemisty was carried out on tibia or liver sections

after deparafinization and antigen retrieval as described in Table 2.1. Rabbit IgG antibody was used as negative control except for detection of IHH. 10 µg/ml IHH antibody was incubated with 40 µg/ml recombinant IHH as absorption control. Mouse testis sections were used as positive control (data not shown).

Blocking solutions and biotinylated secondary antibody were as per the Cell and Tissue Staining Kit (anti-rabbit or anti-goat) for all antibodies except phos-hisH3. For phos-hisH3, tibia sections were blocked with 5% normal horse serum and incubated with goat-anti-rabbit fluorescein isothiocyanate (FITC) secondary antibody (1 in 1000 dilution). Sections were counterstained with Mayer's hematoxylin or Prolong-Gold DAPI (P36931, ThermoFisher, Australia) and evaluated under an Olympus BX51 microscope fitted with Soft Imaging System's Colorview III camera and analySIS® LS software. The number of cells staining positive for Caspase 3, phos-hisH3, Ki67, $p57^{kip2}$, CyclinB1, Cyclin D1, phosphorylated pRb (phos-pRb), phosphorylated p130 (phos-p130), E2F1, E2F4, GHR, IGF1 and IHH in each zone was determined using Olympus analySIS® LS Research Olympus Soft Imaging Solutions (version 3.1) software. The number of chondrocytes within a 200µm wide strip that encompassed all zones was determined and repeated twice more. Chondrocyte number in each zone was averaged to give the final value per animal and presented as a percentage of the total number of cells per area counted. For immunostaining analyses of GHR, tyrosine phosphorylated-JAK2 (Y-phos-JAK2), -STAT5 (Y-phos-STAT5), -STAT5A (Y-phos-STAT5A), and serine phosphorylated-STAT5 (S-phos-STAT5) on liver sections, captured images were analyzed using Image J with a compatible IHC profiler plugin for analyzing cytoplasmic and nuclear staining pattern (Chatterjee et al. 2013; Varghese et al. 2014).

2.11 Statistics

The number of animals used in bone morphology, endocrine level measurement and IHC analysis was justified based on previous lab studies and literatures (Derrick-Roberts et al.

2016; Derrick-Roberts et al. 2014; Macsai et al. 2012; Metcalf et al. 2009; Sun et al. 2004). The number of animals used for gene expression analysis and local regulation of chondrocytes was justified with power analysis $p<0.05$ and power=80%. Statistical significance of variance (age and diseases state as independent variables) was determined by a two-way ANOVA with a Tukey's HSD post-hoc analysis using GraphPad Prism version 7.0 (GraphPad Software Inc., California, USA). Statistical significance of variance (diseases as variables) was determined by a Student's t-test using Microsoft Excel 2010 and 2016. Statistical significance was assumed when $p<0.05$.

Table 2.1 Antigen retrieval and dilution used for primary antibodies in immunohistochemical analysis.

Antibody	Source and cat #	Antigen retrieval	Dilution
Activated caspase 3 (Asp175)	CST #9661	10mM sodium citrate buffer, 60°C, O/N; 0.01U/ml chondroitinase ABC, 37°C, 1hr	1:300
Caspase 3	CST #9662		1:1000
Cyclin D1(SP4)	ThermoFisher MA5-14512	10mM sodium citrate buffer, 60°C, O/N	1:50
E2F1	Abcam ab179445		
pRb (phospho S780)	Abcam ab47763		
Cyclin B1 (H433)	Santa Cruz sc-752		1:100
E2F4	Abcam ab53060		
STAT5 (phospho Y694/Y699)	Santa Cruz sc-11761		
STAT5A (phosphor Y694)	Abcam ab30648		
IHH N-terminus	R&D system AF1705		1:20
JAK2(phosphor Y1007/Y1008)	Abcam ab32101		1:25
GHR	Abcam ab202964		1:200
Histone H3 (phosphor Ser10)	CST #9701		
IGF1	Abcam ab9572		
Rb2/p130 (phospho S952)	Abcam ab68136		
STAT5 (phosphor S726/S731)	ThermoFisher PA5-36767		
Isotype (IgG)	Abcam ab27478		

Antibodies were purchased from Santa Cruz Biotech, USA, ThermoFisher, USA, Abcam, Australia, Cell Signalling (CST), Danvers, MA, USA and R&D system, USA.

3 Development of bone pathology in MPS mouse models

3.1 Introduction

MPS, a group of lysosomal storage disorders, are caused by a single enzyme deficiency. Reduced longitudinal bone growth leading to short stature is a common feature observed in MPS I, II, IVA, IVB, VI and VII patients (Melbouci et al. 2018; Neufeld & Muenzer 2001). Although children may fall within the normal height (length) range at birth, their growth progressively slows, and they fall below the third percentile for height by two to three years of age (Hendriksz et al. 2013; Montaño et al. 2008; Neufeld & Muenzer 2001) as GAG accumulates in connective and skeletal tissues. Longitudinal bone growth in MPS is not amenable to current therapies, including BMT/HSCT, or ERT. Genes and underlying mutations in human MPS have been well characterised; however, the pathological cascade in MPS bone growth initiated by accumulated lysosomal storage is poorly understood, thus limiting the development of therapies.

Animal models of MPS, either naturally occurring or via targeted disruption of genes encoding lysosomal enzymes of GAG degradation, have been employed to study bone pathology in MPS (Abreu et al. 1995; Birkenmeier et al. 1989; Crawley et al. 1997; Herati et al. 2008; Macsai et al. 2012; Metcalf et al. 2009; Nuttall et al. 1999; Schuchman et al. 1989). Although skeletal deformities in some of these MPS animal models have been characterized, the growth pattern of long bones of MPS animals has not been detailed. The aim for this chapter was to characterise the development of bone growth in five MPS mouse models (MPS I, MPS IIIA, MPS VII ($Gus^{mps/mps}$ (severe) and $Gus^{tm(L175F)Sly}$ (attenuated) strains) and MPS IX). This chapter hypothesize that these five mouse models mimic their corresponding human MPS, that is, MPS I and MPS VII ($Gus^{mps/mps}$ (severe) and $Gus^{tm(L175F)Sly}$ (attenuated) strains) mice have shortened long bones, while MPS IIIA and MPS IX mice have normal bone length. A detailed time-course of the endochondral bone development was performed, as well as further characterization of growth plate

abnormalities in the severe MPS VII mouse model ($Gus^{mps/mps}$) using histomorphometric analyses.

3.2 MPS VII mouse models are good representatives of the corresponding human MPS for short stature

MPS I, MPS IIIA, MPS VII ($Gus^{mps/mps}$ and $Gus^{tm(L175F)Sly}$ strains) and MPS IX femur (Figure 3.1A), tibia (Figure 3.1B) and L5 vertebra (Figure 3.1C) lengths were measured on radiographs of 6-month old mice (Chapter 2.3.1). Femur length was significantly decreased in murine MPS I, MPS VII severe strain ($Gus^{mps/mps}$) and MPS VII attenuated strain ($Gus^{tm\ (L175F)Sly}$) reaching 95.5±0.7%, 92.6±1.1%, and 66.8±1.3% of normal length respectively. MPS IIIA and MPS IX femur lengths were not different to normal, being 100.2±0.7% and 99.0±2.3% of normal at maturity, respectively. Tibia lengths were significantly reduced in murine MPS VII severe strain ($Gus^{mps/mps}$) and MPS VII attenuated strain ($Gus^{tm\ (L175F)Sly}$), reaching 80.9±3.3% and 96.3±0.6% of normal length respectively. Tibia lengths were the same as normal in murine MPS I, MPS IIIA and MPS IX. L5 vertebra height was significantly decreased only in the murine MPS VII severe strain ($Gus^{mps/mps}$), reaching 85.6±1.6% of normal. There was no difference in L5 height between murine MPS I, MPS IIIA, attenuated MPS VII ($Gus^{tm(L175F)Sly}$), MPS IX strains and normal mice.

Femoral and tibial growth in the 3 models that displayed growth retardation was further analyzed from 14 days of age until 6 months of age (Chapter 2.3.1). Murine MPS VII ($Gus^{mps/mps}$) differed from their normal littermates in showing marked decrease in femoral (Figure 3.2A) and tibial length (Figure. 3.2 D) from 14 days of age onwards. Femur lengths of MPS VII severe strain ($Gus^{mps/mps}$) were 83.5±3.2% of normal at 14 days of age ($p<0.05$) and were progressively decreased from this age onwards. Tibia length of MPS VII severe strain ($Gus^{mps/mps}$) were 91.0±2.9% of normal ($p<0.05$) at 14 days of age and were also significantly shorter than normal mice from this age onwards. Femoral and tibial growth

rates of these mice from 14 days to 1 month of age were significantly decreased to 77.0±7.0% and 57.0±6.3% of normal ($p<0.05$). The femur of attenuated MPS VII ($Gus^{tm\ (L175F)Sly}$) mice were significantly shortened from 3 months of age onwards (Figure 3.2E). The defect appeared earlier at P14 in the tibia of the same animals (Figure 3.2H). However, differences in growth velocity of the femur and tibia between attenuated MPS VII and normal mice did not reach statistical significance (Figure 3.2J). Bone shortening in murine MPS I was observed only in femur at 3 months and 6 months of age (Figure 3.2F and I). Not surprisingly, femoral and tibial growth rate of MPS I mice were not significantly different to those in normal mice from the same colony (Figure 3.2J).

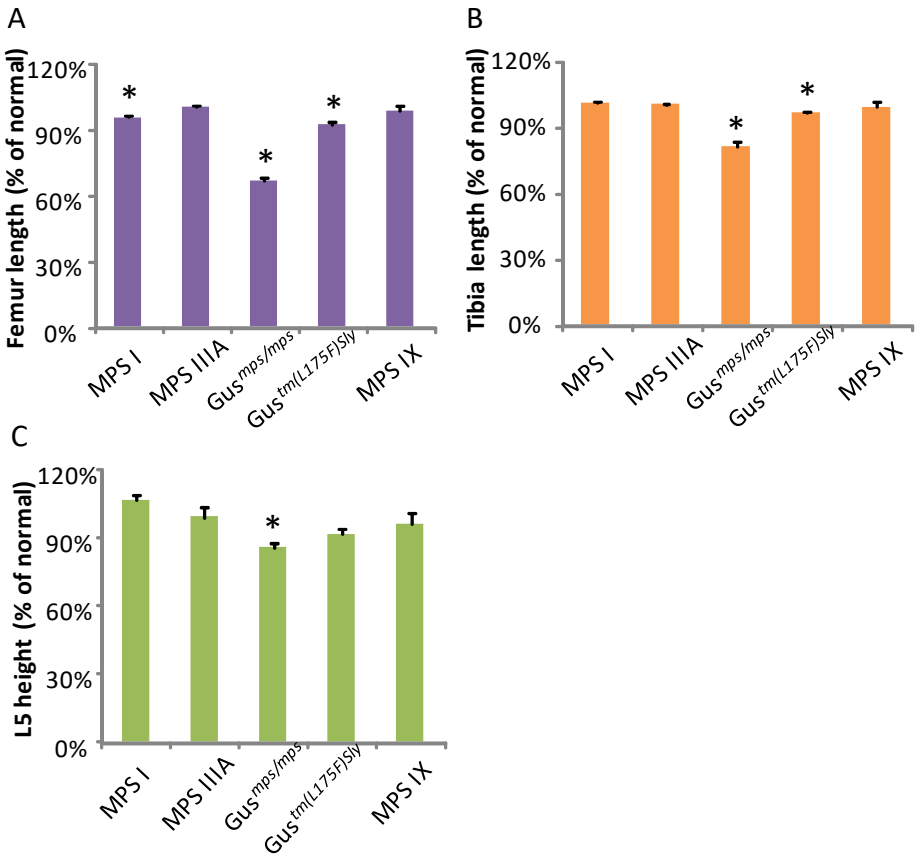

Figure 3.1 Mature bone length of MPS murine models. Femur (A) and tibia length (B) and L5 vertebrae height (C) presented as a percentage of age-matched normal bone length in MPS I, IIIA, MPS VII ($Gus^{mps/mps}$), MPS VII mice ($Gus^{tmSly(L175F)}$) and MPS IX mice at 6-month of age. Results are expressed as the mean ± S.E.M. The number of animals used was listed in Table B1 of Appendix B.

* denotes a significant difference to normal mice ($p<0.05$, Student's t-test).

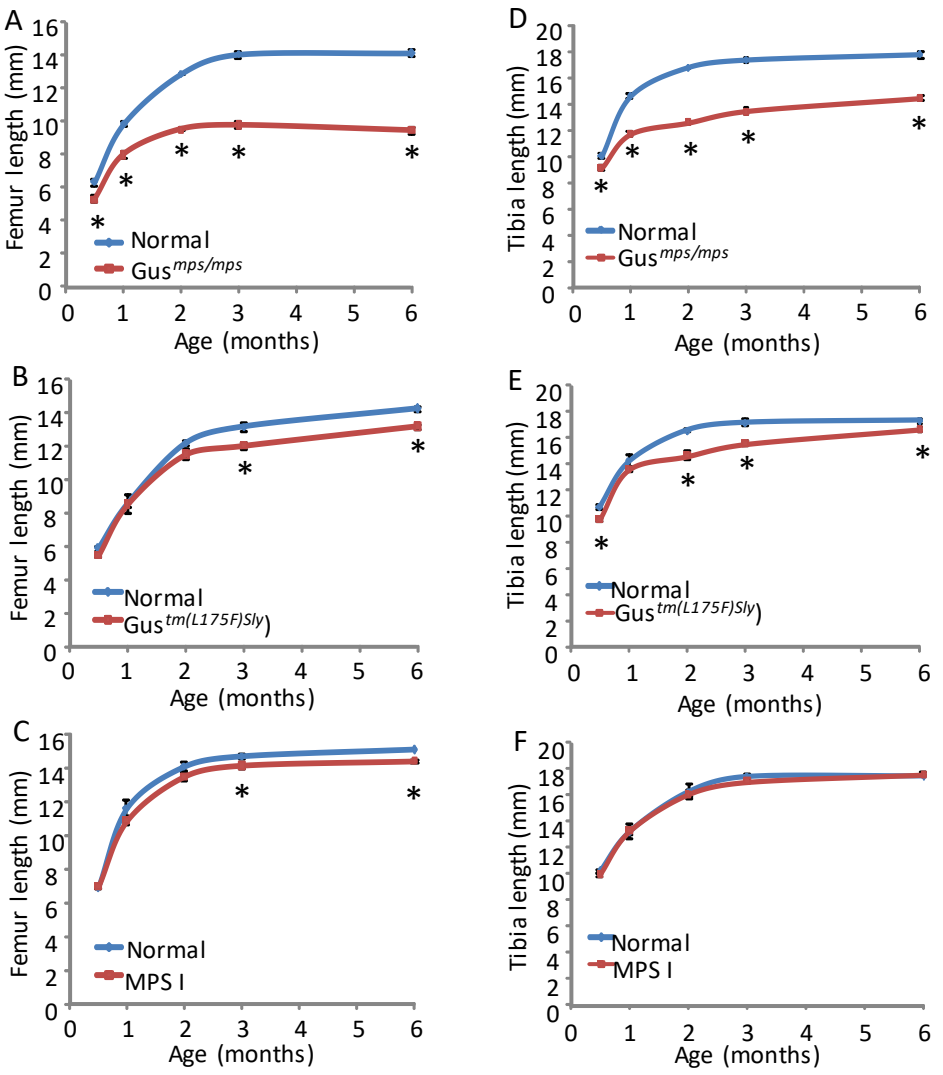

G

	Femur growth rate		Tibia growth rate	
	0.5-1m	1-2m	0.5-1m	1-2m
$Gus^{mps/mps}$	77±7%*	50±2.5%*	57±6%*	39±5%*
$Gus^{tm(L175F)Sly}$	130±6%	83±9%	107±4%	61±3%*
MPS I	84±6%	107±9%	110±5%	93±9%

Figure 3.2 Quantitative analysis of longitudinal bone growth in MPS murine models.

Femur (A-C) and tibia (D-F) length in MPS I, MPS VII ($Gus^{mps/mps}$) and MPS VII mice ($Gus^{tmSly(L175F)}$) from P14 to 6 months of age. (G) Growth rate (% of normal) of MPS mice during P14 to 1 and 1 to 2 months of age. Mean ± S.E.M. The number of animals used was listed in Table B1 of Appendix B.

* denotes significant difference to normal mice ($p<0.05$, Student's t-test).

3.3 MPS VII epiphyseal and diaphyseal morphology during embryonic and early postnatal stages

3.3.1 MPS VII mice exhibit delayed endochondral bone formation and thickened growth plate

Bone length was already significantly reduced in MPS VII (*Gus*$^{mps/mps}$), hereafter referred to as MPS VII mice, at 14 days of age (Figure 3.1A and D) To gain insights into the differences in bone development between normal and severe MPS VII mice, safranin-O/fast green stained sections of proximal tibiae (Chapter 2.3.2) were assessed from embryonic stage E12.5-17.5, (Figure 3.3A) to postnatal 6 months (Figure. 3.3C). Between E12.5 to E13.5, mesenchymal condensation to chondrocytes in the presumptive tibia was observed (Figure. 3.3A and B). One day after, chondrocytes became hypertrophic at the site of the future POC. Sections through the tibia of MPS VII mice showed no apparent difference in morphology from the normal control up to E14.5.

In normal mice, marrow elements were observed in the central area in 10/13 (77%) of normal tibia by E15.5, when the POC and bone collar are first observed. The marrow cavity and central bone elements continued to expand until E18.5 when the POC was fully developed (Figure 3.3A, E18.5). Flattened chondrocytes appeared at E15.5, and the columnar structure of proliferating and hypertrophic chondrocytes were clearly observed by E18.5 in the growth plate (Figure 3.3C). In contrast, formation of the primary centre of ossification was delayed in approximately 67% of MPS VII tibiae (deposition of marrow cavity observed in 4 out of 12 MPS VII mice, while hypertrophic chondrocytes still present in the diaphysis of 8 out of 12 MPS VII mice) at E15.5 (Figure. 3.3A). The morphology of chondrocytes in the growth plate were similar to the normal controls at this stage (Figure. 3.3C). A marrow cavity containing bone elements was observed in all MPS VII tibiae at E16.5 (Figure 3.3A), suggesting formation of the POC in prenatal MPS VII tibiae appeared

one day later than the normal controls. Flattened proliferating chondrocytes and enlarged hypertrophic chondrocytes with poor columnar arrangement were observed in MPS VII epiphysis at E18.5 (Figure 3.3C). While the POC continued to expand accompanied by longitudinal bone growth in both normal and MPS VII tibia during the remainder of the embryonic and early postnatal period, the MPS VII metaphysis was consistently shorter than normal mice.

In the normal tibia, hypertrophic chondrocytes were observed in the future SOC at P7. Bone marrow cells appeared in the proximal epiphyseal cartilaginous region of normal tibia by P10 (Figure. 3.4A). Hypertrophic chondrocytes were also observed in the MPS VII tibiae at P7 but a distinguishable SOC was not observed at P10 (Figure 3.4A). A large invasion of bone marrow cells into the SOC region occurred in normal tibial epiphyses by P11. In contrast, formation of SOC was delayed in approximately 83% of MPS VII mice (observed in 5 out of 6 MPS VII mice). Formation of the SOC did initiate in 17% of MPS VII mice at this age and all MPS VII mice showed evidence of bone deposition in the SOC by P12 (Figure 3.4A). Expansion of the SOC in MPS VII mice was less than that of normal at P14 and 2 months of age (Figure 3.4A) and occupied 10.0±2.7% and 42.0±3.0% of the total epiphyseal area respectively (Figure 3.4B). Despite the delay, there was a change of the shape of the SOC from spherical to hemispherical in both normal and MPS VII epiphysis as mice aged.

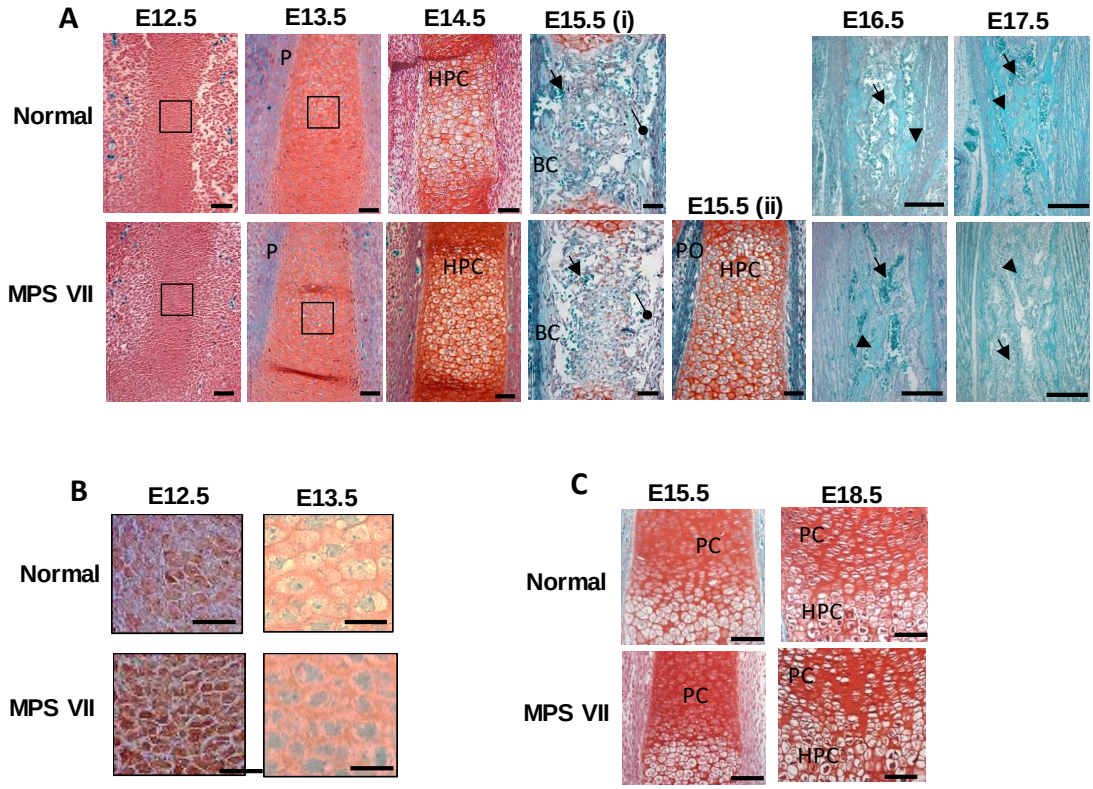

Figure 3.3: Formation of the POC and growth plate in the embryo. Sagittal sections of the tibial POC were stained with safranin O/fast green and an image taken at the mid-anlage/diaphyseal region (A). At E15.5 an example of an MPS VII tibia with a POC (E15.5(i)) and an MPS VII tibia with no evidence of POC formation (E15.5 (ii)) is shown. A higher magnification of the boxed area at E12.5 and E13.5 is shown in (B). Safranin O/fast green stained sections showing the proximal tibial growth plate (C). Scale bar=100 µm in A and C. Scale bar = 20 µm in B. P= perichondrium, HPC = hypertrophic chondrocytes, BC = bone collar, PO = periosteum, PC = proliferative chondrocytes. Black arrow = bone marrow, oval arrow = blood vessel, arrow head = bone. The number of animals used was listed in Table B2 of Appendix B.

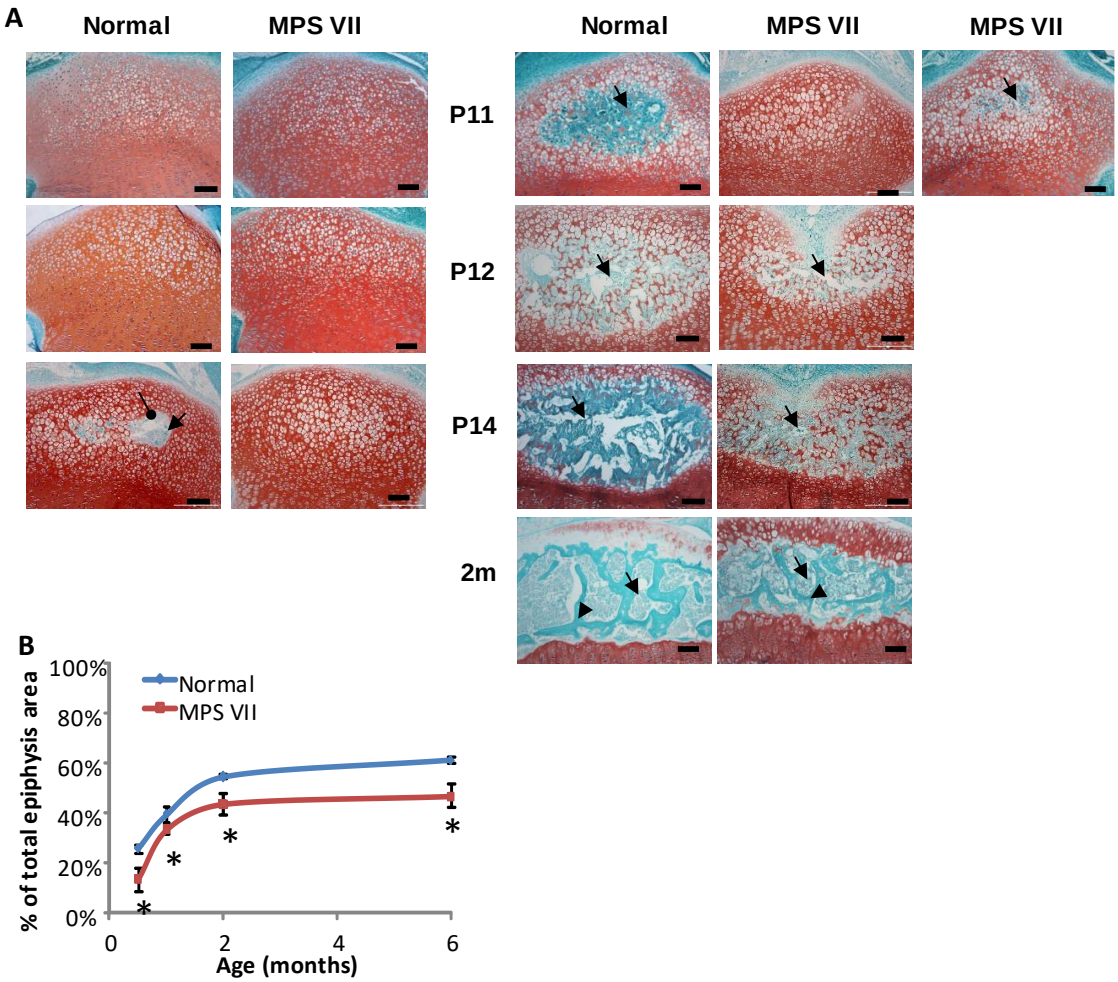

Figure 3.4 Formation of the SOC and expansion of the growth plate in the postnatal tibia. Sagittal sections through the proximal tibial epiphysis were stained with safranin O/fast green and showed the formation of the SOC (A). Scale bar=100 µm. At P11, two phenotypes of MPS VII epiphysis were shown, representing the absence of the SOC (middle) and presence of the SOC (right) in epiphysis of MPS VII mice. Black arrow, bone marrow. Oval arrow, blood vessel. Arrow head, bone. Quantitative analysis of the area of the proximal tibial epiphysis occupied by SOC (C). Mean ± S.E.M. The number of animals used was listed in Table B2 and B4 of Appendix B.

* denotes a significant difference to normal mice ($p<0.05$, Student's t-test).

3.3.2 MPS VII mice have lengthened RZ and HZ in the tibia growth plate

Histological analyses of MPS proximal tibia sections (Chapter 2.3.2) revealed an abnormal growth plate in MPS VII mice (Figure 3.5A). The growth plate was enlarged, especially in the RZ, and columnar arrangement of the chondrocytes was disrupted in severe MPS VII ($Gus^{mps/mps}$) mice. Attenuated MPS VII mice ($Gus^{tmSly(L175F)}$) also displayed a thickened growth plate with a slightly disorganized structure, while MPS I tibial growth plate was comparable to normal mice.

By P14 it was clear that the growth plate in MPS VII mice was abnormally enlarged with a larger RZ and HZ. While PZ chondrocytes lined up in long columns in the normal mice, MPS VII chondrocytes lost their columnar arrangement in the PZ (Figure. 3.5B). To further confirm the observed differences and gain a detailed understanding of the abnormalities in MPS VII growth plate morphology, growth plate zone height, the number of chondrocytes and lacunae size of the three distinct zones (the RZ, PZ and HZ) were quantified (Chapter 2.3.3).

Total growth plate height declined with age in both normal and MPS VII mice (Figure 3.6A). However, total growth plate height in MPS VII mice was significantly higher from 1 month of age onwards ($p<0.05$) than normal mice. Measurement of individual growth plate zone heights were carried out in mice of P14, 1 month and 2 months only, as individual zones were difficult to distinguish in older animals. A significant higher RZ height ($p<0.05$) was observed in MPS VII mice at all time points when compared to normal (Figure 3.6B). There were no statistically significant changes in the growth plate RZ height between different time points in the normal mice; however, the RZ height of growth plate significantly increased between 1 and 2 months in MPS VII mice ($p<0.05$). The heights of the PZ were unchanged from normal in MPS VII mice (Figure 3.6C). The PZ of the growth plate became thinner in both normal and MPS VII mice as they aged ($p<0.05$). MPS VII HZ

height was significantly lower than normal controls at P14, the same as normal at 1 months of age and significantly higher than normal at 2 months of age ($p<0.05$) (Figure 3.6D). While the height of the HZ of normal mice tibial growth plate significantly decreased with age ($p<0.05$), no significant changes in MPS VII growth plate HZ height were observed between different time points.

3.3.3 Enlarged chondrocytes due to lysosomal storage

The horizontal diameter of lacunae in the growth plate were measured to compare the size of normal and MPS VII chondrocytes (Chapter 2.3.3). MPS VII chondrocytes were significantly larger than normal chondrocytes (Figure 3.7A) in the RZ at P14, 1 month and 2 months of age. PZ chondrocytes were elongated only at 1 month of age in MPS VII growth plate (Figure 3.7B). HZ chondrocytes in MPS VII growth plate enlarged horizontally from 1 month of age onwards (Figure 3.7C). TEM observations (Chapter 2.4) clearly revealed enlarged and vacuolated chondrocytes in the RZ of MPS VII mice (Figure 3.7D). MPS VII PZ chondrocytes had condensed nuclei, with accumulated storage of GAGs inside the cells. Similar vacuolated structure was observed in the HZ of MPS VII growth plate.

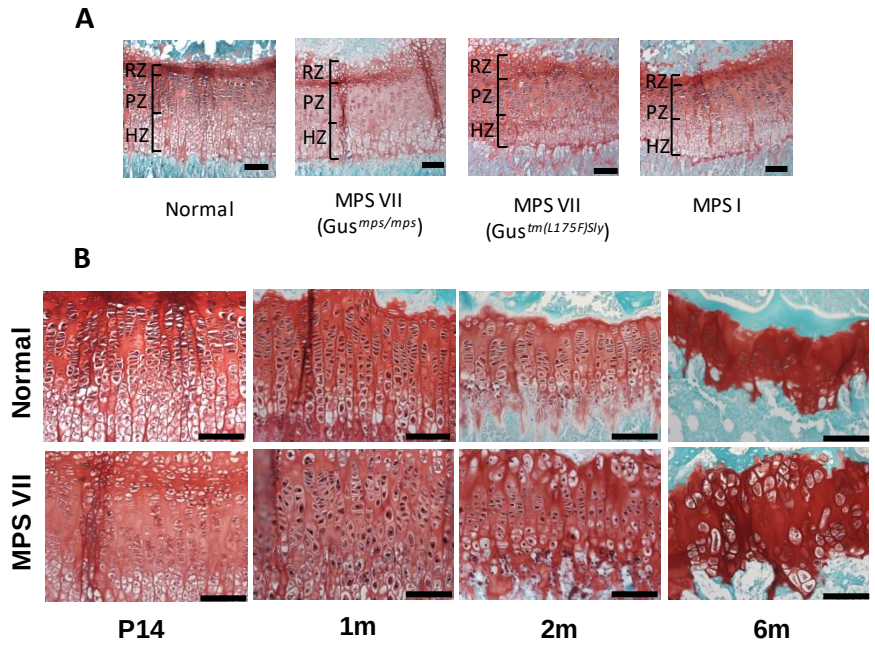

Figure 3.5 Histology of the growth plate in normal and MPS mice. Sagittal sections through (A) the proximal tibial growth plate of normal, MPS VII (Gus$^{mps/mps}$), MPS VII mice (Gus$^{tm(L175F)Sly}$) and MPS I at P14. (B) the proximal tibial epiphysis showed the development of the growth plate in normal and MPS VII mice from P14 to 6 months. Sections were stained with safranin O/fast green. The number of animals used were listed in Table B3 of Appendix B. Scale bar= 100µm.

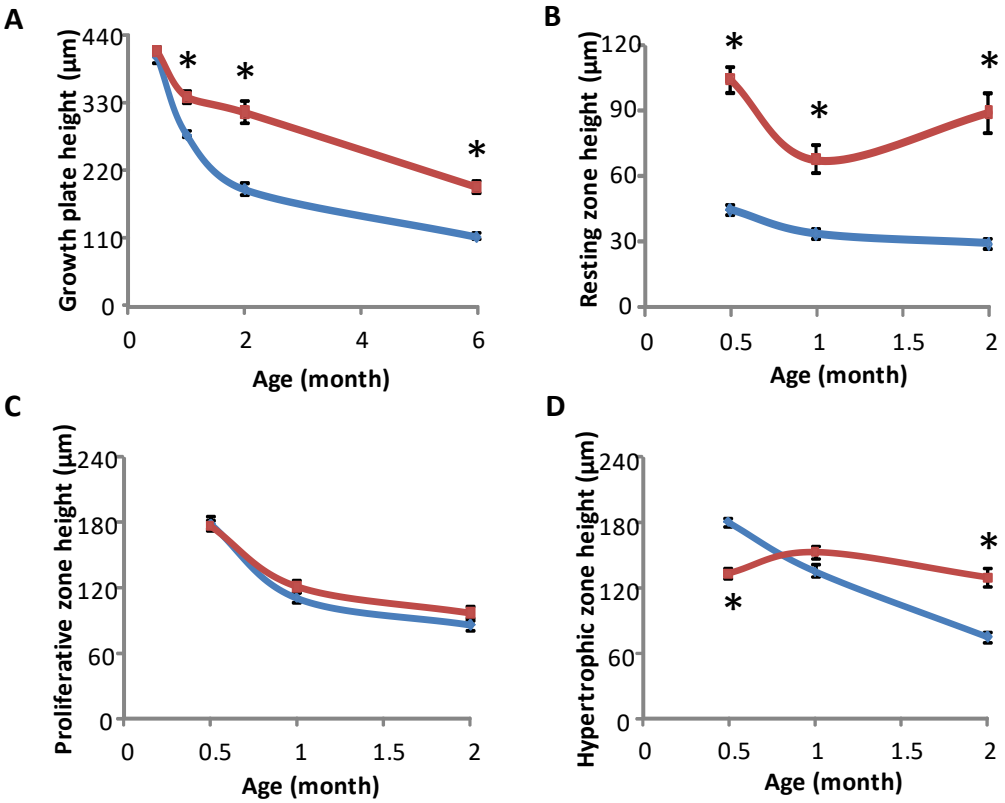

Figure 3.6 Histomorphometric analysis of the growth plate in normal and MPS VII mice. Quantitative analyses of (A) total height, (B) resting zone height, (C) proliferative zone height, and (D) hypertrophic zone height of the growth plate in normal and MPS VII mice from P14 to 2 months. Mean ± S.E.M. The number of animals used were listed in Table B3 of Appendix B.

* denotes a significant difference to normal ($p<0.05$, Two-way ANOVA, Tukey's post-hoc test).

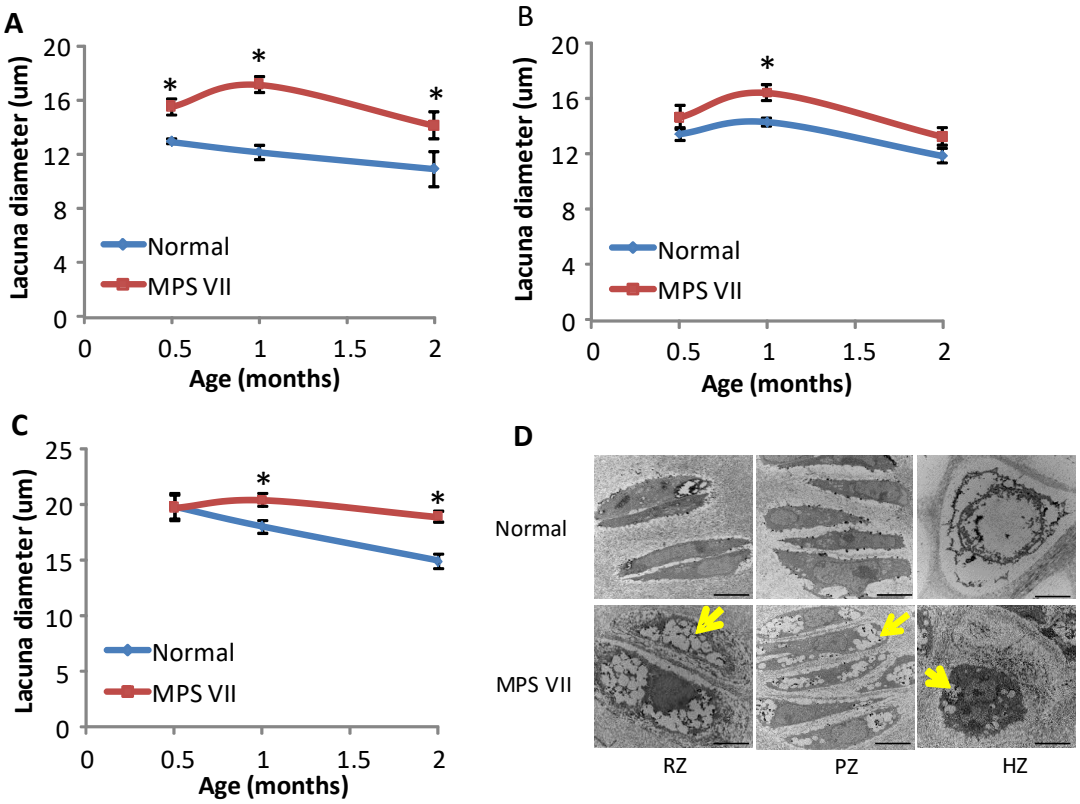

Figure 3.7 Chondrocyte size and GAG storage in the growth plate. Chondrocyte size in the (A) resting zone (RZ), (B) proliferative zone (PZ) and (C) hypertrophic zone (HZ) of the growth plate in 2 months old normal and MPS VII mice. Results are expressed as the mean ± S.E.M. The number of animals used were listed in Table B3 of Appendix B. TEM (D) of chondrocytes of RZ, PZ and HZ of P14 normal and MPS VII growth plate. Yellow arrow, lysosomal storage. Scale bar = 5 µm.

* denotes significant difference between normal and MPS VII ($p<0.05$, Two-way ANOVA, Tukey's post-hoc test).

3.4 Decreased number of PZ chondrocytes is not due to apoptosis in the MPS VII growth plate

In the RZ, no difference in the cell number (Chapter 2.3.3) was observed between normal and MPS VII mice at P14 and 1 month of age (Figure 3.8A). However, at 2 months of age, a significant increase in the number of cells per mm^2 was observed in MPS VII mice (2471±118 cells/mm^2) compared to normal mice (1600±157 cells/mm^2; $p<0.05$). The number of chondrocytes in the PZ of normal mice tended to be consistent with ages, while cell number in the proliferating zone of MPS VII mice decreased with age and was significantly reduced compared to normal (Figure 3.8B; $p<0.05$). The number of cells in the HZ of normal mice increased with age (Figure 3.8C). More hypertrophic cells were observed in MPS VII mice (2623±72 cells/mm^2) at P14 when compared to normal mice (2255±55 cells/mm^2; $p<0.05$), while MPS VII mice had fewer hypertrophic cells (2152±85 cells/mm^2) at 2 months of age when compared to normal mice (2935±93 cells/mm^2; $p<0.05$).

To determine whether the changes in cell number in the growth plate of MPS VII mice are the result of increased apoptosis, the expression of apoptosis associated genes was evaluated by real-time PCR analysis (Chapter 2.9). *Bcl2* expression was also elevated significantly in MPS VII growth plate; however, the ratio of *Bcl/Bax* was not significantly different from normal (Figure 3.9A). Expression of *FasL* was absent from both normal and MPS VII growth plate, while expression of *FasR* was slightly increased without reaching statistical significance. *Casp3* expression was significantly increased in the whole growth plate of MPS VII mice (Figure 3.9B, $p<0.05$), which was confirmed by increased immunostaining of uncleaved Caspase3 in the MPS VII growth plate when compared to normal mice (Figure 3.9C). However, the expression of cleaved/activated Caspase 3 was absent from both normal and MPS VII growth plate, suggesting that growth plate chondrocytes was were not undergoing apoptosis.

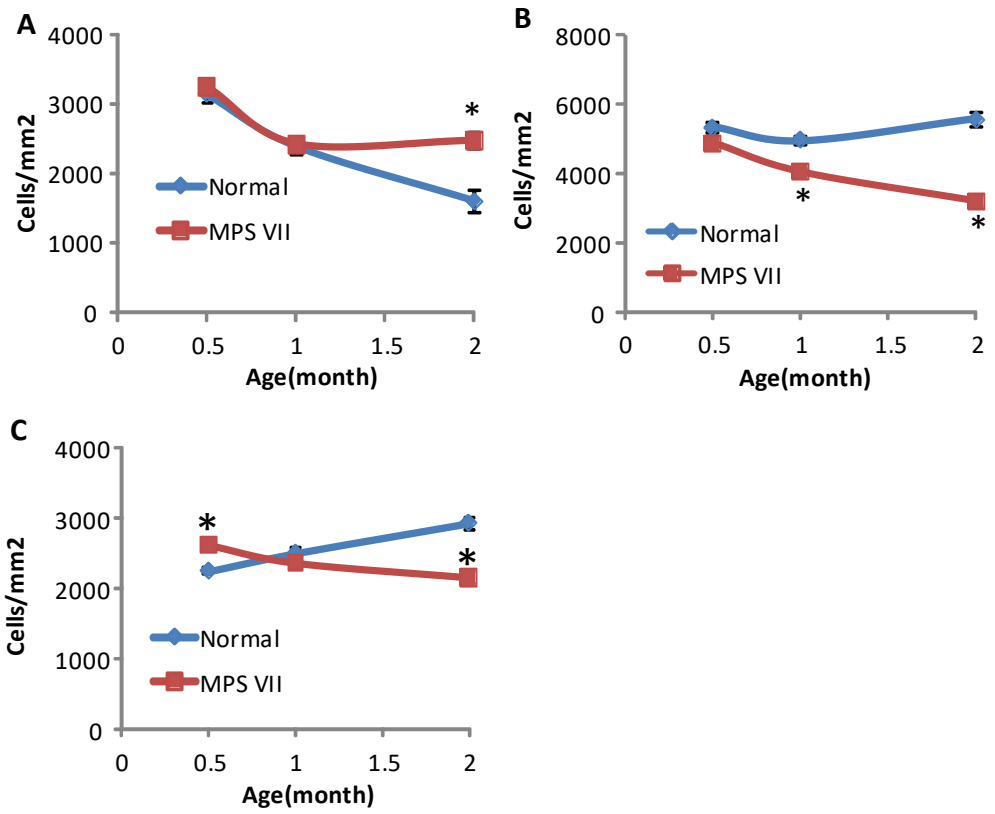

Figure 3.8 The number of chondrocytes in the growth plate of normal and MPS VII mice. The number of chondrocytes in the (A) resting zone, (B) proliferative zone and (C) hypertrophic zone of normal and MPS VII mice aged P14 to 2 months. Results are expressed as the mean ± S.E.M. The number of animals used were listed in Table B3 of Appendix B.

* denotes significant difference between normal and MPS VII ($p<0.05$, Two-way ANOVA, Tukey's post-hoc test).

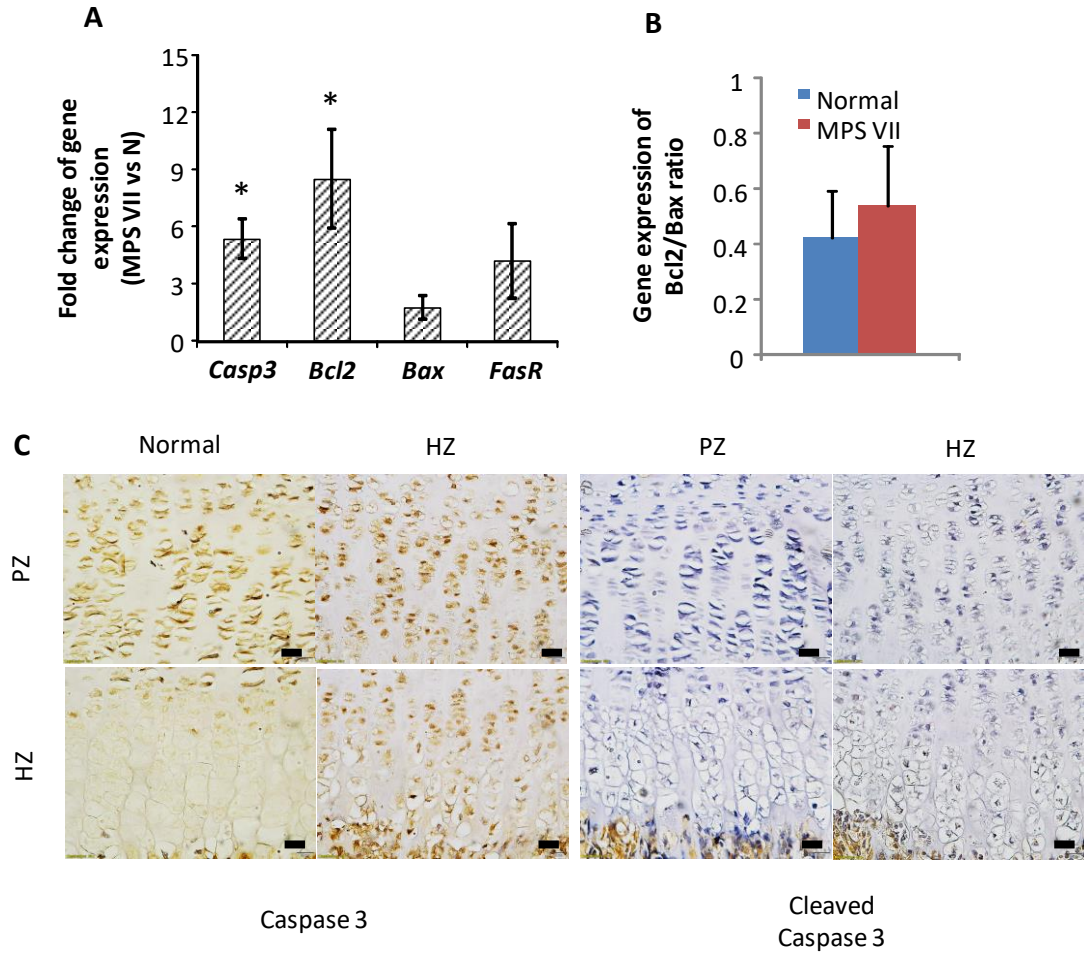

Figure 3.9 Apoptosis in the growth plate of normal and MPS VII mice. (A) Gene expression of *Caspase 3*, *Bcl2*, *Bax* and *FasR* in P14 MPS VII growth plate was expressed as the fold change compared to normal growth plate. Gene expression was normalized to *cyclophilin A* and the fold change in the expression of genes from MPS VII growth plate compared to normal growth plate was calculated using the ΔΔCt method of n=5 replicates. (B) Ratio of *Bcl2/Bax* gene expression in P14 normal and MPS VII growth plate. (C) Immunohistochemistry of Caspase 3 and cleaved Caspase 3 was determined in P14 normal and MPS VII proximal tibia. Results are expressed as the mean ± S.E.M. of n=3 replicates. Bar scale = 20 µm.

* denotes significant difference between normal and MPS VII ($p<0.05$, Student's t-test).

3.5 Discussion

Bone elongation is severely compromised in patients with MPS I (Neufeld & Muenzer 2001; Rozdzynska-Swiatkowska et al. 2015), II (Rozdzynska-Swiatkowska et al. 2015), IVA (Montaño et al. 2008), IVB (Kubaski et al. 2016), VI (Neufeld & Muenzer 2001) and VII (Montano et al. 2016; Sly et al. 1973)). Growth retardation of MPS patients starts in early childhood and becomes progressively worse with age (Montaño et al. 2008; Neufeld & Muenzer 2001) as GAG accumulates in connective and skeletal tissues. GAG storage is observed in chondrocytes and osteoblasts of foetal MPS VII mice at 15 days post cotium (dpc) and 18 (dpc) respectively (Vogler et al. 2005). However, it is unknown how this early storage impacts cartilage and bone development. The purpose of this chapter was to determine which murine model best reproduces the reduced bone length phenotype of human MPS and to use this model to characterise tibial development from the foetus to skeletal maturity.

Initial evaluation of long bone and vertebral lengths at maturity showed that bone length in mouse models of MPS IIIA, MPS VII ($Gus^{mps/mps}$), MPS VII ($Gus^{tm\ (L175F)Sly}$) and MPS IX paralleled the corresponding human disorders (Fischer et al. 1998; Imundo et al. 2011; Natowicz et al. 1996; Neufeld & Muenzer 2001). Much like humans with MPS IIIA or MPS IX and other MPS IIIA animal models (Fischer et al. 1998; Imundo et al. 2011; Natowicz et al. 1996; Neufeld & Muenzer 2001), the lengths of bones in murine MPS IIIA and MPS IX were not pronouncedly different to normal mice at maturity. Long bone and vertebral growth was most severely affected in the severe MPS VII ($Gus^{mps/mps}$) mouse model, which exhibited shortened bones from a very young age. Bone length discrepancies in murine $Gus^{mps/mps}$ are consistent with human (Montano et al. 2016; Sly et al. 1973), canine (Herati et al. 2008; Smith, LJ et al. 2012) and feline MPS VII (Fyfe et al. 1999; Wang, P et al. 2015). Mice with the attenuated form of MPS VII ($Gus^{tm(L175F)Sly}$) also displayed significantly

decreased lengths of femur and tibia (but not vertebral) bones, but the discrepancy compared to normal mice was less than that observed in the $Gus^{mps/mps}$ strain. Unlike the $Gus^{mps/mps}$ strain, femur lengths were not significantly different to normal mice at younger ages in the $Gus^{tm(L175F)Sly}$ strain. The L175F mutation in murine MPS VII is analogous to the L176F mutation that affecting 20% of MPS VII patients who display a mild phenotype (Tomatsu et al. 2002; Wu, BM et al. 1994). In contrast, bone length in the murine MPS I model did not represent human MPS I (Neufeld & Muenzer 2001; Silveri et al. 1991). Only the femur was modestly shortened in murine MPS I at older ages (3 and 6 months of age). Tibia lengths were relatively normal at all ages. These are in agreement with previous study that long bone lengths (tibia and humerus) in MPS I mice at 8 months of age were relatively normal, except for a modest reduction in femur lengths in females (Liu, Y et al. 2005). Bone lengths of canine MPS I (Herati et al. 2008) are not significantly different to normal controls, and feline MPS I models (Haskins et al. 1983) had no obvious dwarfism.

The discrepancy of bone shortening between the three mouse models (MPS VII ($Gus^{mps/mps}$), MPS VII ($Gus^{tm\ (L175FSly)}$) and MPS I) may be attributed to the fact that growth plate is much more impaired in severe MPS VII mice than the others (Figure 3.5A). The severity of growth plate dysfunction in MPS is probably affected by residual enzyme activity. GAG has been shown to dramatically accumulate due to the deficiency of β-glucuronidase in the growth plate of MPS VII animals (Metcalf et al. 2009). The $Gus^{mps/mps}$ mice had 0.34-1% normal β-glucuronidase activity (Birkenmeier et al. 1989; Macsai et al. 2012; Vogler et al. 1990). This theory can be supported by observations in other MPS animal models. MPS VII dogs and cats, which have severely shortened bones, have approximately 0.2% and 0% of normal β-glucuronidase activity, respectively (Schuchman et al. 1989; Wang, P et al. 2015). As the $Gus^{tm(L175F)Sly}$ mice have 1% normal β-glucuronidase activity (Derrick-Roberts et al. 2014; Tomatsu et al. 2002), this lead to less accumulated GAGs, resulting in a less severely disorganized growth plate (Figure 3.5A) and less shortened long bones (Figure 3.2B & E).

In contrast, the enzyme activity of *α-L*-iduronidase in MPS I dogs and cats, whose bone length are relatively normal, were approximately 4% and 2.4% of normal, respectively, compared to <1% in human MPS I (Bunge et al. 1998; Herati et al. 2008; Oussoren et al. 2013; Traas et al. 2007). Therefore, it is likely that MPS VII animals have more severely shortened bone growth than MPS I animals because MPS VII animals have less enzyme activity. However, MPS I mice had approximately 0.2% of normal *α*-L-iduronidase enzyme activity (Clarke, LA et al. 1997; Liu, Y et al. 2005), and with this residual enzyme activity it would be expected to display a bone length phenotype closer to human MPS I. At present, there is no explanation for the discrepancy in bone length phenotype between murine and human MPS I.

Among the three mouse models with bone length deficits, the reduction in femur length tended to be more severe that in the tibia, especially for MPS I whose femur was significantly shortened while the tibia was relatively normal at maturity. During pregnancy the femur growth rate is higher than that in the tibia; while after birth the tibia has the highest grow rate compared to other limbs in mice (Patton & Kaufman 1995). The 'overtake' nature of tibia growth may therefore contribute to the observed difference of bone shortening between femur and tibia.

The naturally occurring MPS VII ($Gus^{mps/mps}$) mouse model exhibited the most severe bone shortening phenotype, which replicates the pathology observed in human patients (Neufeld & Muenzer 2001; Sly et al. 1973), making it an ideal model for investigating the pathology of bone defects in MPS. The results of this chapter are consistent with a single study of bone shortening in MPS VII mice (Metcalf et al. 2009), and extends this observation to a comparison of the time course of EO progression in MPS VII mice to normal mice. Histological analyses suggested that the conversion from cartilage to bone during EO was delayed in MPS VII mice. The time of first appearance of POC in the normal tibia was at

E15.5, which is consistent with previous studies (Dao et al. 2012; Patton & Kaufman 1995; Wang, Y et al. 2015). It is notable that MPS VII hindlimbs showed some variations in the initiation of POC from one embryo to another. Initiation of the POC was not observed in approximately 67% of MPS VII mice at E15.5 but was observed in all MPS VII mice at E16.6, suggesting that MPS VII mice have a slower development of the POC than that of normal mice.

The SOC of normal mouse tibia formed at around P10. In MPS VII mice, the development of the SOC was delayed by approximately two days. Prenatally hypertrophic chondrocytes trigger invasion of blood vessels, bone cells and bone marrow cells from the perichondrium to direct matrix mineralization and differentiation of perichondrial cells to osteoblasts (Carlevaro, M. F. et al. 2000; Long 2012; Takahara et al. 2004). Postnatal formation of the SOC is similar to the formation of the POC, but its establishment involves formation of cartilage canals (Burkus, Ganey & Ogden 1993; Wang, Y et al. 2015). In this chapter, the delayed POC and SOC appearance in MPS VII suggested that there was a defect during the conversion from cartilage to bone, which maintained the chondrocytes in a hypertrophic state, thus possibly delaying the degradation of cartilage matrix and invasion of blood vessels.

Growth plate height in normal mice decreases with age as bones grow in length. However, total growth plate height in MPS VII mice was significantly higher than normal from 1 month of age onwards. Although decrease of the growth plate height still occurred in MPS VII mice, the process appeared to be slower than normal, leaving a thicker than normal growth plate at maturity, which was consistent with previous observation of thickened growth plates in MPS VII feline and MPS I murine model (Nuttall et al. 1999; Russell et al. 1998). The thickened growth plate is possibly the result of an impaired conversion of

chondrocytes from resting to proliferation and from hypertrophic to bone, as the RZ and HZ of MPS VII were greatly enlarged in the growth plate.

The RZ in MPS VII growth plate was significantly enlarged, accompanied with elevated number, size and density of chondrocytes. Consistently, increased zone height and enlarged cells were also observed in the RZ of MPS VI cat tibia growth plate (Abreu et al. 1995; Nuttall et al. 1999). These anomalies suggested the transition of chondrocytes from the resting to the proliferative stage (Abad et al. 2002) would be limited. TEM observations suggested that the enlarged chondrocytes in the RZ was due to accumulation of storage inside the cells (Figure 3.7D). However, it is still not clear whether accumulation of storage in the MPS VII RZ chondrocytes prevent them from progressing to proliferation.

Chondrocyte proliferation and hypertrophy both contribute to linear bone growth. Decreased or delayed chondrocyte proliferation in the growth plate therefore may lead to shortened bones. In MPS VII mice, the PZ height and size of PZ chondrocytes were not significantly different to normal mice; however, a marked decrease in the number of cells was observed, which was consistent with previous findings that the number of chondrocytes per column in the PZ of 3 weeks old MPS VII mice decreased to approximately 60% of normal (Metcalf et al. 2009). Early cell death caused by increased apoptotic activity may cause the decrease in the number of proliferative chondrocytes. Apoptosis in the cartilage is induced by activation of Caspase 3 (Matsuo et al. 2001). The balance between *Bax* and *Bcl2* levels and the *FasL/FasR* system can also determine the fate of cells in cartilage (Ju et al. 1995; Oltvai, Milliman & Korsmeyer 1993). These results suggested that the decrease in MPS VII PZ chondrocytes is not due to increased apoptosis but is due to a decreased proliferation rate in the affected growth plate (Metcalf et al. 2009).

At the end of chondrocyte hypertrophy, chondrocytes progress to cell death and the matrix becomes mineralized and converted into bone. In MPS VII mice, HZ height remained

constant over the time points, while it decreased with age in normal mice. MPS VII HZ chondrocytes had increased chondrocyte size but decreased cell number. The constant zone height observed in the HZ suggested that MPS VII mice tend to maintain the growth plate chondrocytes in the hypertrophic state, delaying the maturation of chondrocyte and progression into bone. These findings are consistent with previous observations in MPS VI cats and rats that the HZ height and chondrocyte size were significantly increased as compared to age-matched normal (Abreu et al. 1995; Nuttall et al. 1999) and was accompanied by a decrease in the HZ cell number (Simonaro et al. 2005). The decreased number of chondrocytes undergoing hypertrophy in MPS VII growth plate may also be attributed to a delay in the transition of chondrocytes from proliferating to hypertrophic state in MPS.

In summary, this chapter has demonstrated that murine MPS VII mouse models, especially the severe strain ($Gus^{mps/mps}$), provide good representations of short stature similar to patients with MPS. Findings of morphological abnormalities in MPS VII growth plate suggested a progressive defect in bone development that is caused by the delay of the programmed EO in the growth plate. The transition steps includes (i) the initiation of proliferation, which requires strictly regulated cell cycle progression (ii) cessation of proliferation which is mediated through the withdrawal from the cell cycle accompanied by hypertrophic differentiation, and (iii) blood vessel invasion preceding bone deposition. Programmed proliferation and hypertrophic differentiation of chondrocytes require strictly regulated cell cycle progression and the guidance of signalling pathways involving endocrine, and paracrine/autocrine factors. Therefore, the delay observed during the transition steps of EO in MPS VII growth plate could be due to disruptions of the cell cycle progression and/or dysfunction of signalling pathways. In the next chapter, cell cycle progression of MPS VII chondrocytes in the growth plate will be discussed in detail.

4 Normal cell cycle progression is disrupted in MPS VII growth plate chondrocytes

4.1 Introduction

Growth of endochondral bone proceeds through a strict temporal and spatial sequence of events as growth plate chondrocytes divide, synthesize matrix, and undergo hypertrophic differentiate in order to create an environment suitable for new bone deposition (Byers et al. 1992; Byers et al. 1997; Gibson & Flint 1985). Central to this process is the synchronized entry into and exit out of the cell cycle by growth plate chondrocytes in order to initiate proliferation and subsequent hypertrophic differentiation. The time chondrocytes spend on completing a cell cycle varies in growth plates growing at different rates, leading to the differential growth of long bones (Wilsman et al. 1996). Chondrocytes in growth plates that grow slowly spend a longer time in the G1 phase of the cell cycle. DNA replication, or S phase, predominately occurs in the PZ of the growth plate. Chondrocytes in the PZ pass through the G2 phase and progress through the M phase rapidly for division. Chondrocytes positioned proximally in a column seem to have a higher probability of division than those positioned distally (Farnum & Wilsman 1993). Transition of proliferative chondrocytes to terminal differentiation occurs predominately in the pre-HZ. The decisions of whether a chondrocytes progress through the cell cycle to divide again or alternatively exit the cell cycle are made during the G1 phase (Zetterberg & Larsson 1985). Upregulation of CKIs ensures chondrocytes withdrawal from the cell cycle during this step. Therefore, the appropriate level and timing of expression of proteins including cyclins, CDKs, E2F, pocket proteins and CKIs in the chondrocytes are essential for normal endochondral bone growth.

Although several studies have shown disruption of the cell cycle genes that govern transition from G1 to S phase result in shortened bones (Cobrinik et al. 1996; Lee, MH et al. 1996; Zhang, P et al. 1997), the status of cell cycle progression in MPS growth plate has not been investigated. This chapter therefore aimed to investigate the regulation of EO through cell

cycle progression in MPS VII mice. The hypothesis of this chapter is that the synchronised entry and exit from the cell cycle are disrupted in MPS VII growth plate.

4.2 More MPS VII chondrocytes were in the G1 phase and committed to enter S phase

Cells throughout the normal growth plate were positive for Ki67 antigen, a marker for all active phases of the cell cycle (Figure 4.1A). The number of cells positive for Ki67 in the MPS VII growth plate was greater than normal in the PZ (Figure. 4.1B) (175.0±13.7% of normal, $p<0.05$) and HZ (251.5±36.1% of normal, $p<0.05$), respectively, suggesting more MPS VII chondrocytes were in the cell cycle.

Cells positive for Cyclin D1 were observed predominantly in the early (upper cells in the columns) PZ of normal growth plate and to a lesser extent in the RZ, while HZ chondrocytes were negative for Cyclin D1 (Figure 4.1C). In MPS VII, higher but not statistically significant levels of Cyclin D1 staining was observed in the RZ and PZ of the growth plate. In contrast to normal, the number of cells stained positive for Cyclin D1 were also observed in the late (lower cells in the columns) PZ and HZ of MPS VII growth plate. In the HZ, 6.8±1.6% of MPS VII chondrocytes were positive for Cyclin D1 (Figure. 4.1D, $p<0.05$), indicating these cells were still in G1 phase.

Cells positive for pocket protein phos-pRb were mainly observed in the normal RZ and PZ, with limited positive staining observed in the HZ (Figure. 4.2A&B, $p<0.05$). While in MPS VII, the number of chondrocytes positive for phos-pRb was increased in the HZ (Figure 4.2B, 387.1±46.9% of normal, $p<0.05$), suggesting that dephosphorylation of pocket proteins for cell cycle withdrawal was limited in MPS VII HZ chondrocytes. Cells positive for phso-p130, were observed throughout the normal growth plate (Figure. 4.2C). In MPS VII growth plate, the number of cells positive for phos-p130 in the three zones was not

significantly different to that of normal (Figure. 4.2 C&D). The expression of phosphorylated p107 was not observed in the growth plate region of either normal or MPS VII mice (data not shown).

E2F1, the activator E2F protein essential for G1 to S phase transition, was mainly observed in the RZ and early PZ chondrocytes of normal growth plate (Figure. 4.3A&B, $p<0.05$), and to a significantly lesser extent by the HZ chondrocytes, especially in the pre-HZ region. However, the number of cells stained positive for E2F1 in the MPS VII growth plate were significantly increased to 123.8±14.2%, 170.3±13.0%, 279.6±9.1% of normal in the RZ, PZ and HZ, respectively (Figure. 4.3B, $p<0.05$). The staining of E2F1 in the MPS VII growth plate was not limited to early PZ chondrocytes and pre-HZ chondrocytes but was also observed in late PZ and late HZ chondrocytes (Figure 4.3A).

E2F4, the most abundant transcription repressor of the E2F family, was predominantly expressed by the PZ chondrocytes of normal growth plate, and to a lesser extent by the RZ and HZ cells (Figure 4.3C). In MPS VII growth plate, the number of cells stained positive for E2F4 were significantly decreased to 13.8±7.1% of normal growth plate and 8.8±4.5% of normal growth plate in the RZ and PZ, respectively (Figure 4.3 D).

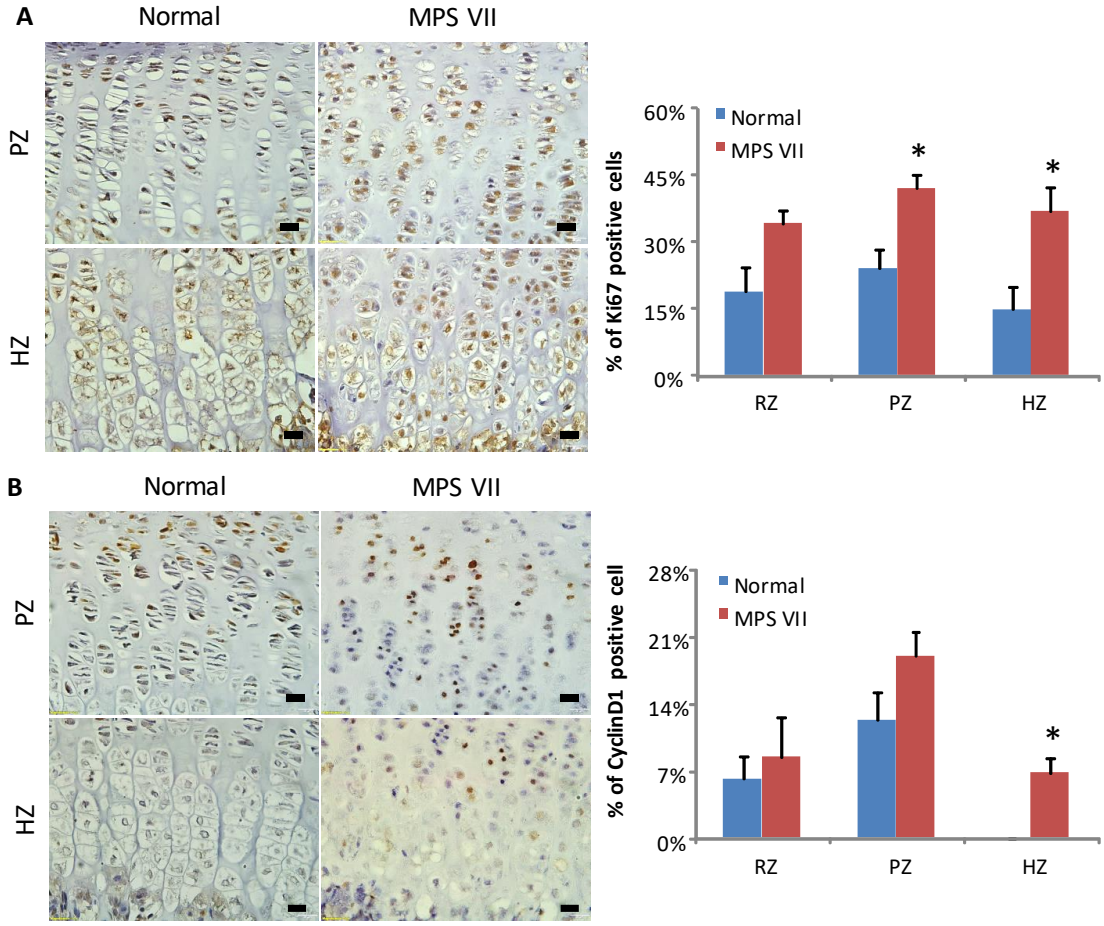

Figure 4.1 Immunohistochemical staining of P14 growth plate for Ki67 and CyclinD1.

IHC and quantification of cells positive for Ki67 (A) and CyclinD1 (B). Results were presented as the percentage of positive cells in the RZ, PZ and HZ, mean ± S.E.M. of n=3 replicates. Scale bar=20µm.

*denotes significant differences between normal and MPS VII mice ($p<0.05$, Student's t-test).

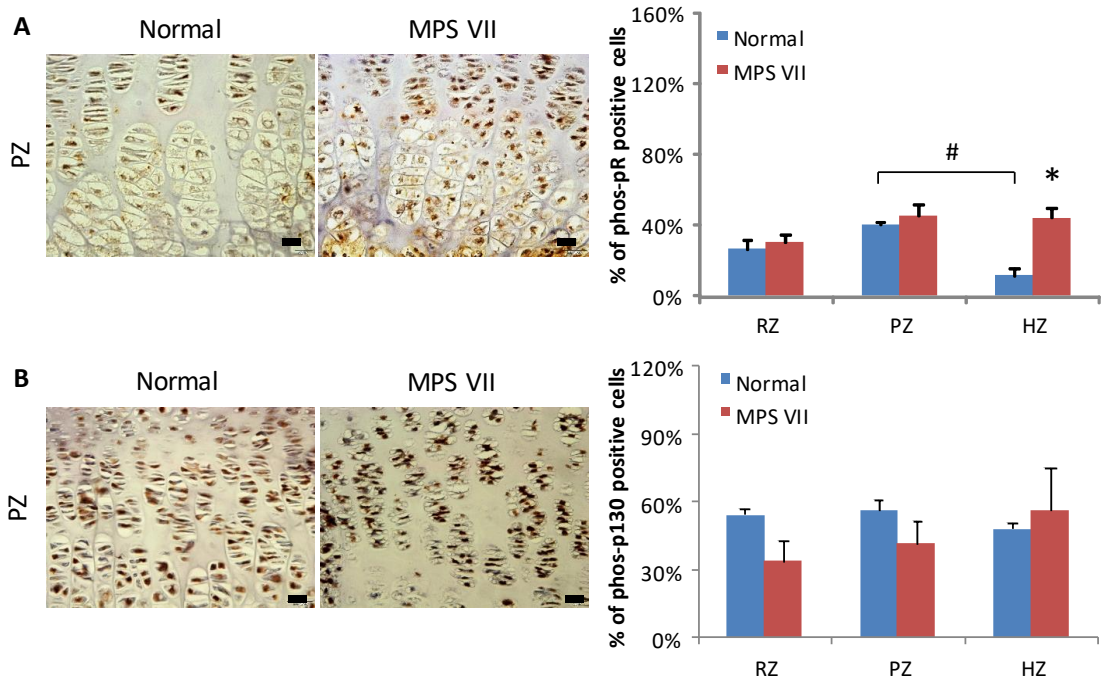

Figure 4.2 Immunohistochemical staining of P14 growth plate for pocket proteins. IHC and quantification of cells positive for phosphorylated pRb (phos-pRb) (A) and phosphorylated p130 (phos-p130) (B). Results were presented as the percentage of positive cells in the RZ, PZ and HZ, mean ± S.E.M. of n=3 replicates. Scale bar=20μm.

*denotes significant differences between normal and MPS VII mice.

# denotes significant differences between zones of normal growth plate ($p<0.05$, Two-way ANOVA, Tukey's post hoc test).

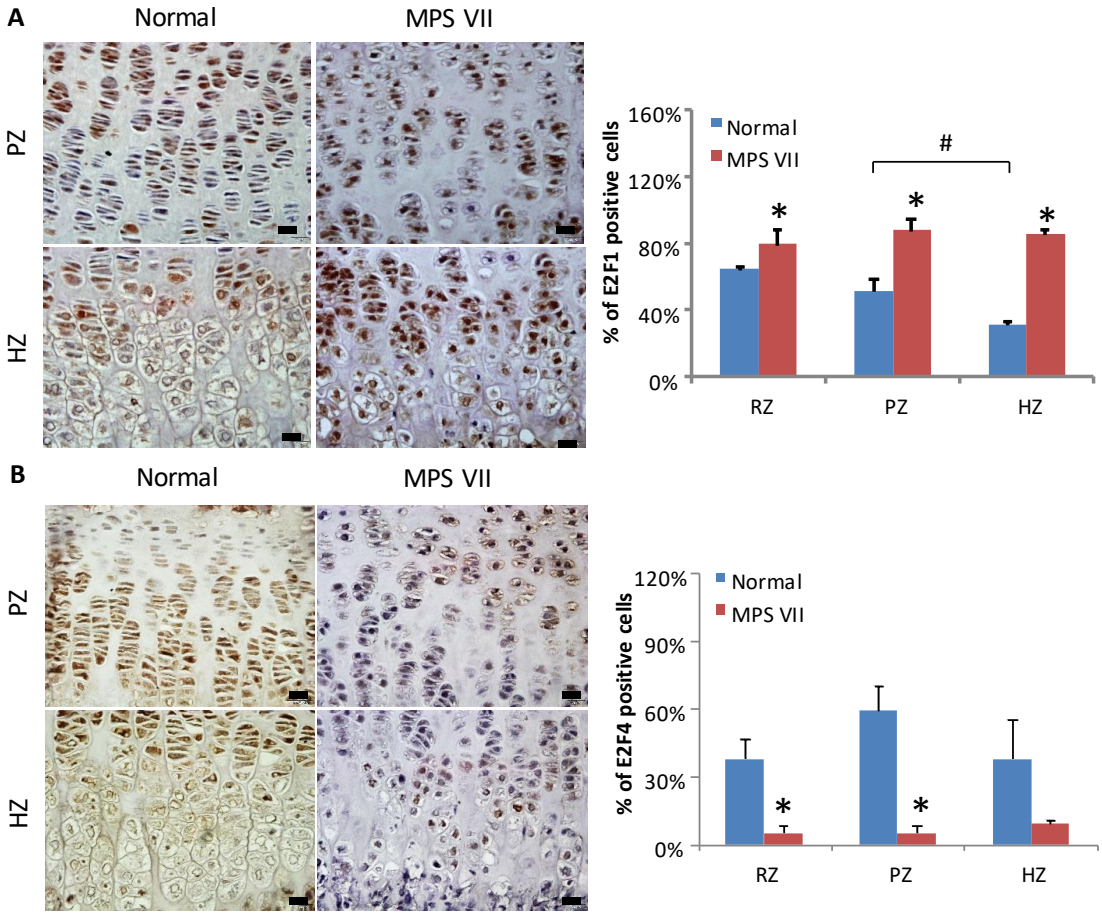

Figure 4.3 Immunohistochemical staining of P14 growth plate for E2Fs. IHC and quantification of cells positive for E2F1 (A) and E2F4 (B). Results were presented as the percentage of positive cells in the RZ, PZ and HZ, mean ± S.E.M. of n=3 replicates. Scale bar=20μm.

*denotes significant differences between normal and MPS VII mice.

# denotes significant differences between zones of normal growth plate ($p<0.05$, Two-way ANOVA, Tukey's post hoc test).

4.3 Fewer MPS VII chondrocytes progressed to M phase

Normal PZ chondrocytes were positive for phos-hisH3, a marker of cells undergoing mitosis (Figure 4.4A). The number of chondrocytes staining for phos-hisH3 decreased to 52.4±14.9% of normal in MPS VII PZ (Figure 4.4B, $p<0.05$). Neither chondrocytes of normal nor MPS VII growth plate stained positive for phisH3 in the HZ (Figure 4.4A). Staining of CyclinB1 was observed in both normal and MPS VII chondrocytes in all three zones of the growth plate (Figure 4.4C). The number of MPS VII chondrocytes stained positive for CyclinB1 was not significantly different compared to that of normal (Figure 4.4D).

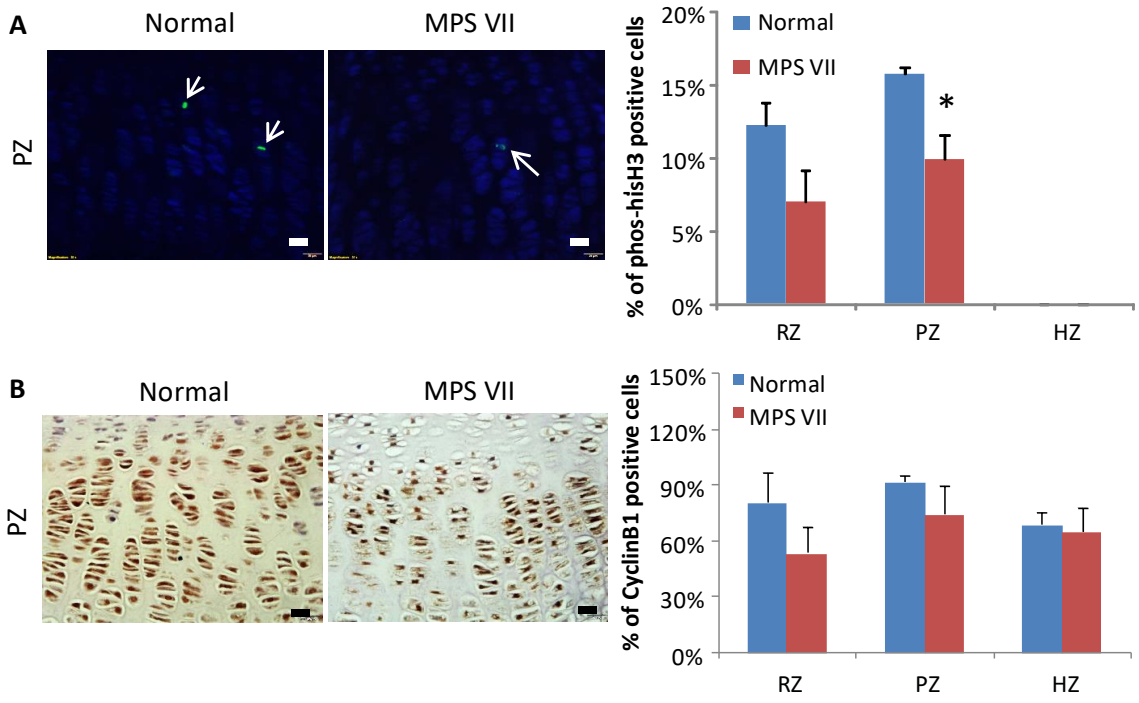

Figure 4.4 Immunohistochemical staining of P14 growth plate for mitosis markers. IHC and quantification of cells positive for phosphorylated hisH3 (phos-hisH3) (A) and CyclinB1 (B). Results were presented as the percentage of positive cells in the RZ, PZ and HZ, mean ± S.E.M. of n=5 replicates for phos-hisH3 and n=3 replicates for CyclinB1. Scale bar=20μm.

*denotes significant differences between normal and MPS VII mice ($p<0.05$, Student's t-test).

4.4 Fewer MPS VII chondrocytes progressed to cell cycle withdrawal

Expression of cyclin/CDK inhibitor $p57^{kip2}$, a marker for terminally differentiated cells destined to exit the cell cycle, was observed predominately in the HZ of normal growth plate (Figure 4.5A & B, $p<0.05$), while the number of HZ cells positive for $p57^{kip2}$ was significantly reduced to 50.9±10.9% of normal in MPS VII growth plate (Figure 4.5A & B).

Figure 4.5 Immunohistochemical staining of P14 growth plate for $p57^{kip2}$.

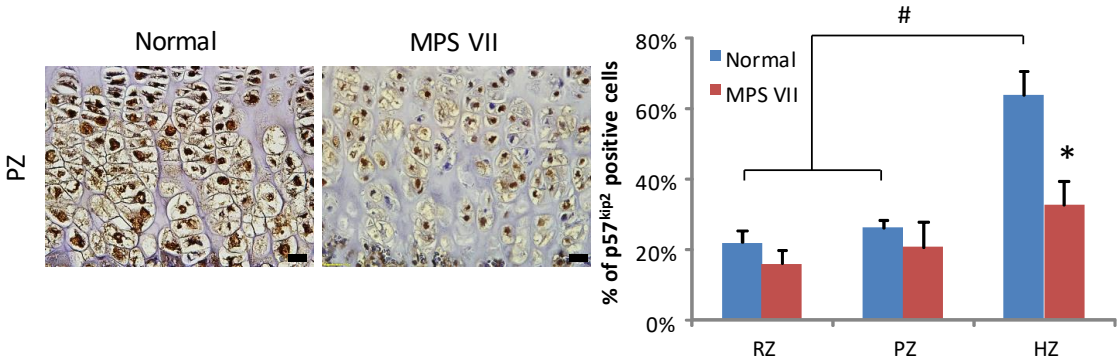

Quantification of cells positive for $p57^{kip2}$ were presented as the percentage of positive cells in the RZ, PZ and HZ, mean ± S.E.M. of n=3 replicates. Scale bar=20μm.

*denotes significant differences between normal and MPS VII mice.

# denotes significant differences between zones of normal growth plate ($p<0.05$, Two-way ANOVA, Tukey's post hoc test).

4.5 Discussion

Cell cycle regulation is essential for chondrocyte proliferation and hypertrophy, in which the entry of chondrocytes into M phase results in mitotic division and the withdrawal of chondrocytes from the cell cycle allows the transition to hypertrophic phenotype. In this chapter, the expression of multiple markers that represent different phases of the cell cycle and several regulators that control cell cycle progression in the growth plate region of normal and MPS VII mice were analyzed.

Under normal circumstances, most chondrocytes in the PZ undergo G1/S transition, DNA replication and mitotic division. Cells positive for Ki67, a nuclear protein, are considered to have entered the cell cycle. A higher percentage of chondrocytes in the PZ of MPS VII mice were positive for Ki67, suggesting more MPS VII chondrocytes were in the cell cycle. The balance of the activator and repressor E2F proteins regulate G1/S phase transition of the cell cycle. While free E2F1 promotes transcription of genes required for DNA replication (Gaubatz et al. 2000), nuclear E2F4/pocket protein (pRb, p130 or p107) complexes (Moberg, Starz & Lees 1996) inhibit this process. The elevated expression of E2F1 and reduced expression of E2F4 in the PZ of MPS VII growth plate therefore suggest that more MPS VII chondrocytes in the PZ were in the G1 phase and had committed to enter S phase. Since the differential proliferation rate of the growth plates is attributed to the differences in the time that PZ chondrocytes of the growth plates spend in the G1 phase (Wilsman et al. 1996), the longer time of MPS VII chondrocytes stayed in the G1 phase would lead to slower proliferation rate.

Furthermore, a decrease in the number of PZ chondrocytes that expressed the M phase marker phos-hisH3 was observed in MPS VII mice, indicating that fewer MPS VII chondrocytes progressed to mitotic division. Comparison of CyclinB1 expression, which is highly expressed during the G2 and early M phase between normal and MPS VII growth

plate, suggested that the failure of MPS VII chondrocytes in progressing to mitotic division was not caused by deficiency of CyclinB1 protein. Clearly, MPS VII PZ chondrocytes entered the cell cycle and had the potential to replicate DNA, but they failed to progress to mitotic division. As a result, the number of chondrocytes was reduced in PZ of MPS VII growth plate (Figure 3.8B). A previous study (Metcalf et al. 2009) showed a significantly reduced rate of proliferation in 3 weeks old MPS VII mice using BrdU incorporation. As BrdU is incorporated into the newly synthesized DNA during S phase, reduction in BrdU staining in the PZ suggested that fewer MPS VII chondrocytes were cable of progressing to DNA replication. The observation of elevated E2F1 expression in the PZ indicated a prolonged status of MPS VII chondrocytes at the G1 phase (Figure 4.3), while the mitotic division (M phase) (Figure 4.4A) were inhibited. These findings were similar to the response of cancer cells to S phase blockage using hydroxyurea or aphidicolin (Chen et al. 2013; Cho et al. 2005; Hung, Jamison & Schreiber 1996; Iwasaki, T et al. 1995), also suggesting that mid-late S phase, when DNA replicates, were inhibited in MPS VII PZ.

Cell cycle withdrawal is required for hypertrophy and normal HZ chondrocytes are positive for $p57^{kip2}$. The decision to progress to cell division or cell cycle withdrawal is made in the G1 phase (Zetterberg & Larsson 1985). Expression of Cyclin D1, which is a cartilage specific isoform of the D type cyclins, was limited to normal RZ and PZ chondrocytes (Long, Schipani, et al. 2001). Expression of this marker was not observed in the normal HZ, where cell cycle withdrawal is the major event. In contrast, MPS VII HZ chondrocytes continued to express Cyclin D1, but failed to express sufficient $p57^{kip2}$, indicating that instead of exiting from the cell cycle, these MPS VII chondrocytes were still in the G1 phase, which was also consistent with the observation of increased Ki67 staining in the HZ of MPS VII growth plate. This theory was further supported by elevated immunostaining of E2F1 and phos-pRb in MPS VII HZ. Downstream of Cyclin D1/CDK activity is the E2F/pRb complexes. During G0/G1 phase, where senescent chondrocytes exit the cell

cycle, upregulation of CKI (such as $p57^{kip2}$) inhibits Cyclin D1/CDK activity, which lead to dephosphorylation of pRb. E2F1 is therefore blocked by activated pRb (unphosphorylated form) allowing for cell cycle withdrawal. The level of E2F1 and phos-pRb in normal chondrocytes was downregulated during the transition from the proliferative to hypertrophic phenotype. In contrast, persistence of these two proteins in the HZ of MPS VII growth plate suggested that although these chondrocytes were morphologically hypertrophic, they were more typical of proliferative cells, failing to undergo phenotypical changes for hypertrophic differentiation.

A previous study has shown that overexpression of *E2f1* disturbed the differentiation of chondrocytes in the HZ of the growth plate, which leads to delayed EO and shorter long bones in transgenic mice (Scheijen et al. 2003). Therefore, the lower number of HZ chondrocytes observed in MPS VII growth plate (Figure .8C) may be partially due to the persistence of E2F1.

This chapter demonstrated for the first time that the pace of cell cycle progression in growth plate chondrocytes is disrupted *in vivo*. During the course of this thesis, a report was published showing MPS I and MPS II fibroblasts were less likely to progress to S and G2/M phase *in vitro* (Moskot et al. 2016), suggesting that disruption of the cell cycle progression may occur in more than one cell type in MPS. MPS VII is characterized by storage of HS, DS and CS. While the participation of DS in cell cycle regulation has not been reported, HS and CS can participate in cell cycle progression through interactions with BMP, WNT and IHH signalling pathways (Cortes, Baria & Schwartz 2009; De Leonardis et al. 2014; Manton et al. 2007; Zhang, F et al. 2007).

By utilizing immunohistochemistry, the changes in cell cycle progress across the three distinct zones (the RZ, PZ and HZ) were clearly defined. However, the intracellular localization of the cell cycle regulators was not determined. The functions of E2F4 and

CyclinB1 are dependent on their localization within the cells. Nuclear translocation allows E2F4 to form complexes with pocket proteins, which block E2F1 activity (Lindeman et al. 1997), and enables formation of CyclinB1-CDK1 complexes to activate downstream genes that are crucial for mitosis (Porter & Donoghue 2003). It is possible that proteins like E2F4 and CyclinB1 are mis-localized within MPS VII chondrocytes as accumulation of GAG storage would alter cellular structure. Therefore, future examination of nuclear/cytoplasmic ratios of E2F4 and CyclinB1 in growth plate chondrocytes using Immuno-EM techniques may strengthen the understanding of the disturbance of cell cycle progression in the MPS VII growth plate.

Collectively, in comparison to normal growth plate, more chondrocytes in the PZ stayed within the G1 phase of the cell cycle in the MPS VII growth plate. Although these cells were committed to enter S phase, fewer PZ cells were capable of progressing to DNA replication and subsequent mitotic division, and fewer HZ cells progressed to cell cycle withdrawal for terminal differentiation. This chapter demonstrated that progression through the G1 phase, mitotic division and cell cycle withdrawal were disrupted in growth plate chondrocytes of MPS VII mice, and thus pointed to potential targets for correcting growth plate dysfunctions, especially the reduced proliferation and hypertrophy of chondrocytes. Since the pace of cell cycle progression in the growth plate is strictly regulated by a complex network of endocrine and paracrine/autocrine factors, which therefore mediates the elongation of bones, in the next chapters, expression of such factors in MPS VII mice will be investigated to provide better understanding of the mechanism behind bone shortening in MPS.

5 Endocrine factors involved in linear bone growth are dysregulated in MPS VII mice

5.1 Introduction

EO is strictly regulated by a complex network of signalling pathways, controlling the pace and onset of chondrocyte proliferation and differentiation. These pathways include systemic factors that travels through the bloodstream, such as GH, T3, glucocorticoids, estrogen, testosterone, circulating IGF1 (Clarke, BL & Khosla 2009; Fernandez-Cancio et al. 2008; van der Eerden, Karperien & Wit 2003), as well as local factors like IHH and paracrine/autocrine IGF1.

GH is the major hormone supporting longitudinal bone growth. GH is secreted by the pituitary gland in a pulsatile manner and primarily acts on the liver where it stimulates the production of IGF1 (Butler & Le Roith 2001), IGFALS and IGFBP, including IGFBP3, the most abundant form in the circulation (Baxter, Martin & Beniac 1989). This signalling pathway is mediated through the JAK2/STAT5 signalling cascade (Piwien-Pilipuk, Huo & Schwartz 2002; Teglund et al. 1998). Liver-derived IGF1 contributes to 75% of IGF1 in the circulating pool (Sjogren et al. 1999; Yakar et al. 1999). IGF is then delivered to bone and bound by bone/cartilage-derived IGFR1, regulating EO. GH is also delivered to bone and stimulate longitudinal bone growth through GHR (Gevers et al. 2002).

T3 supports bone growth mainly by promoting chondrocyte hypertrophy (Robson et al. 2000; Stevens et al. 2000). T3 stimulates IGF1 mRNA expression in chondrocytes (Ohlsson, Nilsson, Isaksson, Bentham, et al. 1992) and osteoblasts (Varga, Rumpler & Klaushofer 1994) and increases IGF1 secretion from bone organ cultures (Lakatos et al. 1993). T3 also plays a critical role in IGF1 signalling and bone acquisition during the pre-pubertal period (Xing et al. 2012), suggesting that the action of T3 on bone growth is age-dependent.

IHH is highly expressed by chondrocytes in the growth plate, but has also be found in lungs, liver, kidneys, gastrointestinal tract, ovarian and prostate (Lim et al. 2014; Liu, C et al. 2015;

Matz-Soja et al. 2014; McMahon, Ingham & Tabin 2003; Valentini et al. 1997). IHH regulates proliferation and the transition of chondrocytes to hypertrophy in conjunction with PTHrP (Koyama et al. 1996; Maeda et al. 2007; St-Jacques, Hammerschmidt & McMahon 1999; Vortkamp et al. 1996). Although IHH is found in the circulation, there is little evidence suggesting a role for circulating IHH in bone growth.

Lysosomal GAG storage has been observed in the pituitary gland, thyroid gland, hepatocytes and Kupffer cells in the liver of children with MPS II (Nagashima et al. 1976; Oda et al. 1988), suggesting endocrine function is likely impaired. Limited information is available on endocrine status in MPS patients. Gardner (2011) and Polgreen (2008) reported GH deficiency and GH insensitivity in some children with MPS IH post HSCT. Hypothyroidism has also been reported in one case of MPS IH/S patient (Mohanalakshmi, V. & S. 2014). Despite low IGF1 level, normal to high GH level has been reported in three siblings with MPS II, suggesting GH insensitivity (Toledo et al. 1991). Consistently, one single study found an increased expression of IGFBP1 and IGFBP2 in MPS VII mouse liver, indicating the bioavailability of IGF1 may be altered (Woloszynek et al. 2004).

However, the mechanism behind these altered endocrine levels in MPS is not fully understood. The aim of this chapter was to characterize the regulation of bone growth at endocrine level in MPS VII mice. Based on the observation of lysosomal GAG storage in the pituitary gland, thyroid gland and liver cells of MPS patients, this chapter hypothesis that the level of GH, IGF1 and T3 is altered in the circulation of MPS VII mice. The level of GH, IGF1, IGFBP3, IGFALS, T3 and IHH was measured in the serum from normal and MPS VII mice at P14, 1, 2 and 6 months of age. Furthermore, GH-induced hepatic IGF1 production and expression of major factors along the GH/IGF1 axis in the liver of normal and MPS VII mice were examined.

5.2 Serum analyses of endocrine factors in MPS VII mice

5.2.1 Circulating GH level was not affected in young MPS VII mice, but ghrelin-induced GH secretion was altered in MPS VII mice at 2 months of age.

The circulating GH level was measured in serum samples from normal and MPS VII mice at P14 and 1 month of age (Chapter 2.2.1). The level of GH was not altered in MPS VII mice at P14 (101.7±21.1% of normal mouse level, Figure 5.1A). Although not statistically significant, GH level of MPS VII mice decreased to 58.7±16.6% of normal at 1 month of age (Figure 5.1A).

It is difficult to monitor pulsatile GH secretion in mice, which requires frequent collection of blood due to constraints on their blood volume. Since ghrelin stimulates GH release from the pituitary gland (Kojima et al. 1999), exogenous ghrelin was used as an amplifier of GH pulsatility to investigate if GH secretion is affected by the progression of disease in MPS VII mice (Chapter 2.6). Administration of saline had no stimulatory effect on GH secretion in either normal or MPS VII mice at different ages. Administration of ghrelin greatly stimulated GH secretion in both normal and MPS VII mice at 1 and 4 months of age (Figure 5.1B & D), and the GH level was not significantly different between normal and MPS VII mice 5 min and 15 min after ghrelin injection at both ages. At 2 months of age, administration of ghrelin stimulated GH secretion in normal mice 5 min and 15 min after injection (Figure 5.1C). In contrast, ghrelin-induced GH secretion in MPS VII mice was significantly reduced to that in normal mice, reaching only 26.8±11.5% and 22.7±10.1% of the normal levels (Figure 5.1C, $p<0.05$) 5 min and 15 min after injection, respectively. The levels of ghrelin-induced GH secretion in MPS VII mice at 2 months of age were not significantly different to those of age-matched mice with saline injection.

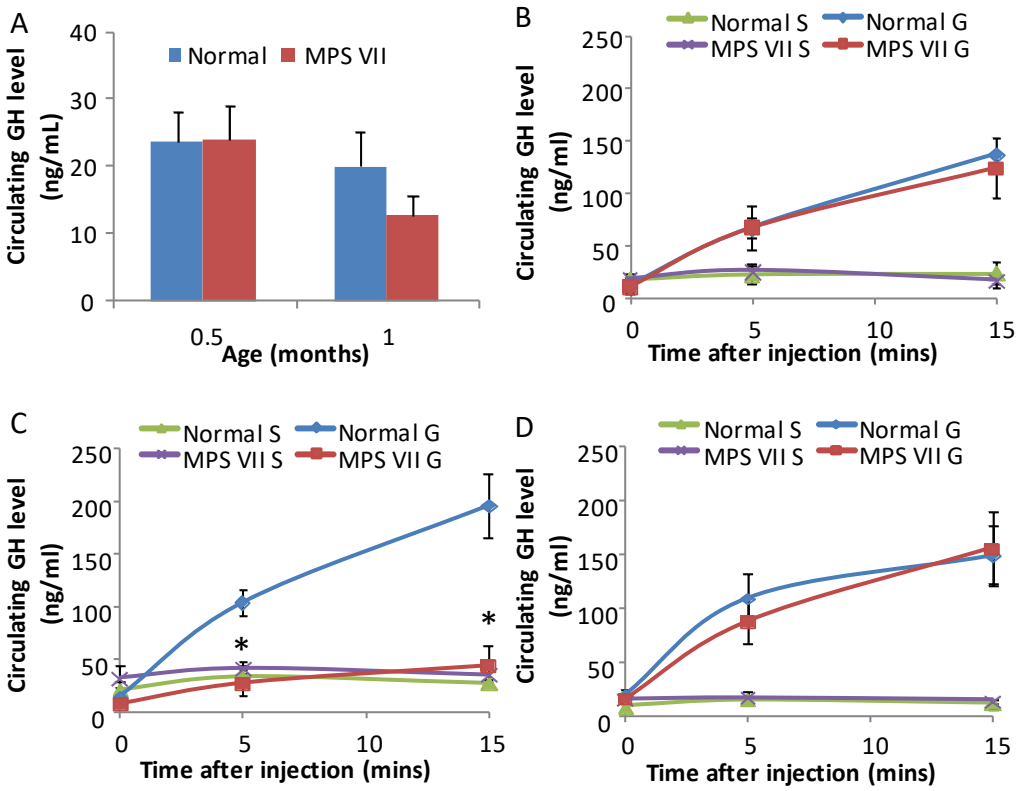

Figure 5.1 Ghrelin-induced GH secretion was decreased in young adult MPS VII mice.

Circulating GH level (A) in normal and MPS VII mice at 14 days and 1 month of age (n=11 replicates). The effect of ghrelin administration on GH secretion in normal and MPS VII mice at 1 month (B), 2 months (C) and 4 months (D) of age (n≥6 replicates for ghrelin (G), and n≥3 replicates for saline (S)). Results are presented as the mean±S.E.M. * denotes significant differences of ghrelin-induced GH level between normal and MPS VII mice, $p<0.05$, Student's t-test.

5.2.2 Young MPS VII mice had decreased level of IGF1, IGFBP3 and IGFALS in the circulation

IGF1, IGFBP3 and IGFALS levels in mouse serum at different ages were determined by ELISA as shown in Figure 5.2A, B & C. Serum IGF1 level in both normal and MPS VII mice raised during P14 to 2 months, and slightly decreased at 6 months of age. Young MPS VII mice (P14) showed a 58% reduction in circulating IGF1 (Table 5.1)

The patterns of circulating IGFBP3 and IGFALS levels were similar to that of circulating IGF1. In both normal and MPS VII, IGFBP3 and IGFALS level increased from P14 onwards, peaked at 2 months of age and decreased slightly at maturity. A 30% and a 60% reduction were observed on the circulating IGFBP3 level and IGFALS level respectively in MPS VII mice at P14 (Table 5.1). The molar ratio of IGF1: IGFBP3: IGFALS changed from 1:3.6:4.4 in normal to 1:6.1:4.4 in MPS VII mice at P14, also suggesting the stability of the ternary complex was altered in the circulation of MPS VII mice. However, circulating IGF1, IGFBP3 and IGFALS levels in MPS VII mice were not significantly different to those of normal mice at 1, 2 or 6 months of age.

Table 5.1 Circulating IGF1, IGFBP3 and IGFALS levels in MPS VII mice

	Normal	**MPS VII**
IGF1	242.9±29.5 ng/ml*	102.2±11.3 ng/ml
IGFBP3	3276.7±300.4 ng/ml*	2283.2±235.5 ng/ml
IGFALS	9351.2±1215.7 ng/ml*	3737.5±773.5 ng/ml

Circulating IGF1, IGFBP3 and IGFALS level in normal and MPS VII mice at P14. Results are presented as the mean ± S.E.M of n=9 replicates.

* denotes significant difference between normal and MPS VII mice ($p<0.05$, Student's t-test).

Serum IGF1 level was also measured in attenuated MPS VII (Gus$^{tm(L175F)Sly}$ strain), which displayed a mild bone shortening (Chapter 3.2, Figure 3.1 & 3.2), and MPS IIIA mice, which has normal bone length (Chapter 3.2, Figure 3.1) (Figure 5.2D). Interestingly, attenuated MPS VII (Gus$^{tm(L175F)Sly}$ strain) mice had a significantly higher serum IGF1 level than that of severe MPS VII mice; however, this level (63.2±7.5% of normal mice) was still significantly decreased as compared to the normal and MPS IIIA mice. In contrast, MPS IIIA mice had serum IGF1 level similar to that of normal mice (121.9±26.3% of normal mice), which was significantly higher than that of severe MPS VII mice. These findings indicated a correlation between bone shortening and the circulating IGF1 level in MPS mice.

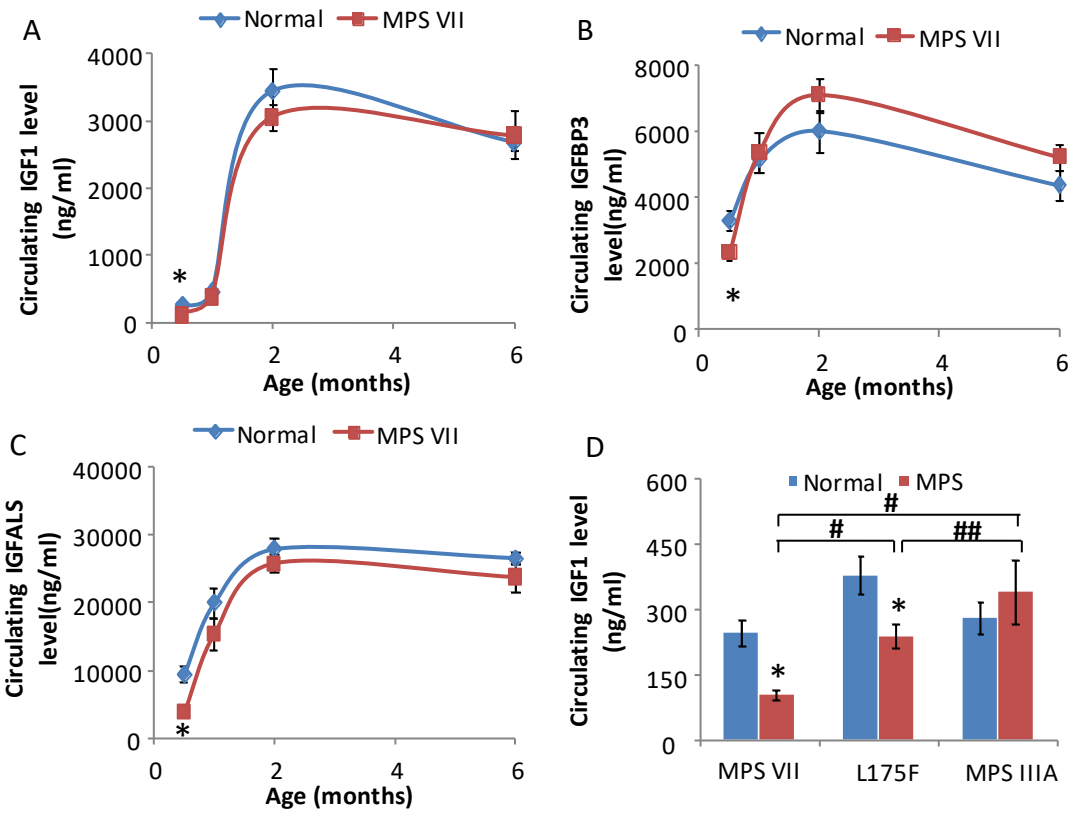

Figure 5.2 Circulating IGF1, IGFBP3 and IGFALS levels were significantly decreased in P14 MPS VII mice. Circulating IGF1 (A), IGFBP3 (B) and IGFALS (C) level in normal and MPS VII mice at P14, 1 month, 2 months and 6 months of age (n≥9 replicates). (D) Comparison of circulating IGF1 level in normal, severe MPS VII ($Gus^{mps/mps}$), attenuated MPS VII (L175F represents $Gus^{tm(L175F)Sly}$) and MPS IIIA mice at P14 (n≥8 replicates). Results are presented as the mean ± S.E.M.

* denotes significant difference between normal and MPS mice.

# denotes significant difference between severe MPS VII and L175F or MPS IIIA mice.

denotes significant difference between L175F and MPS IIIA mice.

($p<0.05$, two-way ANOVA, Tukey's post hoc).

5.2.3 Circulating T3 level was not affected in MPS VII mice

Circulating T3 level was constant in both normal and MPS VII mice from 14 days to 6 months of age (Figure 5.3A). The level of circulating T3 in MPS VII mice was not significantly different to those of normal mice at P14 (114.2±15.4% of normal), 1 month (95.3±14.3% of normal), 2 months (111.9±6.0% of normal) and 6 months of age (85.5±7.3% of normal).

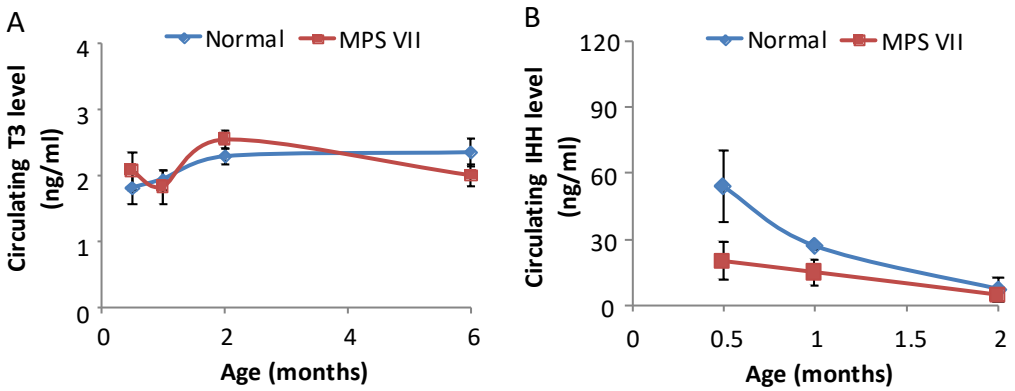

Figure 5.3 Circulating T3 and IHH levels in MPS VII mice were not significantly different from those of normal. (A) Circulating T3 level in normal and MPS VII mice at P14, 1 month, 2 months and 6 months of age (n≥9 replicates). (B) Circulating IHH level in normal and MPS VII mice at P14, 1 month and 2 months of age (n=replicates). Results are presented as the mean ± S.E.M.

5.2.4 Circulating IHH level was slightly decreased in MPS VII mice

In normal mice, the circulating IHH level of mice was 54.0±16.5 ng/ml at 14 days of age and decreased with age (Figure 5.3B) such that at 6 months of age, the serum IHH level was no longer detectable. Circulating IHH level in MPS VII mice followed a similar pattern as that of normal mice and declined with age (Figure 5.3B). The circulating IHH level of MPS VII decreased to 37%, 57% and 67% of those of normal mice at P14, 1 month and 2 months of age, respectively, but did not reach statistical significance. At 6 months of age, serum IHH level of MPS VII mice was also not detectable.

5.3 Liver derived IGF1 production

5.3.1 GH-induced secretion of IGF1 was limited in MPS VII hepatocytes

To further investigate the mechanism behind reduced level of circulating IGF1 in MPS VII mice, the effect of GH on IGF1 secretion by both normal and MPS VII hepatocytes was assessed *in vitro*. Normal hepatocytes produced IGF1 in response to GH stimulation in a dose dependent manner (Figure 5.4A). IGF1 level secreted by normal hepatocytes was 0.4 ± 0.22 pg/µg when cultured in the absence of GH, and it increased gradually with increasing concentrations of GH, and reached the peak (1.51 ± 0.09 pg/ µg) when cultured with 500 ng/mL GH. In contrast, MPS VII hepatocytes produced significantly less IGF1 and did not display a dose-dependent increase. IGF1 levels secreted by MPS VII hepatocytes were 0.16 ± 0.05 pg/µg and 0.21 ± 0.06 pg/µg when cultured without GH and with 500 ng/mL GH, respectively.

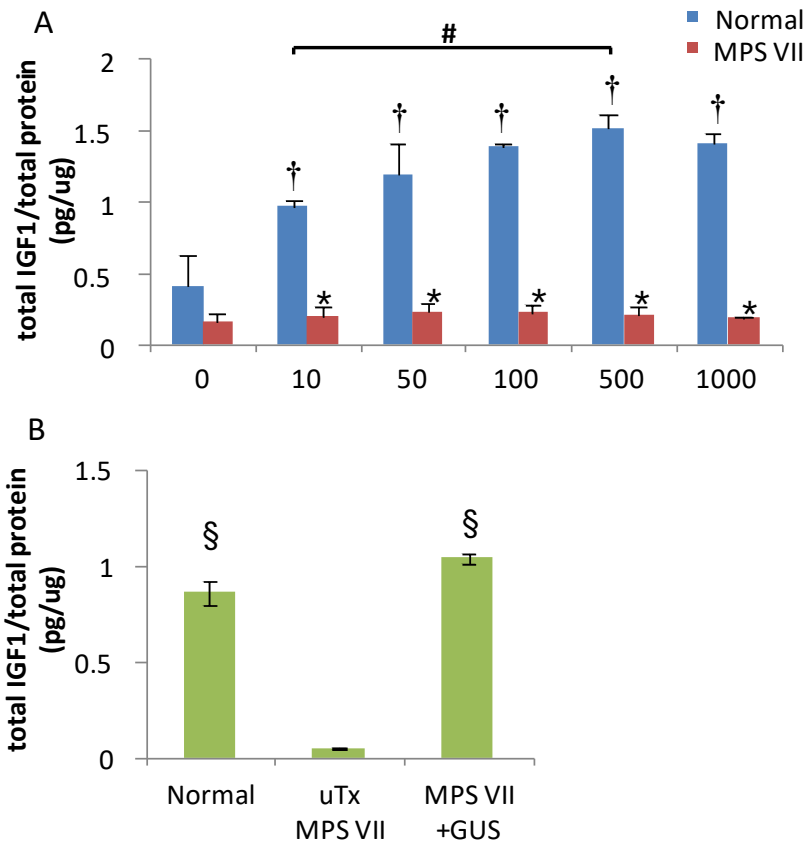

Figure 5.4 GH-induced IGF1 production was limited in MPS VII hepatocytes but was rescued by β-glucuronidase (GUS). IGF1 secretion by (A) normal and MPS VII hepatocytes after 24hr of GH stimulation; and (B) normal and untreated MPS VII hepatocytes and β-glucuronidase rescued MPS VII hepatocytes after 24hr of GH stimulation (500ng/ml). Results are presented as mean ± S.E.M.

* denotes significant difference of IGF1 secretion between normal and MPS VII hepatocytes.

† denotes significant difference of IGF1 secretion by normal hepatocytes between GH doses and 0 ng/ml.

# denotes significant difference of IGF1 secretion by normal hepatocytes between stimulation of 10ng/ml GH and 500ng/ml GH.

§ denotes significant difference of IGF1 secretion by normal hepatocytes or GUS rescued MPS VII hepatocytes to untreated (uTx) MPS VII hepatocytes.

($p<0.05$, Two-way ANOVA, Tukey's post-hoc test).

5.3.2 IGF1 secretion in MPS VII hepatocytes was rescued by β-glucuronidase (GUS)

MPS VII hepatocytes were cultured in medium supplemented with β-glucuronidase (Chapter 2.7.3) to investigate whether IGF1 secretion by MPS VII hepatocytes is rescued by β-glucuronidase. Figure 5.4B shows that while untreated MPS VII hepatocytes failed to increase the IGF1 level (4.8±0.4% of normal) in response to GH stimulation, MPS VII hepatocytes supplied with β-glucuronidase produced an IGF1 level (120.5±3.1% of normal) that was equivalent to that of normal cells.

5.3.3 Low IGF1 production in MPS VII liver was not due to deficiency of GHR but an impaired hepatic JAK2-STAT5 signalling

In the liver, GH binds to GHR and subsequently activates phosphorylation of JAK2 and STAT5. The latter then forms a dimer structure and translocates into the nucleus, where it targets and induces transcription of *Igf1*. Hepatic GH signalling was therefore investigated in MPS VII liver using real-time PCR and immunohistochemistry analyses.

Real-time PCR analyses revealed that the levels of expression of *Ghr*, *Igf1*, *Igfbp3*, *Igfals*, and *Stat5a* and *Stat5b* were not altered in the liver of MPS VII mice (Figure 5.5A) when compared to those of normal mice. However, a 5.6-fold higher level of *Igfr1* expression was observed in the MPS VII liver when compared to normal liver (Figure 5.6A, $p<0.05$).

Hepatocyte cytoplasm stained positive for GHR in both normal and MPS VII liver (Figure 5.5B). Consistent with gene expression analyses, immunostaining of GHR within the MPS VII liver was at a similar level to that within the normal liver. Positive staining of Y-phos-JAK2 was observed only in the nucleus of hepatocytes (Figure 5.5B) of both normal and MPS VII mice. More MPS VII liver cells were positive for Y-phos-JAK2 (145.5±12.3% of normal, $p<0.05$, Figure 5.5C).

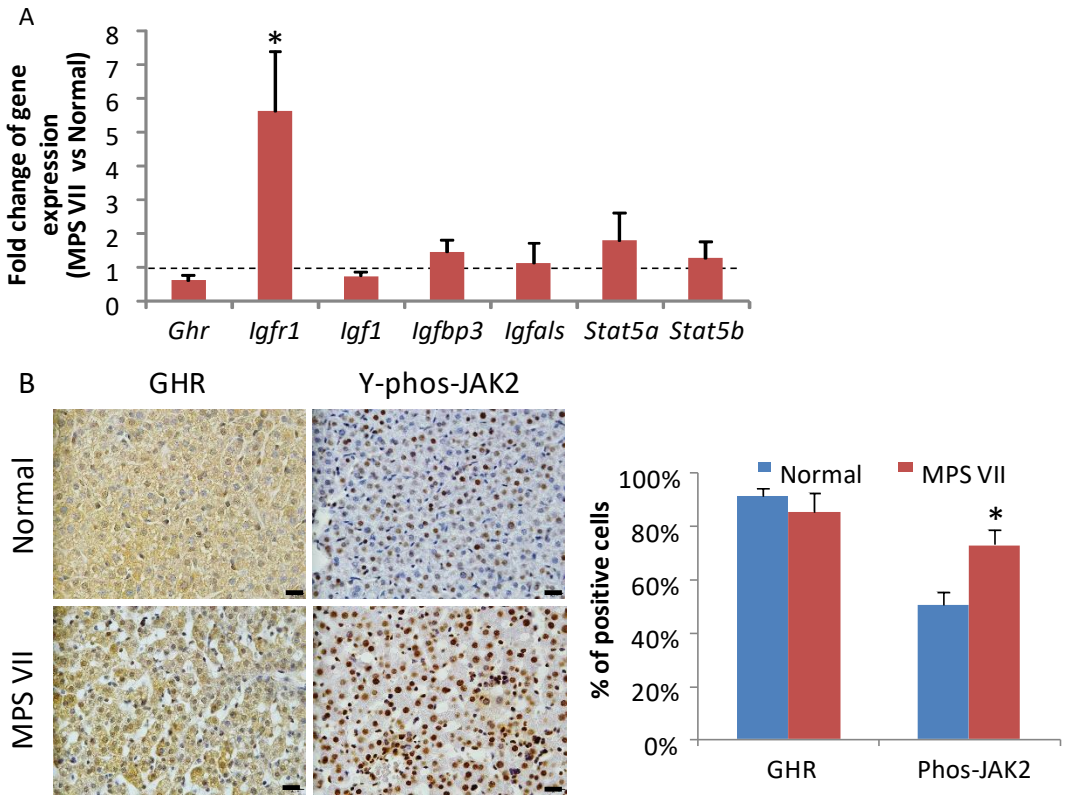

Figure 5.5 MPS VII liver had elevated phosphorylated JAK2 in the nuclei. (A) Gene expression analysis of essential growth factors of GH/IGF1 axis in the liver. (B) IHC and quantification of hepatocytes positive for for GHR and Y-phos-JAK2. Scale bar=20µm. Results are presented as percentage of positive stained cells to total cells. Results were presented as the mean ± S.E.M. of n=5 replicates.

*denotes significant differences between normal and MPS VII mice ($p<0.05$, Student's t-test).

Y-phos-STAT5 was located within the cytoplasm of hepatocytes of both normal and MPS VII mice (Figure 5.6A). Fewer cells within the MPS VII liver (80.6±7.6% of normal, $p<0.05$, Figure 5.6B) stained positive for Y-phosp-STAT5 when compared to those within the normal liver. Immunostaining of Y-phos-STAT5A was not detected in neither normal nor MPS VII liver (data not shown). Immunostaining of S-phos-STAT5 was found in the nuclei of hepatocytes and was not significantly different between normal and MPS VII mice.

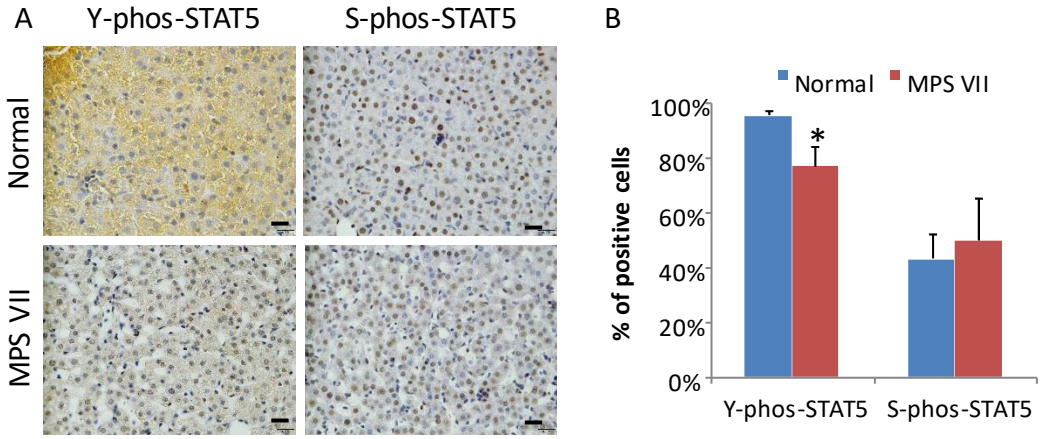

Figure 5.6 Immunohistochemical staining of D14 mice liver for Y-phos-STAT5 and S-phos-STAT5. IHC (A) and quantification (B) of hepatocytes positive for Y-phos-STAT5 and S-phos-STAT5. Scale bar=20μm. Results are presented as percentage of positive stained cells to total cells, mean ± S.E.M of n=5 replicates.

*denotes significant differences between normal and MPS VII ($p<0.05$, Student's t-test).

5.4 Discussion

During childhood, bone growth is regulated by circulating GH, IGF1 (Baker et al. 1993; Liu, JP et al. 1993), thyroid hormones and glucocorticoids, whereas sex steroids contribute to this process later during puberty. MPS children have normal thyroid hormone levels but a high proportion of patients display GH insensitivity (Gardner et al. 2011; Toledo et al. 1991). The overall endocrine status of MPS children is still uncertain. In this chapter, the status of GH, IGF1, IHH and T3 in normal and MPS VII mice at different ages was determined.

GH does not affect postnatal growth in mice until after 14 days of age (Isaksson et al. 1987; Lupu et al. 2001; Zhou, Y et al. 1997). Therefore, GH secretion in normal and MPS VII mice was assessed from P14. Basal secretion of GH in the circulation of young MPS VII mice was not pronouncedly different to that of normal mice at P14 and 1 month of age. Acylated ghrelin injection greatly stimulated GH secretion, acting through the ghrelin receptor/GH secretagogue receptor (GHSR) (Kojima et al. 1999), in both normal and MPS VII mice at 1 and 4 months of age. A failure of GH secretion in MPS VII mice in response to ghrelin stimulation was observed at 2 months of age. However, it is still not understood what causes this age-specific failure of ghrelin-induced GH secretion in MPS VII mice.

Young MPS VII mice had a markedly reduced circulating IGF1 level, which is likely to be the most direct cause of the observed bone shortening at the same ages. GH and IGF1 mediate postnatal bone growth coordinately during pubertal and post-pubertal periods; however, early postnatal bone growth is mediated predominately by IGF1 and to a less extent by GH (Mohan, S. et al. 2003). Liver-derived IGF1 is the major source of circulating IGF1 and is predominately mediated by GH. GH-induced IGF1 production by MPS VII hepatocytes was markedly reduced *in vitro*, suggesting that decreased IGF1 level in MPS VII may be due to an impaired GH/IGF1 signalling pathway in the liver. The significantly

reduced circulating levels of IGFALS and IGFBP3, which are mainly synthesized by hepatocytes and Kupffer cells respectively, lead to increased stability of the ternary complex and thus resulted in less available IGF1 for bone growth. However, the reduction of bioactive IGF1 in MPS VII mice was not caused by deficiency of *Igf1*, *Igfbp3* or *Igfals* in the liver at the transcription level.

The initial steps of GH-induced IGF1 production in the liver includes autophosphorylation of GHR and cytoplasmic JAK2. In the liver of MPS VII mice, expression of GHR was not altered at either the transcription or protein level, suggesting the reduced IGF1 production was not caused by deficiency of GHR. Surprisingly, phosphorylation of JAK2 at tyrosine 1007/tyrosine 1008 site, which is the initial step for activation of JAK2 (Feng et al. 1997), was absent from cytoplasm of the hepatocytes in both normal and MPS VII liver, but more Y-phos-JAK2 was observed in the nuclei of MPS VII hepatocytes. Nuclear JAK2 has been previously observed in rat liver but its function is not yet known (Lobie et al. 1996; Ram & Waxman 1997). A previous study found that accumulation of phosphorylated STAT5 in vitamin A-deficient liver was induced by decreased expression of SHP-1, which subsequently decreased expression of the nuclear JAK2 (Murray et al. 2005). The observed accumulation of nuclear Y-phos-JAK2 in MPS VII liver therefore may be associated with the reduction of Y-phos-STAT5. However, it is not clear whether elevated nuclear phosphorylation of JAK2 is involved in the decreased secretion of hepatic IGF1 in MPS VII mice or not.

GH-induced IGF1 production also requires dimerization and nuclear translocation of STATs, mainly STAT5B in the liver (Hosui & Hennighausen 2008). Both tyrosine and serine phosphorylation of STAT5 (Gebert, Park & Waxman 1997) can be activated by GH. Cytoplasmic Y-phos-STAT5 was markedly decreased in MPS VII liver, while nuclear S-phos-STAT5 was not significantly different to that of normal livers. Gene expression of

Stat5a and *Stat5b* was not altered in MPS VII liver, indicating that the reduced Y-phos-STAT5 expression was not due to changes at transcription level. Tyrosine phosphorylation of STAT5B (Y-phos-STAT5B) was not examined in this chapter due to the absence of commercially available antibody against Y-phos-STAT5B. In both normal and MPS VII liver, Y-phos-STAT5A was not expressed (data not shown), supporting that STAT5A is less abundant and less necessary for tyrosine phosphorylation in the liver (Waxman et al. 1995). Gene expression of *Igf1*, *Igfbp3* and *Igfals* in MPS VII liver was not significantly different from normal liver. Together, these findings suggest that nuclear translocation of STAT5 is not affected in MPS VII liver, and thus the transcription of its downstream targeting genes (*Igf1*, *Igfbp3* and *Igfals*) is not altered. However, the decreased secretion of IGF1 by MPS VII liver is likely to be a result of the decreased cytoplasmic tyrosine phosphorylation of STAT5 through an unknown mechanism, which affects IGF1 secretion at the post-transcriptional level (Figure 5.7).

Healthy hepatocytes express low levels of IGFR1 and it is not directly involved in GH-induced IGF1 production (Butler et al. 1994). However, MPS VII liver expressed an elevated level of *Igfr1*. Previous reports have observed overexpression of IGFR1 in hepatocytes of subjects with chronic hepatitis B, chronic hepatitis C and liver cirrhosis (Kim, Park & Lee 1996; Stefano et al. 2006; Tao et al. 2000). Thus, elevated expression of *Igfr1* in MPS VII liver most likely indicates abnormal liver function rather than a role in IGF1 production.

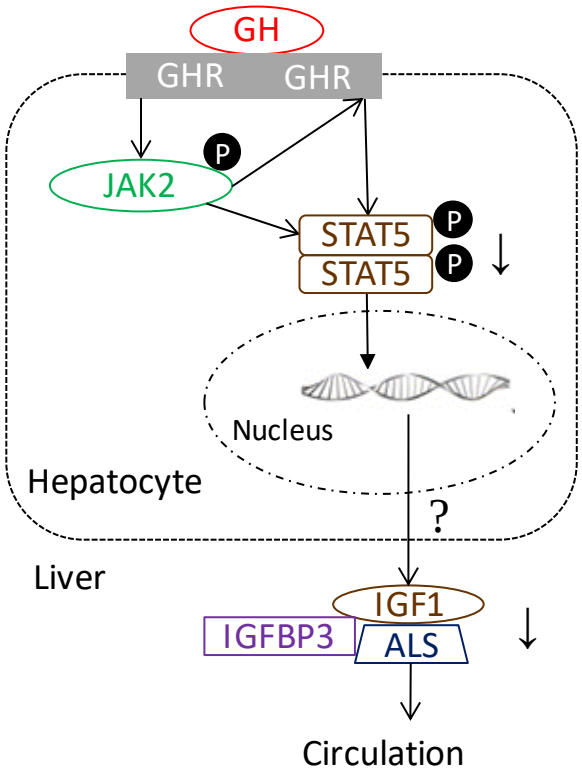

Figure 5.7 GH-mediated IGF1 production is impaired in MPS VII liver. Binding of GH triggers dimerization of the cell surface GHR, which activates JAK2 through phosphorylation. Activated JAK2 lead to phosphorylation of the GHR and subsequently cytoplasmic transcription factors including STAT5A and STAT5B. In MPS VII liver, cytoplasmic phosphorylation of STAT5 is diminished. Phosphorylated STATs dimerize and translocate to the nucleus, where they bind onto the promoter of target genes (etc. *Igf1, Igfbp3 and Igfals*). Nuclear phosphorylation of STAT5 is at normal level in MPS VII liver. However, the levels of IGF1, IGFALS and IGFBP3 in the circulation of MPS VII mice are lower than normal.

Addition of β-glucuronidase to MPS VII hepatocytes rescued IGF1 production. It is likely that exogenous β-glucuronidase reversed the effects on poor IGF1 secretion by removing the GAG storage in MPS VII hepatocytes *in* vitro (Derrick-Roberts et al. 2014; Macsai et al. 2012). This indicates that disruption of lysosomal machinery is responsible for the reduced IGF1 production in MPS VII liver. Intravenous administration of exogenous enzymes produced by lentivirus mediated gene therapy to MPS animal models has been reported to efficiently reduce GAG storage in MPS liver (Cotugno et al. 2010; Derrick-Roberts et al. 2014). Thus, *in vivo* correction of the reduced IGF1 production is achievable in MPS since current therapies such as ERT and GT deliver most GAG degradation enzymes to the liver efficiently.

Circulating T3 level was not pronouncedly different in MPS VII mice at different ages. T3 has been reported to promote bone growth, especially during the pre-pubertal period (Xing et al. 2012), and is likely to act through IGF1 signalling (O'Shea et al. 2005; Wang, L, Shao & Ballock 2010) and the IHH/PTHrP loop (Stevens et al. 2000). While hypothyroidism has been reported in a case of MPS I patient with short stature (Mohanalakshmi, V. & S. 2014), another study reported normal circulating level of thyroid stimulating hormone and thyroxine in MPS VI patients (Decker et al. 2010). However, findings in this chapter suggested that bone shortening in MPS VII mice was not caused by a deficiency of T3.

Circulating IHH level was decreased in P14 MPS VII mice, but the reduction did not reach statistical significance. A direct function of circulating IHH on linear bone growth have not been previously reported; however, some studies suggest that the Hedgehog signaling pathway has positive effects on hepatic IGF1 production (Matz-Soja et al. 2014; Vokes et al. 2008). It is possible that circulating IHH contributes partially to bone shortening in MPS VII mice through modulating hepatic IGF1 production. In addition, serum IHH levels decreased with age in both normal and MPS VII mice. If circulating IHH indeed can

promote bone growth through regulating hepatic IGF1, its activity is age-dependent, which is highly expressed during early postnatal period; or even prenatal period as IHH is an essential morphogen for embryonic development (Ingham & McMahon 2001).

This is the first study to investigate the level of endocrine factors in a MPS animal model at different ages. The results showed that while the circulating GH level was similar in young normal and MPS VII mice, ghrelin-induced GH secretion was greatly reduced in MPS VII mice at 2 months of age. MPS VII mice had greatly reduced IGF1, IGFBP3 and IGFALS levels in the circulation and an altered IGF1: IGFBP3: IGFALS ratio which resulted in less bioavailable IGF1. The reduced IGF1 level was caused by impaired GH-induced IGF1 secretion in the liver. Although the detailed mechanism underlying failure of IGF1 production is still not clear, diminished tyrosine-phosphorylated STAT5 expression in MPS VII liver may be involved. Local effects of GH on postnatal longitudinal bone growth have also been proposed, which either acts directly on growth plate chondrocytes (Gevers et al. 2009) or indirectly stimulates local secretion of IGF1 (Mohan, S. et al. 2003; Wang, J et al. 2004). This chapter revealed an alteration in the GH/IGF1 axis in MPS VII mice during longitudinal bone development; and the next chapter will examine the effects of paracrine/autocrine factors on chondrocyte proliferation and differentiation in MPS VII growth plate.

6 The proliferative capacity of growth plate chondrocytes in response to endocrine and paracrine/autocrine factors

6.1 Introduction

Chondrocyte activity in the growth plate is tightly regulated by the coordinated activity of multiple proteins. These proteins include but are not limited to systemic factors GH/IGF1 and T3, autocrine/paracrine factors IGF1 and IHH secreted by growth plate chondrocytes, their cartilage-specific receptors and downstream transcription factors (Mackie et al. 2008).

GH acts on resting, proliferative and pre-hypertrophic chondrocytes through locally expressed GHR (Gevers et al. 2009; Isaksson, Jansson & Gause 1982) and also stimulates the production of IGF1 by resting and proliferative chondrocytes through JAK2/STAT5 signaling (Gevers et al. 2009) and together they play major role in controlling proliferation (Mohan, Subburaman et al. 2003; Wang, J et al. 2004). GHR null mice exhibit retarded growth (Zhou, Y et al. 1997), shortened long bones, narrowed growth plate, reduced PZ and HZ height, and decreased proliferation rate (Lupu et al. 2001). Bone length of GHR null mice (Sims et al. 2000) and growth of GHR deficient patients (Backeljauw & Underwood 2001) were only partially restored by IGF1 treatment, supporting that GH has both direct and IGF1-dependent action on promoting linear bone growth. Cartilage-specific IGF1 (Wang, Y et al. 2006) and IGFR1 (Wang, Y et al. 2011) null mice exhibit reduced proliferation and increased apoptosis of chondrocytes in the growth plate. The former mice had reduced long bone growth, and the latter mice showed disorganized columnar structure of the growth plate and apparent growth retardation. These studies demonstrate the essential roles of GH, IGF1 and their receptors in controlling chondrocyte proliferation in the growth plate.

Under normal condition, T3 acts primarily on RZ and PZ chondrocytes through TR-α (Ballock et al. 1999; Robson et al. 2000). T3 promotes chondrocyte hypertrophy and inhibits chondrocyte proliferation (Robson *et al.* 2000; Stevens *et al.* 2000). The effect of T3 on

growth plate chondrocytes is indirectly mediated via GHR, IGFR1 (O'Shea et al. 2005), PTHrP and PTHrPR (Stevens et al. 2000).

IHH is produced by prehypertrophic chondrocytes and its action is mediated through its receptors PTC and SMO in the growth plate (St-Jacques, Hammerschmidt & McMahon 1999; Zhang, XM, Ramalho-Santos & McMahon 2001). IHH induces chondrocyte proliferation through transcription factors of the GLI family, and inhibits transition of chondrocytes to terminal differentiation via the IHH/PTHrP feedback loop (Hilton et al. 2005; Vortkamp et al. 1996). Deficiency of *Ihh* in mice leads to reduced chondrocyte proliferation and an expanded HZ in the growth plate (St-Jacques, Hammerschmidt & McMahon 1999), whereas overexpression of *Ihh* in mice lead to upregulated PTHrP expression and a delayed transition of chondrocytes from proliferative to hypertrophic phenotypes (Minina et al. 2001). Although its effect on chondrocyte proliferation is parallel to IGF1(Long, Zhang, et al. 2001), IGF1 can stimulate secretion of IHH by chondrocytes (Wang, Y et al. 2006; Yang, ZQ et al. 2017). MPS VII mice have a reduced gene expression level of *Ihh* in the growth plate (Metcalf et al. 2009), however; it is not clear whether the expression pattern of the morphogen IHH is affected in these mice.

The effects of GH, IGF1 and T3 on chondrocyte proliferation have not been reported in MPS cartilage. this chapter aimed to investigate the relationship between local signalling pathways and growth plate dysfunctions in MPS VII mice. As a decreased *Ihh* expression has been reported, this chapter therefore hypotheses that the altered IHH signalling pathway limits proliferative capacity of growth plate chondrocytes in MPS VII mice. The ability of MPS VII chondrocytes to proliferate in response to exogenous GH, T3, IGF1 and IHH was assessed *in vitro*. In addition, the expression pattern of IHH and gene expression levels of components of the IHH/PTHrP feedback loop were examined in the growth plate.

6.2 Cell proliferation was reduced in MPS VII chondrocytes in response to GH stimulation

GH rapidly stimulated cell proliferation in cultured normal growth plate chondrocytes at a concentration of 250 ng/mL, reaching 187.0±7.6% of untreated chondrocytes after 6 days of culture (Figure 6.1A). In contrast, a decrease of cell proliferation was observed in MPS VII chondrocytes on day 2 of culture. Cell proliferation of MPS VII chondrocytes was then slowly stimulated by exogenous GH, reaching 142.0±4.6% of untreated chondrocytes on day 6 of culture. The level of cell proliferation in GH-treated MPS VII chondrocytes was significantly lower than in normal chondrocytes on day 2, 4 and 6 of culture ($p<0.05$), suggesting that MPS VII chondrocytes were less capable of responding to GH stimulation.

To further investigate the cause(s) of the poor response of MPS VII chondrocytes to GH stimulation, transcription levels of genes involved in GH signalling pathway were examined using RNA isolated from the whole growth plate (Chapter 2.7). Expression levels of *Ghr*, *Stat5a* and *Stat5b* in MPS VII growth plate were not significantly different to those of normal growth plate (Figure 6.1B), suggesting that the delayed stimulatory effects of GH on MPS VII chondrocytes were not due to changes in GHR or STAT5s at the transcription level. However, IHC analysis (Figure 6.1C) showed an altered GHR expression pattern in MPS VII growth plate at protein level. While GHR was predominately expressed in the RZ and PZ of normal growth plate, the number of cells stained positive for GHR was reduced to 26.4% and 25.2% of normal in the RZ and PZ of MPS VII growth plate, respectively.

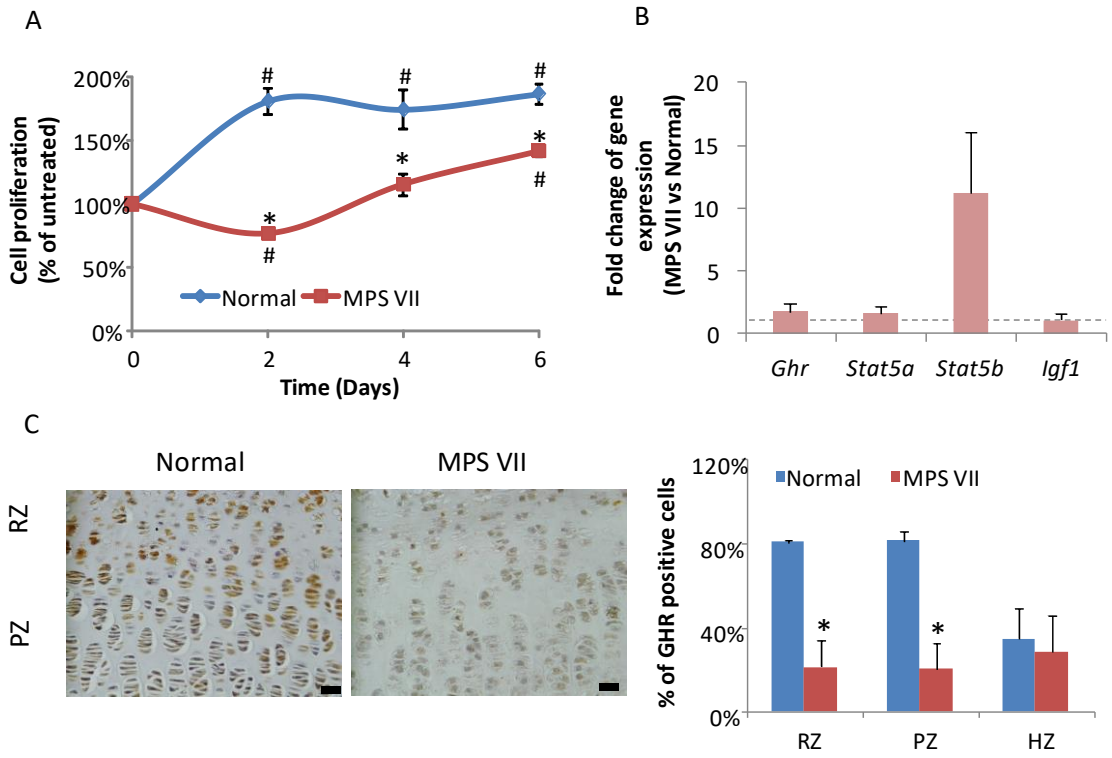

Figure 6.1 GH-induced cell proliferation was limited in MPS VII chondrocytes due to GHR deficiency. Cell proliferation of growth plate chondrocytes in response to GH treatment, results were represented as % of untreated chondrocytes, mean ± S.E.M. of n=3 replicates (A). Expression of genes involved in the GH signaling in the growth plate (B), mean ± S.E.M. of n=5 replicates. Immunohistochemical staining for GHR on P14 normal and MPS VII growth plate (C). Scale bar=50μm. IHC results were presented as percentage of positive stained cells to total cells in each zone, the mean ± S.E.M. of n=3 replicates.

* denotes significant difference between normal and MPS VII chondrocytes.

# denotes significant difference between GH treated and untreated control chondrocytes (Two-way ANOVA, Tukey post-hoc, $p<0.05$).

6.3 Exogenous IGF1 did not stimulate on cell proliferation of chondrocytes in vitro

IGF1 failed to stimulate cell proliferation by either normal or MPS VII chondrocytes (Figure 6.2A). Gene expression levels of *Igfr1*, *Igfbp2* and *Igfbp3* were not significantly different to normal in MPS VII growth plate (Figure 6.2B), suggesting that activation of IGF1 signalling in the MPS VII growth plate was not affected at the transcription level.

The expression pattern of IGF1 protein was then assessed in the growth plate using IHC (Figure 6.2C). IGF1 was predominately expressed in the RZ, early PZ and pre-HZ, and was absent from most HZ chondrocytes in the normal growth plate. The staining pattern of IGF1 in the MPS VII growth plate was not obviously different to normal growth plate in the RZ and PZ. In contrast, the number of HZ cells stained positive for IGF1 increased to 2.2-fold of normal chondrocytes.

6.4 T3 exhibited a rapid stimulatory effect on proliferation of MPS VII chondrocytes in vitro

T3 significantly decreased cell proliferation at concentration of 10ng/ml in cultured normal chondrocytes on day 6 of culture (Figure 6.3A). In contrast, T3 rapidly increased cell proliferation in MPS VII chondrocytes to 126.6±4.6% of untreated control chondrocytes in the first 2 days of culture, which was significantly higher than time-matched normal chondrocytes. Cell proliferation of MPS VII chondrocytes was significantly decreased on day 4 and day 6 of culture as compared to day 2 of culture, reaching 105.2±1.1% and 101.4±6.8% of untreated chondrocytes, respectively, which suggested that the stimulatory effect of T3 on MPS VII chondrocytes was diminished on day 4 and 6 of culture. Gene expression levels of *Trα* and *Trβ* in the MPS VII growth plate were not significantly different to normal growth plate (Figure 6.3B).

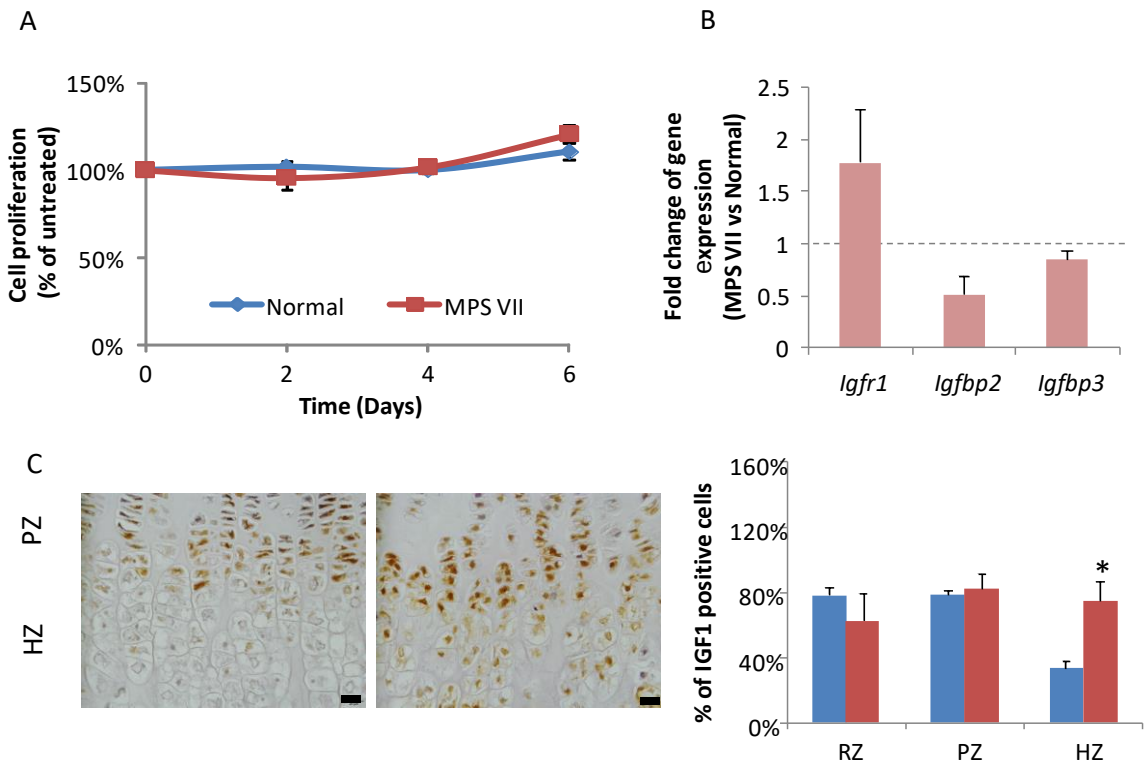

Figure 6.2 Cell proliferation of both normal and MPS VII chondrocytes was not respond to IGF1 treatment. Cell proliferation of normal and MPS VII in response to IGF1 treatment (A). Results were presented as percentage of untreated chondrocytes, mean ± S.E.M. of 3 replicates. Expression of genes involved in the activation of IGF1 signaling in the growth plate (B)**,** mean ± S.E.M. of 5 replicates Immunohistochemical staining for IGF1 on P14 normal and MPS VII growth plate (C). Scale bar=50μm. IHC results were presented as percentage of positive stained cells to total cells in each zone, mean ± S.E.M. of 3 replicates.

*denotes to significant differences between normal and MPS VII mice ($p<0.05$, Student's t-test).

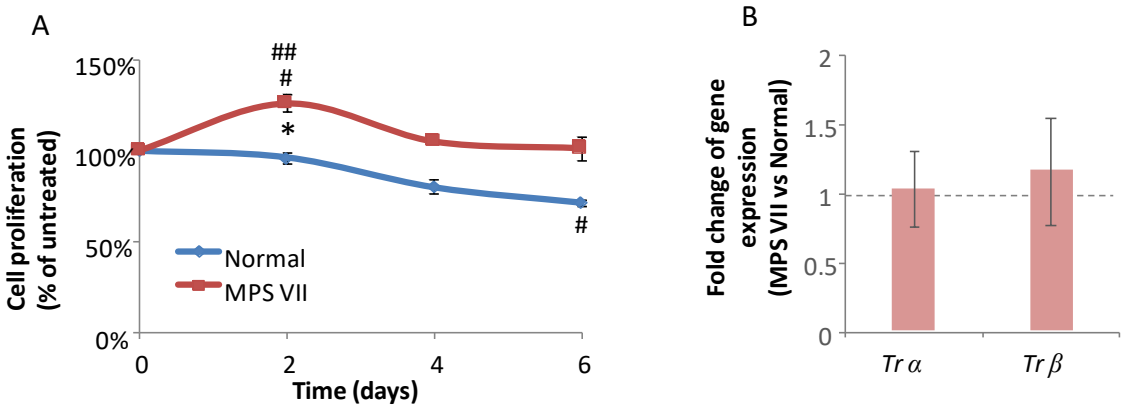

Figure 6.3 Cell proliferation of MPS VII chondrocytes was increased in response to T3 treatment. Cell proliferation of chondrocytes in response to T3 (A). Results were presented as the mean ± S.E.M. of 3 replicates. (B) Gene expression of receptors for T3 in the growth plate**.** Results were presented as the mean ± S.E.M. of 5 replicates.

* denotes significant difference between normal and MPS VII chondrocytes.

# denotes significant difference between T3 treated and untreated control chondrocytes.

denotes significant difference between T3 treated on day 2 and other days of culture (Two-way ANOVA, Tukey post-hoc, $p<0.05$).

6.5 IHH signalling pathway was dysregulated in MPS VII chondrocytes

Cell proliferation of normal chondrocytes exhibited minimal response to exogenous IHH *in vitro* (Figure 6.4A). However, IHH significantly increased cell proliferation in cultured MPS VII chondrocytes on day 2 and 4 of culture.

Expression of essential components of IHH signalling pathway was examined by real-time PCR analysis. As *Ihh* is expressed by pre-hypertrophic and hypertrophic chondrocytes and *Pthrp* is expressed by resting chondrocytes and early proliferating chondrocytes (St-Jacques, Hammerschmidt & McMahon 1999; Vortkamp et al. 1996), RNA isolated from whole growth plate was used to examine the expression of these genes. Micro-dissection of PZ of the growth plate (Chapter 2.9) enriched the genes expressed predominately by the proliferative chondrocytes, including *Smo*, *Ptch1*, *Gli3*, *Pthrpr* and *Sox9.*

Real-time-PCR analysis (Figure 6.4B) showed that the gene expression of *Ihh* significantly decreased to 0.46±0.1 fold of normal in the MPS VII growth plate. In the PZ (Figure 6.4C), *Smo* expression was not obviously changed as compared to normal; however, *Ptch1* expression was significantly elevated at 2-fold of normal ($p<0.05$). IHH downstream repressor *Gli3* expression significantly increased at 4.4±0.9 fold of normal ($p<0.05$).

The expression of PTHrP was not significantly different to normal in the MPS VII growth plate (Figure 6.4B). In the MPS VII PZ, while expression of *Runx2* was at a normal level, expression levels of *Pthrpr* and *Sox9* were significantly increased to 4.4±0.7 and 3.1±0.6 fold of normal, respectively ($p<0.05$, Figure 6.4C).

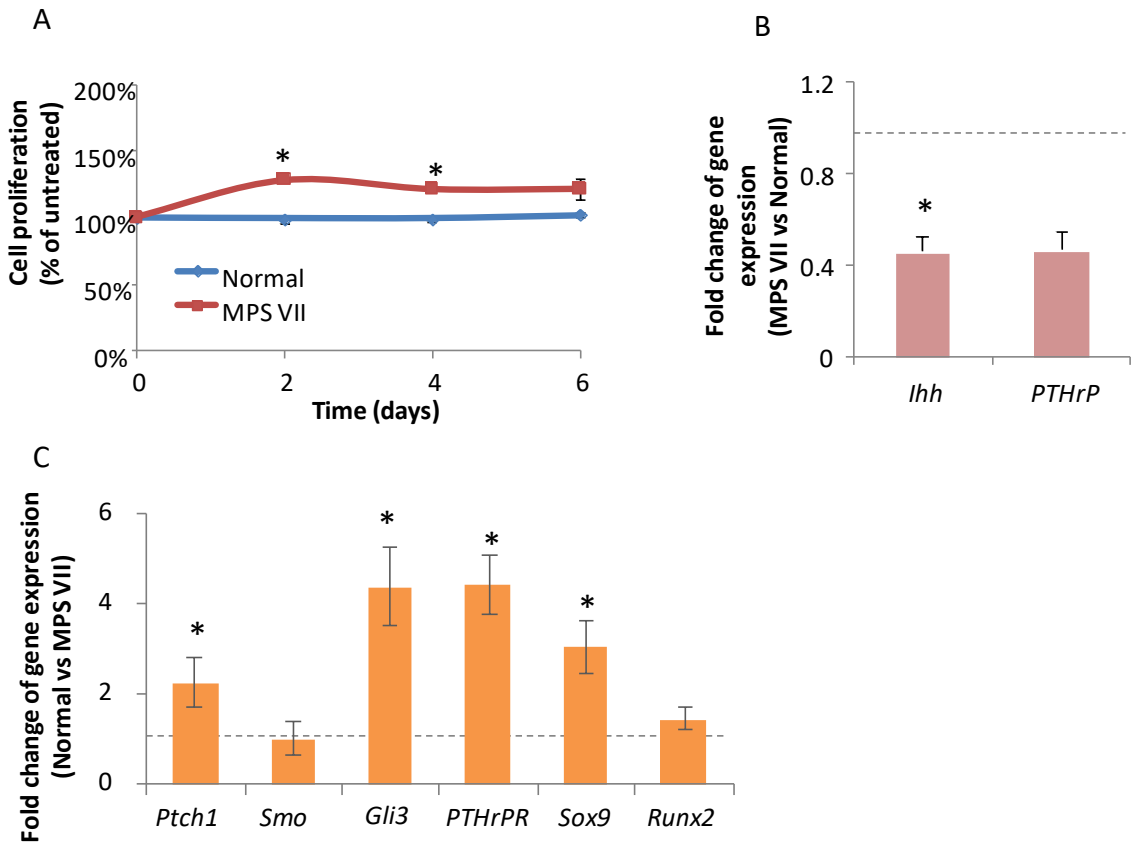

Figure 6.4 Exogenous IHH stimulated cell proliferation of MPS VII chondrocytes. Cell proliferation in response to IHH stimulation (A). Results were presented as the mean ± S.E.M. of 3 replicates. Gene expression of genes involved in IHH/PTHrP loop in the whole growth plate (B), and PZ of the growth plate (C). Results were presented as mean ± S.E.M. of 5 replicates.

* denotes to significant difference of cell proliferation between IHH-treated normal and MPS VII chondrocytes ($p<0.05$, Student's t-test).

To study the expression pattern of IHH in MPS VII growth plate, immunohistochemistry (Chapter 2.10) was used on the tibial growth plates of normal and MPS VII mice at P14, 1 and 2 months of ages. Immunostaining of IHH was observed in P14 normal and MPS VII growth plate (Figure 6.5A) but was absent from the growth plate of both normal and MPS VII mice at 1 and 2 months of ages, suggesting that production of IHH in the growth plate decreases with age in both normal and MPS VII mice. At P14, immunostaining of IHH was predominately observed in the PZ and HZ of normal growth plate (Figure 6.5A). In contrast, the number of chondrocytes positive for IHH staining was significantly decreased to 25% of normal in the PZ of MPS VII growth plate $p<0.05$, Figure 6.5B).

An increase in IHH secretion by normal chondrocytes was observed over the first 2 days of culture (Figure 6.5C). However, IHH secretion by MPS VII chondrocytes was significantly decreased, indicating an impaired secretion of IHH by cultured MPS VII chondrocytes.

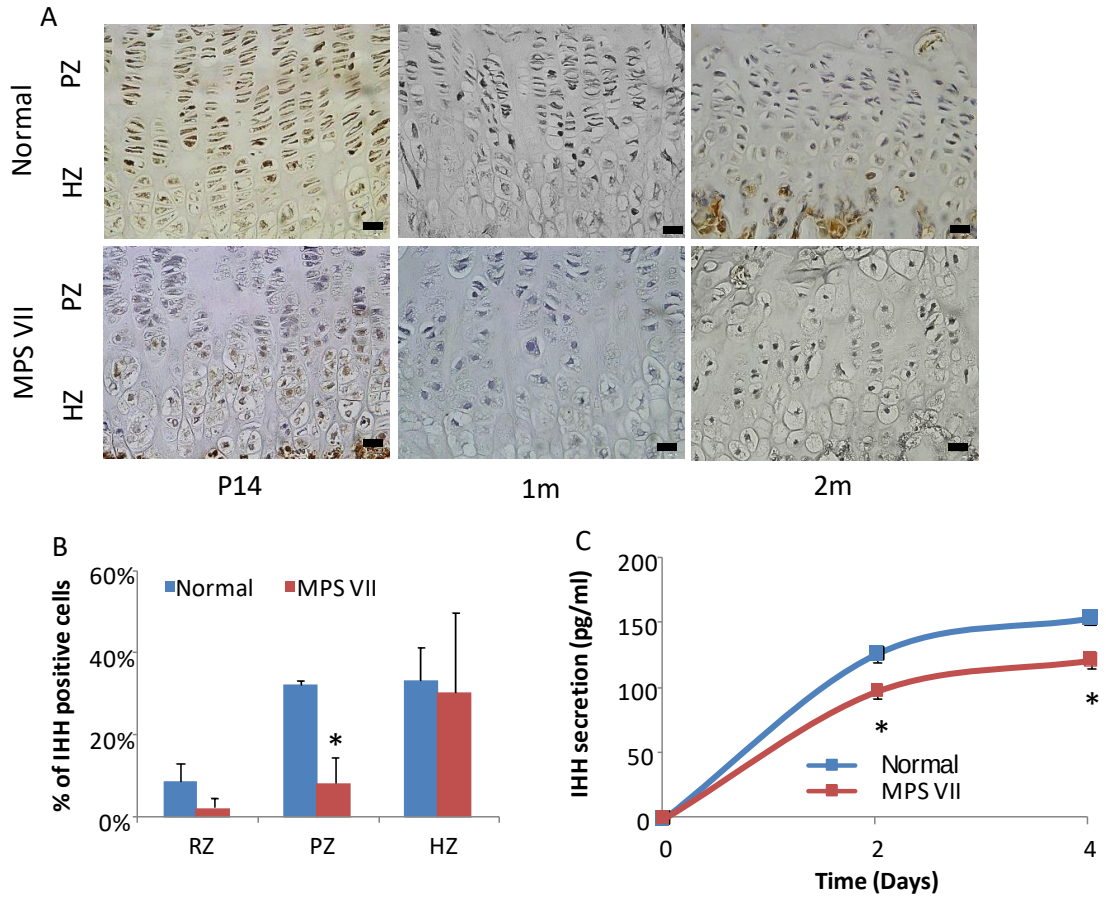

Figure 6.5 IHH production was greatly reduced in MPS VII growth plate. Immunohistochemical staining for IHH on normal and MPS VII mice at P14, 1 month and 2 months of age (A). Quantification results for P14 mice was represented were presented as percentage of positive stained cells to total cells in each zone (B). Level of IHH produced by normal and MPS VII chondrocyte in culture (C). Results were presented as the mean ± S.E.M. of 3 replicates. Scale bar=20μm.

*denotes to significant differences between normal and MPS VII mice ($p<0.05$, Student's t-test).

6.6 Discussion

Proliferation and hypertrophic differentiation of chondrocytes in the growth plate contributes to the elongation of long bones. Proliferation is known to be regulated through multiple signally pathways including GH/IGF1 axis and the IHH/PTHrP loop. Hypertrophic differentiation is regulated by thyroid hormone and also the IHH/PTHrP loop (Mackie et al. 2008). However, the effects of GH, IGF1, T3 and IHH signalling pathways on MPS VII chondrocytes remained unknown. This chapter therefore aimed to investigate the responsiveness of chondrocytes to exogenous GH, T3, IGF1 and IHH and the regulation of their corresponding signaling pathways in MPS VII growth plate.

Exogenous GH stimulated cell proliferation in both normal and MPS VII chondrocytes, but proliferation was greatly reduced in MPS VII. The observed proliferative response to GH stimulation was consistent with previous studies on rabbit and rat (Madsen et al. 1983; Ohlsson, Nilsson, Isaksson & Lindahl 1992) growth plate chondrocytes. GH appears to act on PZ chondrocytes with resting and hypertrophic chondrocytes unresponsive to GH stimulation (Oberbauer & Peng 1995). MPS VII growth plates have a lower proportion of PZ chondrocytes than normal growth plate (Figure 3.8B). Pooled chondrocytes isolated from MPS VII growth plate therefore contained less PZ chondrocytes than normal growth plate. Since GH preferentially acts on proliferative chondrocytes (Oberbauer & Peng 1995), the reduced number of PZ chondrocytes in MPS VII growth plate may explain the reduced proliferative capacity of MPS VII cells. In addition, MPS VII RZ and PZ chondrocytes expressed less GHR than normal chondrocytes. As expression of GHR determines responsiveness to GH (Isaksson et al. 1990), less GHR would also contribute to reduced proliferation of MPS VII chondrocytes.

Exogenous IGF1 failed to promote cell proliferation in both normal and MPS VII chondrocytes. This conflicts with the previous reported ability of IGF1 to stimulate

chondrocyte proliferation (Oberbauer & Peng 1995; Trippel et al. 1989). Differences in the species used (mouse *versus* cow, rabbit and rat), and anatomical site from which chondrocytes were isolated (proximal tibia growth plate *versus* distal radius growth plate and costochondral growth plate) may have contributed to the observed differences. The dose of IGF1 used for chondrocyte culture in this chapter was at a relatively high concentration compared to the literature; however, dose response assessment of IGF1 suggested lower concentrations of IGF1 (25ng/ml-250ng/ml) also did not stimulate chondrocyte proliferation (Figure 2.2).

T3 had an inhibitory effect on cell proliferation of normal chondrocytes, but stimulated cell proliferation of MPS VII chondrocytes on day 2 of culture. T3, which acts through TRs expressed by the resting and proliferative chondrocytes, triggers initiation of proliferation, but subsequently inhibits further proliferation and promotes terminal differentiation (Robson et al. 2000; Williams 2013). Altered ratio of RZ to PZ cells found in MPS VII growth plate (Figure 3.8A and B) may contribute to the greater response to T3 in MPS VII chondrocyte culture.

While IHH had no effects on normal chondrocyte proliferation, it significantly stimulated proliferation of MPS VII chondrocytes. IHH has been shown to promote cell proliferation of PZ chondrocytes isolated from the chick embryo sterna, but not RZ or HZ chondrocytes (Shimo, Tsuyoshi et al. 2008). Sonic hedgehog (SHH) protein, a variant of IHH, stimulated proliferation of chondrocytes isolated from 3 days old murine growth plate, but did not affect the proliferation of chondrocytes from 3 week old mice (Iwasaki, M, Jikko & Le 1999). This study suggested that the function of SHH on proliferation is age dependent and is more effective on young chondrocytes. In the present chapter, normal and MPS VII chondrocytes were isolated from the growth plates of P14 mice, which falls between the above two ages. The unresponsiveness of normal chondrocytes to IHH in culture may

therefore be attributed to the age of the chondrocytes. Chondrocytes from P14 were older and less effective than chondrocytes from 3 days old mice to respond to IHH. In contrast, although MPS VII chondrocytes were obtained from age-matched animals, they expressed an elevated level of *Ptch1* in the PZ, the receptor of IHH. Thus, exogenous IHH stimulated cell proliferation in MPS VII chondrocytes culture.

A reduction of IHH expression was noticed in the whole MPS VII growth plate at the transcription level, which was consistent with a previous finding (Metcalf et al. 2009). The level of IHH protein secreted by MPS VII chondrocytes was also greatly decreased in both the PZ of MPS VII growth plate and in culture. As a result, proliferation of chondrocytes, which is partially regulated by IHH (Long, Zhang, et al. 2001; Razzaque et al. 2005), was reduced (Figure 3.8B). This hypothesis can be supported by the observation of elevated *Gli3* expression in the PZ of MPS VII growth plate (Figure 6.6). Less IHH is available to bind to PTC for downstream activation of SMO, increasing the expression of *Gli3*. Transcription of IHH target genes is therefore repressed and chondrocyte proliferation in MPS VII growth plate is limited. However, in this chapter expression of *Smo* in the MPS VII PZ was not apparently different to that of normal PZ at the transcription level. Further investigations are required to assess if the protein level of SMO or activation of SMO is affected in MPS VII growth plate.

While this chapter focused on the proliferative response of chondrocytes, the results suggested that transition to the hypertrophic phenotype was also altered. In addition to promoting proliferation, IGF1 promotes linear bone growth by controlling the expansion of hypertrophic chondrocytes (Wang, J, Zhou & Bondy 1999). As shown in Figure 6.2C, IGF1 is expressed in the pre-HZ of normal growth plate and is subsequently reduced in the HZ as chondrocytes mature. In contrast, a higher proportion of MPS VII chondrocytes continued

to express IGF1 in the HZ, indicating that transition of MPS VII chondrocytes from proliferation to hypertrophic differentiation is delayed.

The levels of SOX9, PTHrP and its receptor need to be downregulated to allow hypertrophic differentiation of chondrocytes (Huang, W et al. 2001; Kronenberg 2003; Weir et al. 1996). However, elevated gene expression levels of *Pthrpr* and its downstream target *Sox9* were observed in the PZ of MPS VII growth plate. PTHrP is synthesized by RZ chondrocytes, diffusing to the PZ and pre-HZ chondrocytes where it bound by PTHrPR during postnatal growth (Chau et al. 2011; Lee, K et al. 1996; Schipani et al. 1997). Alteration of gene expression level of *PTHrP* in MPS VII growth plate would be masked by the whole growth plate. Therefore, in this chapter, examination of PTHrP level was assessed indirectly by the expression of *Pthrpr* that is expressed by the PZ chondrocytes. Persistent SOX9 protein was observed in canine vertebral chondrocytes during proliferative to hypertrophic maturation (Peck et al. 2015). Thus, it is likely that persistent levels of *Pthrpr* and *Sox9* in the PZ result in delayed transition of MPS VII chondrocytes from proliferation to hypertrophic phenotype (Figure 6.6). In addition, as IHH and PTHrP form a negative feedback loop (Minina et al. 2002; Vortkamp et al. 1996) in the growth plate, an increase of PTHrP would limit IHH secretion by pre-hypertrophic chondrocytes, which could explain the reduced IHH level observed both *in vitro* and *in vivo* in MPS VII chondrocytes.

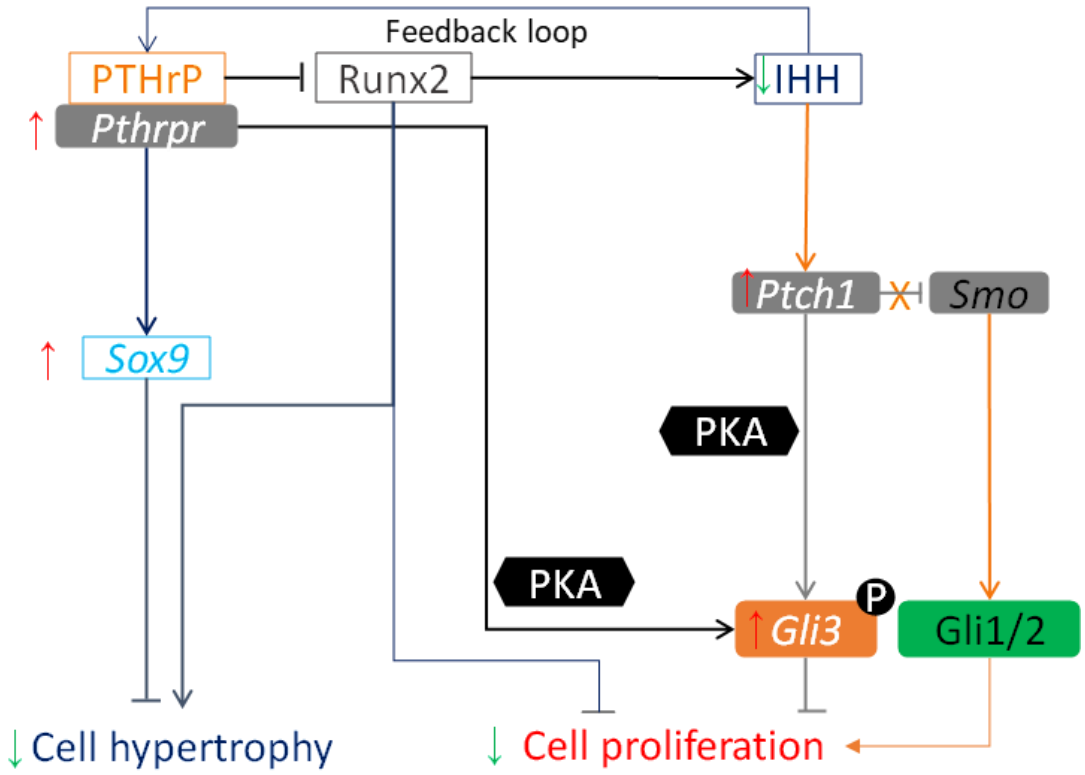

Figure 6.6 Altered IHH/PTHrP signalling in MPS VII growth plate. Chondrocyte proliferation in MPS VII growth plate is inhibited by decreased IHH expression and elevated *Ptch1* and *Gli3*. Transition of MPS VII chondrocytes to hypertrophy is also inhibited by persistent expression of *Pthrpr* and *Sox9*. Arrows indicate stimulatory pathways, while crossed lines indicate inhibitory pathways. Red arrows indicate upregulated genes and green arrows indicate downregulated proteins.

In summary, the regulation of proliferation in MPS VII chondrocytes as well as their transition to hypertrophic differentiation was affected due to dysfunctions of GH, IGF1 and IHH signalling pathways. MPS VII chondrocytes had less capacity to proliferate in response to GH stimulation, due to reduced expression of GHR in the RZ and PZ. Proliferation of chondrocytes may also be limited by the reduction of IHH in MPS VII growth plate. However, exogenous IGF1 does not play a role on chondrocyte proliferation in culture. In addition, this chapter found that more MPS VII HZ chondrocytes continued to express IGF1, indicating a phenotype more characteristic of proliferative chondrocytes. The persistent expression of *Pthrpr* and *Sox9* by PZ chondrocytes also suggested that proliferative phenotype were maintained in MPS VII growth plate instead of transiting to hypertrophic differentiation.

7 General Discussion

The majority of bones in the human skeleton are formed through the process of endochondral ossification that originate from a cartilage template (Abad et al. 2002; Long & Ornitz 2013; Mackie, Tatarczuch & Mirams 2011). This process is controlled by a complex network of endocrine factors, paracrine/autocrine factors, transcription factors as well as cell cycle regulators, which are well characterized under the normal condition. However, limited attention has been given to bone development in MPS patients and animal models. Pathogenesis of reduced bone length in MPS is still not understood. This thesis firstly sought to address the progression of bone growth defects in different MPS mouse models. Second to this, potential signalling pathways that are affected in MPS VII during endochondral bone development were determined.

7.1 Shortened long bone growth in MPS VII mice is a result of dysfunction of the EO from early ages

Initial evaluation of long bone and vertebral lengths at maturity revealed that the reduction in bone lengths at maturity was greatest in the severe MPS VII ($Gus^{mps/mps}$ strain) murine model (Figure 3.1), and were consistent with human (Montano et al. 2016; Sly et al. 1973), canine (Herati et al. 2008; Smith, LJ et al. 2012) and feline MPS VII (Fyfe et al. 1999; Wang, P et al. 2015). Femur and tibia lengths were significantly shorter than normal from P14 of age onwards and growth rate worsened with age (Figure 3.2), which are consistent with MPS patients whose bone growth velocities decline significantly after one year of age (Kubaski et al. 2016; Montano et al. 2016; Montaño et al. 2008; Patel, Suzuki, Maeda, et al. 2014; Quartel et al. 2015; Rozdzynska-Swiatkowska et al. 2015).

7.1.1 MPS VII mice have delayed formation of ossification centres from early ages

Development of the POC and SOC in MPS VII tibia followed the same pattern as in normal mice; however, the process of EO was delayed in utero (development of the POC) and

worsened during postnatal long bone growth (development of the SOC and growth plate) (Figure 3.3-3.5). Chondrocytes started to differnetiate to hypertrophic chondrocytes from the middle of the diaphysis in both normal and MPS VII mice at ~E14.5. Formation of the POC that is characterized by blood vessel invasion and bone deposition initiated at ~E15.5 in normal mice, whereas it was approximately one day delayed in MPS VII mice (Figure 3.3A). This delay in development coincides with the first appearance of storage material in chondrocytes of MPS VII mice (Vogler et al. 2005), suggesting a relationship between cellular storage and the abnormal formation of the POC. Early storage has also been observed in placenta tissue of MPS II and VI patients (Baldo et al. 2011); however, it is still not known whether chondrocytes from MPS human foetus have storage or not. While hypertrophic chondrocytes were first observed at P7 in the middle of epiphysis of both normal and MPS VII mice, initiation of the SOC in most MPS VII mice was observed at P12, which is approximately two days later than that of normal (Figure 3.4A). A similar delay in the deposition of bone in the SOC was observed in MPS VII dog vertebrae, femur and tibia (Peck et al. 2015). Findings from this theise suggested that bone deposition was delayed in MPS VII mice, which was more pronounced in the SOC after birth than the POC *in utero*, coinciding with a greater degree of GAG storage in older chondrocytes.

Both normal and MPS VII chondrocytes underwent hypertrophic expansion at the same time in the POC and SOC. However, in this study hypertrophic expansion was defined by an increase in cell volume (Cooper et al. 2013; Farnum et al. 2002). Their ability and the ability of bone, endothelial and perichondrial cells to support angiogenesis and osteogenesis was not examined. Previous studies have observed decreased expression of MMP13 in 3 weeks old MPS VII tibia (Metcalf et al. 2009) and reduced collagen II degradation, which is mediated by cathepsin K, in MPS I osteoclasts (Wilson, S et al. 2009). These suggested that MPS VII hypertrophic chondrocytes may not express one or more of the enzymes for matrix remodelling (such as MMPs) and growth factors (such as VEGFs) for invasion of

blood vessels to the same extent as normal, leading to the subsequent delay in bone deposition in MPS VII tibia.

These enzymes and growth factors are regulated by paracrine/autocrine factors during bone development. MMP2, MMP3, MMP9 and MMP13 can be induced by PTH/PTHrP (Chiusaroli et al. 2003; Kawashima-Ohya et al. 1998; Selvamurugan et al. 2000). *MMP13* expression can also be promoted by IHH in osteoarthritis cartilage (Wei et al. 2012). Vascularization can be regulated by IGF1 through hypoxia, which upregulates VEGF expression (Piecewicz et al. 2012). Indeed, altered *Ihh* and *Pthrpr* expression in the growth plate (Figure 6.4) and reduced circulating IGF1 level (Figure 5.2) were observed in MPS VII mice. The former would delay chondrocyte hypertrophy (discussed in section 7.1.3), which disrupts the secretion of MMPs and the latter would contribute to poor vascularization and bone deposition (Akeno et al. 2002; Mochizuki et al. 1992), and thus these altered signalling pathways could lead to delayed formation of ossification centres in MPS VII mice. Further studies linking these altered signalling pathways to matrix degradation and vascularization are required to understand the mechanism behind the delayed formation of ossification centres in MPS VII mice.

7.1.2 The number of MPS VII chondrocytes transit to proliferative status was reduced

Histomorphometric analysis showed that the number of chondrocytes was significantly decreased in MPS VII PZ (Figure 3.8B). Chondrocytes proliferation is strictly controlled by synchonized cell cycle progression (Beier 2005; LuValle & Beier 2000). CyclinD1 and its downstream target E2F1 are highly expressed in the RZ and early PZ of the growth plate for G1-S phase transition (Figure 4.1 and 4.3). E2F1 induces transcription of genes involved in DNA replication, such as CyclinE, CyclinA, minichromosome maintenance proteins (MCMs) and DNA polymerases during late G1-S phase (Ohtani, DeGregori & Nevins 1995; Ren et al. 2002). Chondrocytes in the PZ then undergo rapid DNA replication and mitotic

division for several rounds and withdraw from the cell cycle for terminal differentiation to the hypertrophic phenotype.

An increased number of chondrocytes stained postive for Ki67 and E2F1 was observed in MPS VII PZ (Figure 4.3). However, fewer MPS VII chondrocytes stained posititve for phos-hisH3 a marker for mitosis (Figure 4.4). Although the number of chondrocytes in the S phase was not examined in this thesis, a previous study reported a reduced prolfieration rate in MPS VII PZ using BrdU staining, indicating a reduction in DNA replication (Metcalf et al. 2009). These results suggested that although more MPS VII chondrocytes were in the G1 phase and had committed to enter the S phase, progression to DNA replication and mitotic division was reduced through an as yet unknown mechanism.

Upon entry to S phase, regulators of G1-S phase transition, such as Cyclin D1, Cyclin E and E2Fs are dispensable and therefore are degraded by proteasomes in an ubiquitination-dependent manner (Alt et al. 2000; Clurman et al. 1996; Hateboer et al. 1996; Koepp et al. 2001; Lin, DI et al. 2006; Marti et al. 1999). Although it has not been reported that ubiquitination of these proteins are regulated by lysosomal pathways, impairment of the ubiquitin-dependent protein degradation has been observed in MPS VI and other lysosomal storage disorders (Bifsha et al. 2007; Tessitore, Pirozzi & Auricchio 2009). Therefore, it is likely that ubiquitin-dependent degradation of Cyclin D1 and E2F1 would be inhibited by lysosomal storage in MPS VII chondrocytes, resulting in increased levels of these molecules.

Chondrocyte proliferation is also promoted by signalling pathways including GH, IGF1 and IHH (Isaksson, Jansson & Gause 1982; Isgaard et al. 1988; Long, Zhang, et al. 2001). Although the circulating GH level was normal in MPS VII mice (Figure 5.1), fewer MPS VII chondrocytes expressed GHR in the RZ and PZ as compared to normal mice (Figure 6.1). Cell proliferation of MPS VII chondrocytes in response to GH stimulation was greatly

reduced compared to normal chondrocytes (Figure 6.1). GH directly induces resting chondrocytes to proliferate through GHR signalling (Baker et al. 1993; Gevers et al. 2009; Hunziker, Wagner & Zapf 1994; Isaksson, Jansson & Gause 1982). It also promotes proliferation preferentially by the PZ chondrocytes (Oberbauer & Peng 1995). As MPS VII mice exhibited fewer number of chondrocytes in the PZ (Figure 3.7) and fewer of these cells expressed GHR, the proliferative capacity of MPS VII chondrocytes in response to GH was therefore reduced.

MPS VII mice had reduced circulating IGF1 levels (Table 5.1 and Figure 5.2), which is consistent with several cases of MPS patients (Gardner et al. 2011; Toledo et al. 1991). Although GHR, the primary mediator of GH-induced IGF1 production, was deficient (Figure 6.1), local secretion of IGF1 was not affected in MPS VII PZ (Figure 6.2). The relative roles of endocrine (circulating) and autocrine/paracrine (local) IGF1 on skeletal growth are controversial in the last two decades. Liver-specific ablation of *Igf1* gene at birth in mice showed a marked reduction (75% of normal) in the circulating IGF1 level, but normal bone growth at post-weaning ages (Yakar et al. 1999), suggesting that endocrine IGF1 is not necessary for longitudinal bone growth at later postnatal ages. Ablating the *Igf1* gene at 24-28 days after birth reduced circulating IGF1 to a similar level as above (Sjogren et al. 1999). It is likely that the low, but detectable serum IGF1 is sufficient to support normal postnatal bone growth. Decreased growth plate height, but not bone shortening of hepatic *Igf1* and *Igfals* double knockout mice was restored by IGF1 treatment (Yakar et al. 2002), suggesting that endocrine IGF1 promotes linear bone growth through the growth plate. Knockout of GHR in mice lead to reduced endocrine and autocrine/paracrine IGF1 levels, resulting in significantly decreased femur length and bone mass (Wu, Y et al. 2013). However, normalization of endocrine IGF1 level was not sufficient to restore these skeletal phenotypes, indicating that autocrine/paracrine IGF1 is also essential to coordinate linear bone growth. It is likely that circulating IGF1 (75% of which is liver derived) mainly

promotes bone deposition during endochondral ossification, and is essential during embryonic and early postnatal bone growth (Baker et al. 1993; Wang, Y et al. 2006). Circulating IGF1 also promotes chondrocyte proliferation (Yakar et al. 2002). If circulating IGF1 is indeed important for promoting chondrocyte proliferation, the reduced number of PZ chondrocytes (Figure 3.7) would be attributed to the decreased bioactive IGF1 level in the circulation of MPS VII mice.

Findings of deficient GHR in the growth plate and reduced IGF1 level in the circulation in MPS VII mice may explain the failure of GH therapy to improve bone growth in MPS patients (Gardner et al. 2011; Polgreen & Miller 2010; Polgreen et al. 2009; Polgreen et al. 2014). It is possible that GH therapy alone or the dose of GH used in the above trails is not sufficient to benefit bone growth of MPS patients with short stature. Early treatments prior to the onset of bone shortening may have better effects since the function of endocrine IGF1 on linear bone growth is essential for embryonic and early postnatal development (Baker et al. 1993; Wang, Y et al. 2006).

Both gene expression of *Ihh* and the number of chondrocytes that stained positive for IHH were significantly decreased in the PZ of MPS VII growth plate (Figure 6.4 &6.5). These observations were accompanied by an elevated gene expression level of *Gli3*, suggesting a reduction in the IHH signalling pathway, which is associated with the reduced proliferation in the MPS VII growth plate (Long, Zhang, et al. 2001; Razzaque et al. 2005). Secretion of IHH by chondrocytes is stimulated by IGF1(Wang, Y et al. 2006; Yang, ZQ et al. 2017); thus, it is possible that the decreased IHH secretion in the PZ is caused by the reduction of circulating IGF1 in MPS VII mice (Table 5.1 and Figure 5.2). In addition, IHH has been shown to be inhibited by interleukin-1β (IL-1β), a pro-inflammatory cytokine (Thompson, CL et al. 2015). Inflammation occupies a critical role in lysosomal storage disorders (Calogera 2016) and MPS (Simonaro et al. 2005; Simonaro et al. 2010; Simonaro, Haskins

& Schuchman 2001). Although evidence indicating the relationship between inflammation and the altered IHH signalling pathway in MPS has not yet been reported, downregulation of inflammation either by knockout of toll-like receptor 4 or use of anti-inflammatory drugs has been shown to have normalized structure of the growth plate in MPS VII mice and small improvements on bone growth of MPS IV rats receiving ERT, respectively (Eliyahu et al. 2011; Simonaro et al. 2010). Further studies are required to reveal the relationship between inflammation in MPS and the altered signalling pathways observed in this thesis.

However, although GH, IGF1 and IHH are known to promote chondrocyte proliferation, and that CyclinD1 is a downstream target of both IGF1 and IHH (Mairet-Coello, Tury & DiCicco-Bloom 2009; Tian et al. 2014), a direct relationship between GH, IGF1 and IHH and cell cycle regulators has not been shown in this study.

7.1.3 Transition of chondrocyte to hypertrophic differentiation was delay in MPS VII mice

Histomorphometric analysis showed that the number of chondrocytes was lower than normal (Chapter 3.4, Figure 3.8C), suggesting that fewer proliferative chondrocytes differentiate to hypertrophic chondrocytes in MPS VII growth plate. Chondrocytes withdraw from the cell cycle to embark upon hypertrophic differentiation. The decision by chondrocytes to exit the cell cycle is made during G1 phase (Zetterberg & Larsson 1985). Normal chondrocytes in the pre-HZ and HZ express $p57^{kip2}$ highly (Chapter 4.4, Figure 4.5), which downregulates CyclinD1/CDK activity. E2F4 proteins enter the nucleus of these chondrocytes and form complexes with pocket proteins (pRb, p130 and p107) to inhibit E2F1. Transition to S phase is therefore limited and chondrocytes exit the cell cycle for hypertrophic differentiation.

Significantly fewer MPS VII HZ chondrocytes expressed $p57^{kip2}$ (Figure 4.5); instead these cells continued to express CyclinD1 and higher levels of phos-pRb and E2F1 (Figure 4.1, 4.2A & 4.3A). These observations indicated that fewer MPS VII HZ chondrocytes withdrew from the cell cycle for hypertrophic differentiation.

The transition of chondrocytes to the hypertrophic phenotype is also regulated by coordinated signalling pathways including IGF1 signalling pathway and IHH/PTHrP negative feedback loop. While local IGF1 was downregulated in normal HZ, a higher proportion of MPS VII chondrocytes continued to express IGF1 in the HZ (Figure 6.2). Although it has not been reported in cartilage cells, IGF1 downregulates $p57^{kip2}$ and upregulates CylinD1 in cortical precursor cells *in vitro*, which is potentially mediated through the PI3K/AKT/GSK3β-dependent signalling pathway (Isgaard et al. 1988; Mairet-Coello, Tury & DiCicco-Bloom 2009; Schlegel et al. 2010). Thus, the limited cell cycle withdrawal for hypertrophic differentiation may be partially due to the elevated autocrine/paracrine production of IGF1 in the HZ of MPS VII growth plate.

Gene expression of *Pthrpr* and *Sox9* was elevated in the PZ of MPS VII growth plate as compared to age-matched normal PZ (Figure 6.4). Consistent with this finding, persistence of SOX9 protein was observed in MPS VII dog vertebrae epiphyseal chondrocytes during proliferative-hypertrophic turnover (Peck et al. 2015). PTHrP maintains chondrocytes at proliferative stage by promoting SOX9; and delays chondrocyte hypertrophy by repressing RUNX2 and $p57^{kip2}$ (Guo et al. 2006; MacLean et al. 2004). Altered PTHrP signalling in the PZ therefore would maintain the proliferative phenotype of MPS VII chondrocytes through increased expression of *Pthrpr* and *Sox9* and delay their transition to hypertrophic differentiation by inhibiting $p57^{kip2}$-dependent cell cycle withdrawal.

7.2 Summary

While this thesis demonstrated that $Gus^{mps/mps}$ mice representing severe MPS VII displayed the greatest reduction in bone elongation, findings from this thesis also have direct relevance for other MPS types displayed bone growth defects. A detailed picture of long bone development during the latter part of pregnancy and the postnatal period in MPS VII mice has been drawn. In addition, a potential mechanism to explain growth plate dysfunction in MPS VII mice is presented (Figure 7.1). The main findings from this thesis are:

1) Programmed formation of the POC and SOC is delayed in MPS VII mice.

2) Chondrocyte proliferation is reduced in MPS VII growth plate, due to disrupted progression of chondrocytes to mitotic division, reduced circulating IGF1 levels, decreased capacity of MPS VII chondrocytes to respond to GH due to GHR deficiency and reduced secretion of IHH by MPS VII chondrocytes.

3) Hypertrophic differentiation is also delayed as MPS VII HZ chondrocytes maintain proliferative phenotype and do not withdrawal from the cell cycle due to persistent local IGF1 and expression of *Pthrpr* and *Sox9*.

Collectively, these findings suggested that reduced proliferation and hypertrophy in the growth plate are both implicated in bone shortening in MPS VII mice. However, there are some limitations in this thesis. Alteration of cell cycle regulators and local factors were characterized based on the observation of expression pattern in the growth plate using immunohistochemistry but was not quantitatively analysed. In addition, GH is secreted in a pulsatile manner, which would fluctuate widely in elder animals. Although GH level in elder mice was amplified by ghrelin injection, it would better to assess GH level using serum samples collected at short intervals (Huang, L et al. 2014).

To date, no published studies have investigated comprehensively the growth retardation in MPS by studying bone shortening, growth plate dysfunction and regulation of endochondral ossification using murine models. Our novel findings have provided a detailed picture of MPS VII bone phenotype and growth plate dysfunction, which will guide future directions of investigating the mechanism behind the growth failure in MPS. This thesis also has highlighted the fact that bone phenotypes of MPS are established before birth, which may explain the difficulty experienced by clinicians and researchers in improving bone growth by therapies initiated during childhood.

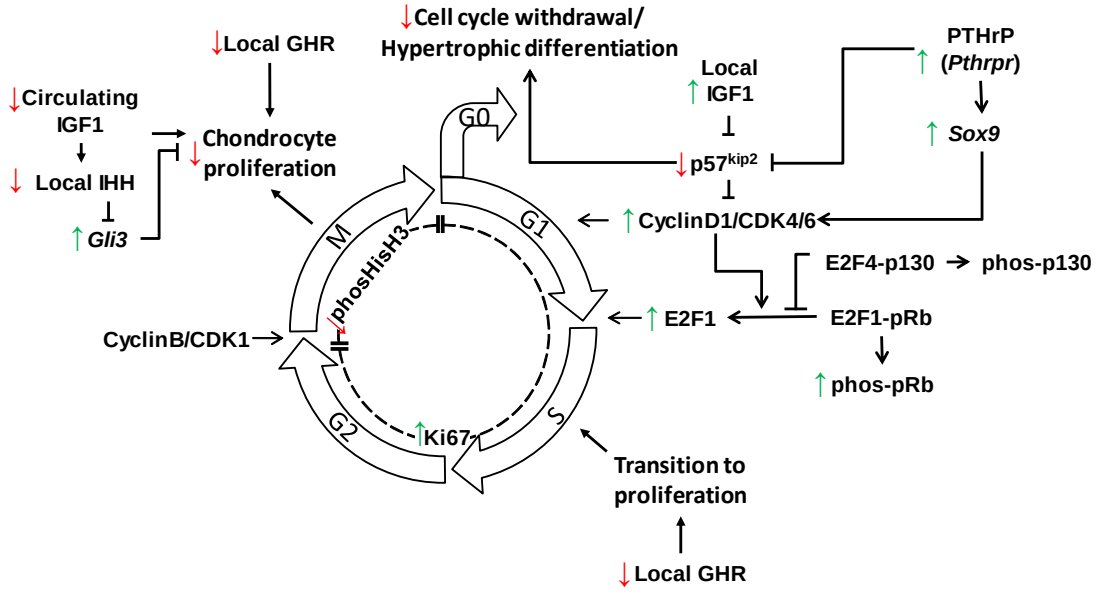

Figure 7.1 Interaction of altered signalling pathways and cell cycle progression in MPS VII growth plate. Transition of chondrocytes to proliferation (DNA replication) is downregulated by GHR deficiency in the RZ and PZ. Later, mitotic division in the PZ chondrocytes is inhibited due to reduced bioactive IGF1 in the circulation and downregulated secretion of IHH by MPS VII chondrocytes. As a result, proliferation of MPS VII chondrocytes is limited. Fewer MPS VII HZ chondrocytes withdraw from the cell cycle for hypertrophic differentiation. This is due to inhibited $p57^{kip2}$ and persistent

CyclinD1 and E2F1 in the HZ, which could be attributed to persistence of local IGF1 and expression of *Pthrpr* and *Sox9* in MPS VII growth plate.

8 Appendices

Appendix A: Materials

Agarose, DNA grade	Progen Biosciences, QLD, Australia
Alician Blue 8GX	Sigma-Aldrich Pty. Ltd., NSW, Australia
Alizarin Red S	ProSciTech Pty. Ltd., QLD, Australia
Bovine Serum Albumin (BSA)	Sigma-Aldrich Pty. Ltd., NSW, Australia
Bradford assay kit	Bio-Rad Laboratories Pty., Ltd., NSW, Australia
Cell and Tissue Staining Kit(anti-rabbit and anti-goat)	R&D systems, Minneapolis, USA
Chloroform	Invitrogen Australia Pty. Ltd., VIC, Australia
Citric acid	Ajax Finechem Pty. Ltd., Seven Hills, NSW
CyQUANT® Direct Cell Proliferation Assay Kit	Molecular Probes, Invitrogen Australia Pty. Ltd., VIC, Australia
dNTPS	Roche Diagnostics, Mannheim, Germany
Diethylpyrocarbonate (DEPC)	Sigma-Aldrich Pty. Ltd., NSW, Australia
Dulbecco's PBS	JRH Biosciences Pty. Ltd., VIC, Australia
EDTA	BDH (Merck) Pty. Ltd., Kilsyth, VIC, Australia
Ethidium Bromide	Sigma-Aldrich Pty. Ltd., NSW, Australia
Fast Green	ProSciTech Pty. Ltd., QLD, Australia

Fetal calf serum Life Technologies Pty. Ltd., VIC, Australia

Fluorescein isothiocyanate (FITC) (#656111) ThermoFisher, Australia

Geltrex LDEV-Free hESC-qualified reduced growth factor basement membrane matrix Thermofisher, Australia

Ghrelin (#AS-24159) AnaSpec Inc, CA, USA

Glycine Ajax Finechem Pty. Ltd., Seven Hills, NSW, Australia

H_2O_2 BDH (Merck) Pty. Ltd., VIC, Australia

Hams F-12 Sigma-Aldrich Pty. Ltd., NSW, Australia

Horse serum (#16050130) ThermoFisher, Australia

Immunocal^{Tm} Decal Corporation, NY, USA

Isoflurane Abbott Australasia Pty. Ltd.

Isopropanol Ajax Finechem Pty. Ltd., Seven Hills, NSW, Australia

Leica CV Mounting Media Leica Microsystems Pty Ltd, NSW, Australia

Lithium Chloride (LiCl) Sigma-Aldrich Pty. Ltd., NSW, Australia

Lithium Carbonate (Li_2CO_3 Ajax Finechem Pty. Ltd., Seven Hills, NSW, Australia

Magnesium Chloride ($MgCl_{2)}$ Roche Diagnostics, Mannheim, Germany

Mayer's hematoxylin ProSciTech Pty. Ltd., QLD, Australia

Mouse GH ELISA kit (EZRMGH-45K) EMD Millipore, USA

Mouse/rat IGF1 Quantikine ELISA kit (MG100)	R&D systems, USA
Mouse IGFALS ELISA kit (MBS912703)	MyBioSourse Inc, San Diego, USA
Mouse IGFBP3 ELISA kit (EMIGFBP3)	ThermoScientific, Australia
Mouse/rat Triiodothyronine ELISA kit (SE120091)	Sigma, Australia
Mouse Indian Hedgehog ELISA kit (MBS706033)	MyBioSource Inc., San Diego, USA
Sodium Chloride (NaCl)	Ajax Finechem Pty. Ltd., Seven Hills, NSW, Australia
Sodium Citrate (Na_3citrate)	Ajax Finechem Pty. Ltd., Seven Hills, NSW, Australia
Sodium Hydroxide (NaOH)	Ajax Finechem Pty. Ltd., Seven Hills, NSW, Australia
SYBRGreen PCR master mix	Applied Biosystems, California, USA
OCT	ProSciTech Pty. Ltd., QLD, Australia
Paraformaldehyde	MP Biomedicals, Ohio, USA
PCR Lysis Reagent	Viagen Biotech Inc., Los Angeles, CA
PCR reaction buffer	Roche Diagnostics, Mannheim, Germany
Penicillin/ Streptomycin	Life Technologies Pty. Ltd., VIC, Australia
Phenol	Invitrogen Australia Pty. Ltd., VIC, Australia
Polybrene	Sigma-Aldrich Pty. Ltd., NSW, Australia
Potassium hydroxide (KOH)	Ajax Finechem Pty. Ltd., Seven Hills, NSW, Australia

Primers and Oligos	GeneWorks, SA, Australia
Prolong-Gold DAPI (P36931)	ThermoFisher, Australia
Proteinase K	Roche Diagnostics, Mannheim, Germany
Proteinase inhibitor (P8340)	Sigma-Aldrich Pty. Ltd., NSW, Australia
pUC19/*HpaII* DNA markers	GeneWorks, SA, Australia
QuantiTect® Reverse Transcription Kit	Qiagen, Maryland, USA
Recombinant mouse growth hormone (cat#D-67335)	PromoKine, Heidelberg, Germany
Recombinant mouse IGF1 (#791-MG)	R&D systems, MN, USA
Recombinant human/mouse IHH (#31705-HH/CF)	R&D systems, MN, USA
RNaqueous® Micro Kit	Ambion, Life technologies, VIC, Australia
RNeasy micro kit	Qiagen, Maryland, USA
Safranin O	ProSciTech Pty. Ltd., QLD, Australia
SAM-HRP	Chemicon, Australia
SDS	Ajax Finechem Pty. Ltd., Seven Hills, NSW, Australia
Sodium Acetate	BDH (Merck) Pty. Ltd., VIC, Australia
Solv21C	United Bioscience, VIC, Australia
SYBR® Green Master Mix	Invitrogen Australia Pty. Ltd., VIC, Australia
Taq DNA polymerase	Roche Diagnostics, Mannheim, Germany

Tris-acetate	Roche Diagnostics, Mannheim, Germany
Trypsin/EDTA	Sigma-Aldrich Pty. Ltd., NSW, Australia
Trizol Reagent	Invitrogen Australia Pty. Ltd., VIC, Australia
3,3′,5-Triiodo-L-thyronine powder (T3, T2877)	Sigma-Aldrich Pty. Ltd., NSW, Australia
4C1N	Sigma-Aldrich Pty. Ltd., NSW, Australia

All other reagents used in this study were of analytical reagent grade and were obtained from:
Ajax Finechem Pty. Ltd., Seven Hills, NSW, Australia
BDH (Merck) Pty. Ltd., VIC, Australia
Sigma-Aldrich Pty. Ltd., NSW, Australia

Appendix B: The number of animals used

Table B1. List of the number of animals used in bone morphology study

Age	MPS I strain		Attenuated MPS VII Gus$^{tm((L175F)Sly}$ strain		Severe MPS VII Gus$^{mps/mps}$ strain		MPS IIIA strain		MPS IX strain	
	Normal	Affected	Normal	Affected	Normal	Affected	Normal	Affected	Normal	Affected
P14	4	4	3	5	6	5	-	-	-	-
1m	6	16	5	4	13	8	-	-	-	-
2m	8	9	6	5	18	9	-	-	-	-
3m	7	8	6	7	7	7	-	-	-	-
6m	6	11	7	6	9	11	5	8	6	4

The number of animals per genotype used for radiographic analysis of bone length in normal and affected mice from MPS I, attenuated MPS VII (Gus$^{tm((L175F)Sly}$ strain), severe MPS VII (Gus$^{mps/mps}$ strain), MPS IIIA and MPS IX P=postnatal day. m=postnatal month.

Table B2. List of the number of animals used in morphology study of proximal tibia

Age	n=	
	N	**VII**
E12.5	5	6
E13.5	6	15
E14.5	8	9
E15.5	13	13
E16.5	7	8
E17.5	5	4
E18.5	8	5
P7	4	3
P8	5	4
P9	5	4
P10	15	8
P11	13	7
P12	12	10
P14	15	12
1m	11	11
2m	12	7
6m	9	5

The number of animals per genotype used for histological analysis of the formation of ossification centres in normal and severe MPS VII mice (Gus*mps/mps* strain). E=embryonic day. P=postnatal day. m=postnatal month.

Table B3. The number of animals used in growth plate histomorphometry study

Age	n=	
	N	**MPS VII**
P14	10	10
1 m	6	8
2 m	5	5
6 m	4	4

The number of animals per genotype used for histomorphometry analysis of the growth plate in normal and severe MPS VII mice (Gus$^{mps/mps}$ strain). P=postnatal day. m=postnatal month.

Table B4. The number of animals used in quantitative analysis of area occupied by the SOC

Age	n=	
	N	**VII**
P14	14	12
1m	11	11
2m	5	7
6m	9	5

The number of animals per genotype used for quantitative analysis of area occupied by the SOC analysis in normal and severe MPS VII mice (Gus$^{mps/mps}$ strain). P=postnatal day. m=postnatal month.

Table B5. List of primers used in qRT-PCR.

Gene	Forward primer (5'-3')	Reverse primer (5'-3')	accession #
Bax	CGAGAGGTCTTCTTCCGGGT	CACAGGGCCTTGAGCACC	NM_007527.3
Bcl2	GCGTCAACAGGGAGATGTCA	GTTCCACAAAGGCATCCCAG	NM_009741.4
Casp3	TCATTCAGGCCTGCCGGGGTAC	TCAGCCTCCACCGGTATCTTCTGG	NM_001284409.1
Col2a1	AGGTGAACAAGGACCCAGAG	AGGATTTCCAGGGGTACCAG	NM_031163.3
CycA	AGCATACAGGTCCTGGCATC	TTCACCTTCCCAAAGACCAC	NM_008907.1
FasR	ATGCACAGAAGGGAAGGAGT	CAGGGTGCAGTTTGTTTCCA	NM_007987.2
FasL	TGGTTGGAATGGGATTAGGA	AAGGCTTTGGTTGGTGAACT	NM_010177.4
Ghr	GGAAGTGAGGCTACACCAGC	TTCAGGGGAACGACACTTGG	NM_010284.2
Gli2	GCTGATGTGGCCCACGAACATCTG	GTGGCTTGCCATGAGGGTCA	NM_001081125.1
Gli3	CAGCCCTGCATTGAGCTTCA	GCGGAGCCTAAGCTTTGCTGTC	NM_008130.2
Mmp13	ACCAGAGAAGTGTGACCCAGCCC	TGCAGGCGCCAGAAGAATCTGTC	NM_008607.2
Ihh	GACTGCTGGCGCGCTTAGCA	GCGGCCGAATGCTCAGACTTGA	NM_010544.2
Igfals	TCACTCAGTTTGGGCAACAA	GGACCACTAGGCTGTTCCAA	NM_008340.3
Igfbp2	GATCTCCACCATGCGCCTT	CAGAGACATCTTGCACTGCT	NM_008342.3
Igfbp3	CCAACCTGCTCCAGGAAACA	GAATCGGTCACTCGGTGTGT	NM_008343.2
Igf1	CCAGAGACCCTTTGCGGGGC	AGCCATAGCCTGTGGGCTTGTTGAA	NM_010512.4
Igfr1	CTGATGTCTGGTCCTTCGGG	CACCCTCCATGACGAAACGA	NM_010513.2
Ptch1	CGGGACTATCTGCACCGGC	AAACTTCGCTCTCAGCCACAG	NM_008957.2
Pthrp	CTCAAACGCGCTGTGTCTGAACATCA	GCGATCAGATGGTGGAGGAAG	NM_008970.3
Pthrpr	CAGGCGCAATGTGACAAGC	TTTCCCGGTGCCTTCTCTTTC	NM_011199.2
Runx2	CCAAGTAGCCAGGTTCAACG	TGGGGAGGATTTGTGAAGAC	NM_001146038.2
Smo	AAGCTCGTGCTCTGGTCCG	TCCACTCGGTCATTCTCACAC	NM_176996.4
Sox9	CGGAGCTCAGCAAGACTCTG	GGGTGGTCTTTCTTGTGCTG	NM_011448.4
Stat5a	CTGAAGATCAAGCTGGGGCA	TGTGACGGATACAGCGAACC	NM_001164062.1
Stat5b	AGCAACCACCTCGAGGACTA	TACTTCCATCACGCCATCAA	NM_001113563.1
Trα	GCTGCTAATGTCAACAGACCG	AATGTTGTGTTTGCGGTGGT	**NM_001113417.1**
Trβ	ACCAGAGTGGTGGATTTTGC	GACATGCCCAGGTCAAAGAT	**NM_007631.2**

Cyclophilin A (*CycA*) was used as a housekeeping gene

Appendix C: Publications

Publication arising from this thesis:

Jiang Z, Derrick-Roberts ALK, Jackson MR, Rossouw C, Pyragius CE, Xian C, Fletcher C and Byers S. Delayed development of ossification centers in the tibia of prenatal and early postnatal MPS VII mice, *Mol Genet Metab*, submitted on 7, March 2018 (accepted for publication)

Published abstract arising from this thesis:

Jiang Z, Rossouw C, Reichstein C, Macsai CE, Jackson MR, Derrick-Roberts ALK, & Byers S. Reduced chondrocyte proliferation and hypertrophy contribute to delayed endochondral bone formation in murine Mucopolysaccharidosis VII, *Mol Genet Metab (2016)*, vol.117, no.2,pp. S62-S63

Byers S, Jiang Z, Reichstein C & Derrick-Roberts ALK, Cell cycle progression is disrupted in murine MPS VII growth plate chondrocytes, *Mol Genet Metab (2017)*, vol. 120, Issues 1–2, pp S33.

Jiang Z, Reichstein C, Derrick-Roberts ALK & Byers S, MPS VII mice display reduced circulating IGF1 and disrupted cell cycle progression in the growth plate, *Mol Genet Metab (2018)* , vol. 123 , Issue 2 , pp S71.

9 References

Abad, V, Meyers, JL, Weise, M, Gafni, RI, Barnes, KM, Nilsson, O, Bacher, JD & Baron, J 2002, 'The role of the resting zone in growth plate chondrogenesis', *Endocrinology*, vol. 143, no. 5, May, pp. 1851-1857.

Abreu, S, Hayden, J, Berthold, P, Shapiro, IM, Decker, S, Patterson, D & Haskins, M 1995, 'Growth plate pathology in feline mucopolysaccharidosis VI', *Calcif Tissue Int*, vol. 57, no. 3, Sep, pp. 185-190.

Ahmed, YA, Tatarczuch, L, Pagel, CN, Davies, HM, Mirams, M & Mackie, EJ 2007, 'Physiological death of hypertrophic chondrocytes', *Osteoarthritis Cartilage*, vol. 15, no. 5, May, pp. 575-586.

Akeno, N, Robins, J, Zhang, M, Czyzyk-Krzeska, MF & Clemens, TL 2002, 'Induction of Vascular Endothelial Growth Factor by IGF-I in Osteoblast-Like Cells Is Mediated by the PI3K Signaling Pathway through the Hypoxia-Inducible Factor-2α', *Endocrinology*, vol. 143, no. 2, pp. 420-425.

Akiyama, H, Lyons, JP, Mori-Akiyama, Y, Yang, X, Zhang, R, Zhang, Z, Deng, JM, Taketo, MM, Nakamura, T, Behringer, RR, McCrea, PD & de Crombrugghe, B 2004, 'Interactions between Sox9 and beta-catenin control chondrocyte differentiation', *Genes Dev*, vol. 18, no. 9, May 1, pp. 1072-1087.

Alberts, B, Johnson, A, Lewis, J, Raff, M, Roberts, K & Walter, P 2008, 'The extracellular matrix of animal connective tissues', in *Molecular Biology of the Cell*, 5th edition edn, Garland Science, New York, pp. 1178-1194.

Allerstorfer, D, Longato, S, Schwarzer, C, Fischer-Colbrie, R, Hayman, AR & Blumer, MJ 2010, 'VEGF and its role in the early development of the long bone epiphysis', *J Anat*, vol. 216, no. 5, May, pp. 611-624.

Alt, JR, Cleveland, JL, Hannink, M & Diehl, JA 2000, 'Phosphorylation-dependent regulation of cyclin D1 nuclear export and cyclin D1-dependent cellular transformation', *Genes Dev*, vol. 14, no. 24, Dec 15, pp. 3102-3114.

Amling, M, Neff, L, Tanaka, S, Inoue, D, Kuida, K, Weir, E, Philbrick, WM, Broadus, AE & Baron, R 1997, 'Bcl-2 lies downstream of parathyroid hormone-related peptide in a signaling pathway that regulates chondrocyte maturation during skeletal development', *J Cell Biol*, vol. 136, no. 1, Jan 13, pp. 205-213.

Arora, RS, Mercer, J, Thornley, M, Tylee, K & Wraith, JE 2007, 'Enzyme replacement therapy in 12 patients with MPS I-H/S with homozygous p.Leu490Pro mutation', *J Inherit Metab Dis*, vol. 30, no. 5, Oct, p. 821.

Backeljauw, PF & Underwood, LE 2001, 'Therapy for 6.5-7.5 years with recombinant insulin-like growth factor I in children with growth hormone insensitivity syndrome: a clinical research center study', *J Clin Endocrinol Metab*, vol. 86, no. 4, Apr, pp. 1504-1510.

Baker, J, Liu, JP, Robertson, EJ & Efstratiadis, A 1993, 'Role of insulin-like growth factors in embryonic and postnatal growth', *Cell*, vol. 75, no. 1, Oct 8, pp. 73-82.

Baldo, G, Matte, U, Artigalas, O, Schwartz, IV, Burin, MG, Ribeiro, E, Horovitz, D, Magalhaes, TP, Elleder, M & Giugliani, R 2011, 'Placenta analysis of prenatally diagnosed patients reveals early GAG storage in mucopolysaccharidoses II and VI', *Mol Genet Metab*, vol. 103, no. 2, 2011/06/01/, pp. 197-198.

Ballock, RT, Mita, BC, Zhou, X, Chen, DH & Mink, LM 1999, 'Expression of thyroid hormone receptor isoforms in rat growth plate cartilage in vivo', *J Bone Miner Res*, vol. 14, no. 9, Sep, pp. 1550-1556.

Ballock, RT & Reddi, AH 1994, 'Thyroxine is the serum factor that regulates morphogenesis of columnar cartilage from isolated chondrocytes in chemically defined medium', *J Cell Biol*, vol. 126, no. 5, Sep, pp. 1311-1318.

Baron, J, Klein, KO, Yanovski, JA, Novosad, JA, Bacher, JD, Bolander, ME & Cutler, GB, Jr. 1994, 'Induction of growth plate cartilage ossification by basic fibroblast growth factor', *Endocrinology*, vol. 135, no. 6, Dec, pp. 2790-2793.

Baxter, RC, Martin, JL & Beniac, VA 1989, 'High molecular weight insulin-like growth factor binding protein complex. Purification and properties of the acid-labile subunit from human serum', *Journal of Biological Chemistry*, vol. 264, no. 20, Jul 15, pp. 11843-11848.

Beier, F 2005, 'Cell-cycle control and the cartilage growth plate', *Journal of Cellular Physiology*, vol. 202, no. 1, pp. 1-8.

Belluoccio, D, Bernardo, BC, Rowley, L & Bateman, JF 2008, 'A microarray approach for comparative expression profiling of the discrete maturation zones of mouse growth plate cartilage', *Biochim Biophys Acta*, vol. 1779, no. 5, May, pp. 330-340.

Bhattacharyya, R, Gliddon, B, Beccari, T, Hopwood, JJ & Stanley, P 2001, 'A novel missense mutation in lysosomal sulfamidase is the basis of MPS III A in a spontaneous mouse mutant', *Glycobiology*, vol. 11, no. 1, Jan, pp. 99-103.

Bhaumik, M, Muller, VJ, Rozaklis, T, Johnson, L, Dobrenis, K, Bhattacharyya, R, Wurzelmann, S, Finamore, P, Hopwood, JJ, Walkley, SU & Stanley, P 1999, 'A mouse model for mucopolysaccharidosis type III A (Sanfilippo syndrome)', *Glycobiology*, vol. 9, no. 12, Dec, pp. 1389-1396.

Bifsha, P, Landry, K, Ashmarina, L, Durand, S, Seyrantepe, V, Trudel, S, Quiniou, C, Chemtob, S, Xu, Y, Gravel, RA, Sladek, R & Pshezhetsky, AV 2007, 'Altered gene expression in cells from patients with lysosomal storage disorders suggests impairment of the ubiquitin pathway', *Cell Death Differ*, vol. 14, no. 3, Mar, pp. 511-523.

Birkenmeier, EH, Barker, JE, Vogler, CA, Kyle, JW, Sly, WS, Gwynn, B, Levy, B & Pegors, C 1991, 'Increased life span and correction of metabolic defects in murine mucopolysaccharidosis type VII after syngeneic bone marrow transplantation', *Blood*, vol. 78, no. 11, Dec 1, pp. 3081-3092.

Birkenmeier, EH, Davisson, MT, Beamer, WG, Ganschow, RE, Vogler, CA, Gwynn, B, Lyford, KA, Maltais, LM & Wawrzyniak, CJ 1989, 'Murine mucopolysaccharidosis type VII. Characterization of a mouse with beta-glucuronidase deficiency', *J Clin Invest*, vol. 83, no. 4, Apr, pp. 1258-1266.

Brennan, BM & Shalet, SM 2002, 'Endocrine late effects after bone marrow transplant', *Br J Haematol*, vol. 118, no. 1, Jul, pp. 58-66.

Buckler, JM, Willgerodt, H & Keller, E 1986, 'Growth in thyrotoxicosis', *Arch Dis Child*, vol. 61, no. 5, May, pp. 464-471.

Bunge, S, Clements, PR, Byers, S, Kleijer, WJ, Brooks, DA & Hopwood, JJ 1998, 'Genotype-phenotype correlations in mucopolysaccharidosis type I using enzyme kinetics, immunoquantification and in vitro turnover studies', *Biochim Biophys Acta*, vol. 1407, no. 3, Sep 30, pp. 249-256.

Burch, WM & Lebovitz, HE 1982, 'Triiodothyronine stimulates maturation of porcine growth-plate cartilage in vitro', *J Clin Invest*, vol. 70, no. 3, Sep, pp. 496-504.

Burkus, JK, Ganey, TM & Ogden, JA 1993, 'Development of the cartilage canals and the secondary center of ossification in the distal chondroepiphysis of the prenatal human femur', *The Yale Journal of Biology and Medicine*, vol. 66, no. 3, May-Jun, pp. 193-202.

Butler, AA, Ambler, GR, Breier, BH, LeRoith, D, Roberts, CT, Jr. & Gluckman, PD 1994, 'Growth hormone (GH) and insulin-like growth factor-I (IGF-I) treatment of the GH-deficient dwarf rat: differential effects on IGF-I transcription start site expression in hepatic and extrahepatic tissues and lack of effect on type I IGF receptor mRNA expression', *Mol Cell Endocrinol*, vol. 101, no. 1-2, May, pp. 321-330.

Butler, AA & Le Roith, D 2001, 'Control of growth by the somatropic axis: growth hormone and the insulin-like growth factors have related and independent roles', *Annu Rev Physiol*, vol. 63, pp. 141-164.

Byers, S, Caterson, B, Hopwood, JJ & Foster, BK 1992, 'Immunolocation analysis of glycosaminoglycans in the human growth plate', *J Histochem Cytochem*, vol. 40, no. 2, Feb, pp. 275-282.

Byers, S, Nuttall, JD, Crawley, AC, Hopwood, JJ, Smith, K & Fazzalari, NL 1997, 'Effect of enzyme replacement therapy on bone formation in a feline model of mucopolysaccharidosis type VI', *Bone*, vol. 21, no. 5, Nov, pp. 425-431.

Calbó, J, Parreño, M, Sotillo, E, Yong, T, Mazo, A, Garriga, J & Graña, X 2002, 'G1 Cyclin/Cyclin-dependent Kinase-coordinated Phosphorylation of Endogenous Pocket Proteins Differentially Regulates Their Interactions with E2F4 and E2F1 and Gene Expression', *Journal of Biological Chemistry*, vol. 277, no. 52, December 27, 2002, pp. 50263-50274.

Calogera, MS 2016, 'Lysosomes, Lysosomal Storage Diseases, and Inflammation', *Journal of Inborn Errors of Metabolism and Screening*, vol. 4, 2016/07/29, p. 2326409816650465.

Carlevaro, MF, Cermelli, S, Cancedda, R & Descalzi Cancedda, F 2000, 'Vascular endothelial growth factor (VEGF) in cartilage neovascularization and chondrocyte differentiation: auto-paracrine role during endochondral bone formation', *J Cell Sci*, vol. 113, no. 1, pp. 59-69.

Carlevaro, MF, Cermelli, S, Cancedda, R & Descalzi Cancedda, F 2000, 'Vascular endothelial growth factor (VEGF) in cartilage neovascularization and chondrocyte differentiation: auto-paracrine role during endochondral bone formation', *J Cell Sci*, vol. 113 (Pt 1), Jan, pp. 59-69.

Chatterjee, S, Malhotra, R, Varghese, F, Bukhari, AB, Patil, A, Budrukkar, A, Parmar, V, Gupta, S & De, A 2013, 'Quantitative Immunohistochemical Analysis Reveals Association between Sodium Iodide Symporter and Estrogen Receptor Expression in Breast Cancer', *PLoS One*, vol. 8, no. 1, p. e54055.

Chau, M, Forcinito, P, Andrade, AC, Hegde, A, Ahn, S, Lui, JC, Baron, J & Nilsson, O 2011, 'Organization of the Indian hedgehog--parathyroid hormone-related protein system in the postnatal growth plate', *J Mol Endocrinol*, vol. 47, no. 1, Aug, pp. 99-107.

Chen, S, Wan, P, Ding, W, Li, F, He, C, Chen, P, Li, H, Hu, Z, Tan, W & Li, J 2013, 'Norcantharidin inhibits DNA replication and induces mitotic catastrophe by degrading initiation protein Cdc6', *Int J Mol Med*, vol. 32, no. 1, Jul, pp. 43-50.

Chinen, Y, Higa, T, Tomatsu, S, Suzuki, Y, Orii, T & Hyakuna, N 2014, 'Long-term therapeutic efficacy of allogenic bone marrow transplantation in a patient with mucopolysaccharidosis IVA', *Mol Genet Metab Rep*, vol. 1, pp. 31-41.

Chiusaroli, R, Maier, A, Knight, MC, Byrne, M, Calvi, LM, Baron, R, Krane, SM & Schipani, E 2003, 'Collagenase Cleavage of Type I Collagen Is Essential for Both Basal and Parathyroid Hormone (PTH)/PTH-Related Peptide Receptor-Induced Osteoclast Activation and Has Differential Effects on Discrete Bone Compartments', *Endocrinology*, vol. 144, no. 9, pp. 4106-4116.

Cho, SH, Toouli, CD, Fujii, GH, Crain, C & Parry, D 2005, 'Chk1 is essential for tumor cell viability following activation of the replication checkpoint', *Cell Cycle*, vol. 4, no. 1, Jan, pp. 131-139.

Clarke, BL & Khosla, S 2009, 'Androgens and Bone', *Steroids*, vol. 74, no. 3, 10/17, pp. 296-305.

Clarke, LA, Russell, CS, Pownall, S, Warrington, CL, Borowski, A, Dimmick, JE, Toone, J & Jirik, FR 1997, 'Murine mucopolysaccharidosis type I: targeted disruption of the murine alpha-L-iduronidase gene', *Hum Mol Genet*, vol. 6, no. 4, Apr, pp. 503-511.

Clurman, BE, Sheaff, RJ, Thress, K, Groudine, M & Roberts, JM 1996, 'Turnover of cyclin E by the ubiquitin-proteasome pathway is regulated by cdk2 binding and cyclin phosphorylation', *Genes Dev*, vol. 10, no. 16, Aug 15, pp. 1979-1990.

Cobrinik, D, Lee, MH, Hannon, G, Mulligan, G, Bronson, RT, Dyson, N, Harlow, E, Beach, D, Weinberg, RA & Jacks, T 1996, 'Shared role of the pRB-related p130 and p107 proteins in limb development', *Genes Dev*, vol. 10, no. 13, Jul 01, pp. 1633-1644.

Cooper, KL, Oh, S, Sung, Y, Dasari, RR, Kirschner, MW & Tabin, CJ 2013, 'Multiple phases of chondrocyte enlargement underlie differences in skeletal proportions', *Nature*, vol. 495, 03/13/online, p. 375.

Cortes, M, Baria, AT & Schwartz, NB 2009, 'Sulfation of chondroitin sulfate proteoglycans is necessary for proper Indian hedgehog signaling in the developing growth plate', *Development*, vol. 136, no. 10, May, pp. 1697-1706.

Cotugno, G, Tessitore, A, Capalbo, A, Annunziata, P, Strisciuglio, C, Faella, A, Aurilio, M, Di Tommaso, M, Russo, F, Mancini, A, De Leonibus, E, Aloj, L & Auricchio, A 2010, 'Different serum enzyme levels are required to rescue the various systemic features of the mucopolysaccharidoses', *Hum Gene Ther*, vol. 21, no. 5, May, pp. 555-569.

Cowell, KR, Jezyk, PF, Haskins, ME & Patterson, DF 1976, 'Mucopolysaccharidosis in a cat', *J Am Vet Med Assoc*, vol. 169, no. 3, Aug 1, pp. 334-339.

Cox-Brinkman, J, Boelens, JJ, Wraith, JE, O'Meara, A, Veys, P, Wijburg, FA, Wulffraat, N & Wynn, RF 2006, 'Haematopoietic cell transplantation (HCT) in combination with enzyme replacement therapy (ERT) in patients with Hurler syndrome', *Bone Marrow Transplant*, vol. 38, no. 1, Jul, pp. 17-21.

Crawley, AC, Niedzielski, KH, Isaac, EL, Davey, RC, Byers, S & Hopwood, JJ 1997, 'Enzyme replacement therapy from birth in a feline model of mucopolysaccharidosis type VI', *J Clin Invest*, vol. 99, no. 4, Feb 15, pp. 651-662.

Daly, TM, Ohlemiller, KK, Roberts, MS, Vogler, CA & Sands, MS 2001, 'Prevention of systemic clinical disease in MPS VII mice following AAV-mediated neonatal gene transfer', *Gene Ther*, vol. 8, no. 17, Sep, pp. 1291-1298.

Dao, DY, Jonason, JH, Zhang, Y, Hsu, W, Chen, D, Hilton, MJ & O'Keefe, RJ 2012, 'Cartilage-specific beta-catenin signaling regulates chondrocyte maturation, generation of

ossification centers, and perichondrial bone formation during skeletal development', *J Bone Miner Res*, vol. 27, no. 8, Aug, pp. 1680-1694.

De Leonardis, F, Monti, L, Gualeni, B, Tenni, R, Forlino, A & Rossi, A 2014, 'Altered signaling in the G1 phase deregulates chondrocyte growth in a mouse model with proteoglycan undersulfation', *J Cell Biochem*, vol. 115, no. 10, Oct, pp. 1779-1786.

de Oliveira, PG, Baldo, G, Mayer, FQ, Martinelli, B, Meurer, L, Giugliani, R, Matte, U & Xavier, RM 2013, 'Characterization of joint disease in mucopolysaccharidosis type I mice', *Int J Exp Pathol*, vol. 94, no. 5, Oct, pp. 305-311.

DeChiara, TM, Efstratiadis, A & Robertsen, EJ 1990, 'A growth-deficiency phenotype in heterozygous mice carrying an insulin-like growth factor II gene disrupted by targeting', *Nature*, vol. 345, 05/03/online, p. 78.

Decker, C, Yu, ZF, Giugliani, R, Schwartz, IV, Guffon, N, Teles, EL, Miranda, MC, Wraith, JE, Beck, M, Arash, L, Scarpa, M, Ketteridge, D, Hopwood, JJ, Plecko, B, Steiner, R, Whitley, CB, Kaplan, P, Swiedler, SJ, Conrad, S & Harmatz, P 2010, 'Enzyme replacement therapy for mucopolysaccharidosis VI: Growth and pubertal development in patients treated with recombinant human N-acetylgalactosamine 4-sulfatase', *J Pediatr Rehabil Med*, vol. 3, no. 2, pp. 89-100.

Derrick-Roberts, AL, Panir, K, Pyragius, CE, Zarrinkalam, KH, Atkins, GJ & Byers, S 2016, 'Reversal of established bone pathology in MPS VII mice following lentiviral-mediated gene therapy', *Mol Genet Metab*, vol. 119, no. 3, Nov, pp. 249-257.

Derrick-Roberts, AL, Pyragius, CE, Kaidonis, XM, Jackson, MR, Anson, DS & Byers, S 2014, 'Lentiviral-mediated gene therapy results in sustained expression of beta-glucuronidase for up to 12 months in the gus(mps/mps) and up to 18 months in the gus(tm(L175F)Sly) mouse models of mucopolysaccharidosis type VII', *Hum Gene Ther*, vol. 25, no. 9, Sep, pp. 798-810.

Domowicz, MS, Cortes, M, Henry, JG & Schwartz, NB 2009, 'Aggrecan modulation of growth plate morphogenesis', *Developmental Biology*, vol. 329, no. 2, pp. 242-257.

Donsante, A, Levy, B, Vogler, C & Sands, MS 2007, 'Clinical response to persistent, low-level beta-glucuronidase expression in the murine model of mucopolysaccharidosis type VII', *J Inherit Metab Dis*, vol. 30, no. 2, Apr, pp. 227-238.

Dy, P, Wang, W, Bhattaram, P, Wang, Q, Wang, L, Ballock, RT & Lefebvre, V 2012, 'Sox9 Directs Hypertrophic Maturation and Blocks Osteoblast Differentiation of Growth Plate Chondrocytes', *Dev Cell*, vol. 22, no. 3, pp. 597-609.

Eliyahu, E, Wolfson, T, Ge, Y, Jepsen, KJ, Schuchman, EH & Simonaro, CM 2011, 'Anti-TNF-Alpha Therapy Enhances the Effects of Enzyme Replacement Therapy in Rats with Mucopolysaccharidosis Type VI', *PLoS One*, vol. 6, no. 8, p. e22447.

Elliger, SS, Elliger, CA, Lang, C & Watson, GL 2002, 'Enhanced secretion and uptake of beta-glucuronidase improves adeno-associated viral-mediated gene therapy of mucopolysaccharidosis type VII mice', *Mol Ther*, vol. 5, no. 5 Pt 1, May, pp. 617-626.

Evers, M, Saftig, P, Schmidt, P, Hafner, A, McLoghlin, DB, Schmahl, W, Hess, B, von Figura, K & Peters, C 1996, 'Targeted disruption of the arylsulfatase B gene results in mice resembling the phenotype of mucopolysaccharidosis VI', *Proc Natl Acad Sci U S A*, vol. 93, no. 16, Aug 6, pp. 8214-8219.

Farnum, CE, Lee, R, O'Hara, K & Urban, JP 2002, 'Volume increase in growth plate chondrocytes during hypertrophy: the contribution of organic osmolytes', *Bone*, vol. 30, no. 4, Apr, pp. 574-581.

Farnum, CE & Wilsman, NJ 1993, 'Determination of proliferative characteristics of growth plate chondrocytes by labeling with bromodeoxyuridine', *Calcif Tissue Int*, vol. 52, no. 2, Feb, pp. 110-119.

Feng, J, Witthuhn, BA, Matsuda, T, Kohlhuber, F, Kerr, IM & Ihle, JN 1997, 'Activation of Jak2 catalytic activity requires phosphorylation of Y1007 in the kinase activation loop', *Mol Cell Biol*, vol. 17, no. 5, pp. 2497-2501.

Fernandez-Cancio, M, Esteban, C, Carrascosa, A, Toran, N, Andaluz, P & Audi, L 2008, 'IGF-I and not IGF-II expression is regulated by glucocorticoids in human fetal epiphyseal chondrocytes', *Growth Hormone & IGF Research*, vol. 18, no. 6, 2008/12/01/, pp. 497-505.

Field, RE, Buchanan, JA, Copplemans, MG & Aichroth, PM 1994, 'Bone-marrow transplantation in Hurler's syndrome. Effect on skeletal development', *J Bone Joint Surg Br*, vol. 76, no. 6, Nov, pp. 975-981.

Fischer, A, Carmichael, KP, Munnell, JF, Jhabvala, P, Thompson, JN, Matalon, R, Jezyk, PF, Wang, P & Giger, U 1998, 'Sulfamidase deficiency in a family of Dachshunds: a canine model of mucopolysaccharidosis IIIA (Sanfilippo A)', *Pediatr Res*, vol. 44, no. 1, Jul, pp. 74-82.

Fisher, MC, Li, Y, Seghatoleslami, MR, Dealy, CN & Kosher, RA 2006, 'Heparan sulfate proteoglycans including syndecan-3 modulate BMP activity during limb cartilage differentiation', *Matrix Biol*, vol. 25, no. 1, Jan, pp. 27-39.

Forrest, D, Hanebuth, E, Smeyne, RJ, Everds, N, Stewart, CL, Wehner, JM & Curran, T 1996, 'Recessive resistance to thyroid hormone in mice lacking thyroid hormone receptor beta: evidence for tissue-specific modulation of receptor function', *EMBO J*, vol. 15, no. 12, Jun 17, pp. 3006-3015.

Fox, JE, Volpe, L, Bullaro, J, Kakkis, ED & Sly, WS 2015, 'First human treatment with investigational rhGUS enzyme replacement therapy in an advanced stage MPS VII patient', *Mol Genet Metab*, vol. 114, no. 2, Feb, pp. 203-208.

Frisk, P, Arvidson, J, Gustafsson, J & Lonnerholm, G 2004, 'Pubertal development and final height after autologous bone marrow transplantation for acute lymphoblastic leukemia', *Bone Marrow Transplant*, vol. 33, no. 2, Jan, pp. 205-210.

Furujo, M, Kosuga, M & Okuyama, T 2017, 'Enzyme replacement therapy attenuates disease progression in two Japanese siblings with mucopolysaccharidosis type VI: 10-Year follow up', *Mol Genet Metab Rep*, vol. 13, Dec, pp. 69-75.

Fyfe, JC, Kurzhals, RL, Lassaline, ME, Henthorn, PS, Alur, PR, Wang, P, Wolfe, JH, Giger, U, Haskins, ME, Patterson, DF, Sun, H, Jain, S & Yuhki, N 1999, 'Molecular basis of feline beta-glucuronidase deficiency: an animal model of mucopolysaccharidosis VII', *Genomics*, vol. 58, no. 2, Jun 1, pp. 121-128.

Garcia, AR, Pan, J, Lamsa, JC & Muenzer, J 2007, 'The characterization of a murine model of mucopolysaccharidosis II (Hunter syndrome)', *J Inherit Metab Dis*, vol. 30, no. 6, Nov, pp. 924-934.

Gardner, CJ, Robinson, N, Meadows, T, Wynn, R, Will, A, Mercer, J, Church, HJ, Tylee, K, Wraith, JE & Clayton, PE 2011, 'Growth, final height and endocrine sequelae in a UK population of patients with Hurler syndrome (MPS1H)', *J Inherit Metab Dis*, vol. 34, no. 2, Apr, pp. 489-497.

Gaubatz, S, Lindeman, GJ, Ishida, S, Jakoi, L, Nevins, JR, Livingston, DM & Rempel, RE 2000, 'E2F4 and E2F5 Play an Essential Role in Pocket Protein–Mediated G1 Control', *Molecular Cell*, vol. 6, no. 3, 2000/09/01/, pp. 729-735.

Gauthier, K, Chassande, O, Plateroti, M, Roux, JP, Legrand, C, Pain, B, Rousset, B, Weiss, R, Trouillas, J & Samarut, J 1999, 'Different functions for the thyroid hormone receptors TRalpha and TRbeta in the control of thyroid hormone production and post-natal development', *EMBO J*, vol. 18, no. 3, Feb 1, pp. 623-631.

Gebert, CA, Park, S-H & Waxman, DJ 1997, 'Regulation of Signal Transducer and Activator of Transcription (STAT) 5b Activation by the Temporal Pattern of Growth Hormone Stimulation', *Molecular Endocrinology*, vol. 11, no. 4, pp. 400-414.

Gerber, HP, Vu, TH, Ryan, AM, Kowalski, J, Werb, Z & Ferrara, N 1999, 'VEGF couples hypertrophic cartilage remodeling, ossification and angiogenesis during endochondral bone formation', *Nat Med*, vol. 5, no. 6, Jun, pp. 623-628.

Gevers, EF, Hannah, MJ, Waters, MJ & Robinson, IC 2009, 'Regulation of rapid signal transducer and activator of transcription-5 phosphorylation in the resting cells of the

growth plate and in the liver by growth hormone and feeding', *Endocrinology*, vol. 150, no. 8, Aug, pp. 3627-3636.

Gevers, EF, van der Eerden, BC, Karperien, M, Raap, AK, Robinson, IC & Wit, JM 2002, 'Localization and regulation of the growth hormone receptor and growth hormone-binding protein in the rat growth plate', *J Bone Miner Res*, vol. 17, no. 8, Aug, pp. 1408-1419.

Gibson, GJ & Flint, MH 1985, 'Type X collagen synthesis by chick sternal cartilage and its relationship to endochondral development', *J Cell Biol*, vol. 101, no. 1, Jul, pp. 277-284.

Giorgiani, G, Bozzola, M, Locatelli, F, Picco, P, Zecca, M, Cisternino, M, Dallorso, S, Bonetti, F, Dini, G, Borrone, C & et al. 1995, 'Role of busulfan and total body irradiation on growth of prepubertal children receiving bone marrow transplantation and results of treatment with recombinant human growth hormone', *Blood*, vol. 86, no. 2, Jul 15, pp. 825-831.

Goldring, MB, Tsuchimochi, K & Ijiri, K 2006, 'The control of chondrogenesis', *J Cell Biochem*, vol. 97, no. 1, Jan 1, pp. 33-44.

Goodrich, DW, Wang, NP, Qian, YW, Lee, EY & Lee, WH 1991, 'The retinoblastoma gene product regulates progression through the G1 phase of the cell cycle', *Cell*, vol. 67, no. 2, Oct 18, pp. 293-302.

Guevara-Aguirre, J, Rosenbloom, AL, Vasconez, O, Martinez, V, Gargosky, SE, Allen, L & Rosenfeld, RG 1997, 'Two-year treatment of growth hormone (GH) receptor deficiency with recombinant insulin-like growth factor I in 22 children: comparison of two dosage levels and to GH-treated GH deficiency', *J Clin Endocrinol Metab*, vol. 82, no. 2, Feb, pp. 629-633.

Guo, J, Chung, UI, Yang, D, Karsenty, G, Bringhurst, FR & Kronenberg, HM 2006, 'PTH/PTHrP receptor delays chondrocyte hypertrophy via both Runx2-dependent and -independent pathways', *Dev Biol*, vol. 292, no. 1, Apr 1, pp. 116-128.

Hall, BK & Miyake, T 1995, 'Divide, accumulate, differentiate: cell condensation in skeletal development revisited', *Int J Dev Biol*, vol. 39, no. 6, Dec, pp. 881-893.

Hardin, DS 2008, 'Treatment of short stature and growth hormone deficiency in children with somatotropin (rDNA origin)', *Biologics : Targets & Therapy*, vol. 2, no. 4, 12/, pp. 655-661.

Harmatz, P, Hendriksz, CJ, Lampe, C, McGill, JJ, Parini, R, Leao-Teles, E, Valayannopoulos, V, Cole, TJ, Matousek, R, Graham, S, Guffon, N & Quartel, A 2017, 'The effect of galsulfase enzyme replacement therapy on the growth of patients with mucopolysaccharidosis VI (Maroteaux-Lamy syndrome)', *Mol Genet Metab*, vol. 122, no. 1-2, Sep, pp. 107-112.

Hartmann, C & Tabin, CJ 2000, 'Dual roles of Wnt signaling during chondrogenesis in the chicken limb', *Development*, vol. 127, no. 14, Jul, pp. 3141-3159.

Hashimoto, S, Setareh, M, Ochs, RL & Lotz, M 1997, 'Fas/Fas ligand expression and induction of apoptosis in chondrocytes', *Arthritis Rheum*, vol. 40, no. 10, Oct, pp. 1749-1755.

Haskins, ME, Aguirre, GD, Jezyk, PF, Desnick, RJ & Patterson, DF 1983, 'The pathology of the feline model of mucopolysaccharidosis I', *Am J Pathol*, vol. 112, no. 1, Jul, pp. 27-36.

Haskins, ME, Desnick, RJ, DiFerrante, N, Jezyk, PF & Patterson, DF 1984, 'Beta-glucuronidase deficiency in a dog: a model of human mucopolysaccharidosis VII', *Pediatr Res*, vol. 18, no. 10, Oct, pp. 980-984.

Haskins, ME, Jezyk, PF, Desnick, RJ, McDonough, SK & Patterson, DF 1979, 'Alpha-L-iduronidase deficiency in a cat: a model of mucopolysaccharidosis I', *Pediatr Res*, vol. 13, no. 11, Nov, pp. 1294-1297.

Hateboer, G, Kerkhoven, RM, Shvarts, A, Bernards, R & Beijersbergen, RL 1996, 'Degradation of E2F by the ubiquitin-proteasome pathway: regulation by retinoblastoma family proteins and adenovirus transforming proteins', *Genes Dev*, vol. 10, no. 23, Dec 1, pp. 2960-2970.

Hendriksz, CJ, Harmatz, P, Beck, M, Jones, S, Wood, T, Lachman, R, Gravance, CG, Orii, T & Tomatsu, S 2013, 'Review of Clinical Presentation and Diagnosis of Mucopolysaccharidosis IVA', *Mol Genet Metab*, vol. 110, no. 0, Sep-Oct 04/10, pp. 54-64.

Hendzel, MJ, Wei, Y, Mancini, MA, Van Hooser, A, Ranalli, T, Brinkley, BR, Bazett-Jones, DP & Allis, CD 1997, 'Mitosis-specific phosphorylation of histone H3 initiates primarily within pericentromeric heterochromatin during G2 and spreads in an ordered fashion coincident with mitotic chromosome condensation', *Chromosoma*, vol. 106, no. 6, Nov, pp. 348-360.

Herati, RS, Knox, VW, O'Donnell, P, D'Angelo, M, Haskins, ME & Ponder, KP 2008, 'Radiographic evaluation of bones and joints in mucopolysaccharidosis I and VII dogs after neonatal gene therapy', *Mol Genet Metab*, vol. 95, no. 3, Nov, pp. 142-151.

Hermosa, BD & Sobel, EH 1972, 'Thyroid in the treatment of short stature', *J Pediatr*, vol. 80, no. 6, Jun, pp. 988-993.

Herskhovitz, E, Young, E, Rainer, J, Hall, CM, Lidchi, V, Chong, K & Vellodi, A 1999, 'Bone marrow transplantation for Maroteaux-Lamy syndrome (MPS VI): long-term follow-up', *J Inherit Metab Dis*, vol. 22, no. 1, Feb, pp. 50-62.

Hilton, MJ, Tu, X, Cook, J, Hu, H & Long, F 2005, 'Ihh controls cartilage development by antagonizing Gli3, but requires additional effectors to regulate osteoblast and vascular development', *Development*, vol. 132, no. 19, Oct, pp. 4339-4351.

Hobbs, JR, Hugh-Jones, K, Barrett, AJ, Byrom, N, Chambers, D, Henry, K, James, DC, Lucas, CF, Rogers, TR, Benson, PF, Tansley, LR, Patrick, AD, Mossman, J & Young, EP 1981, 'Reversal of clinical features of Hurler's disease and biochemical improvement after treatment by bone-marrow transplantation', *Lancet*, vol. 2, no. 8249, Oct 3, pp. 709-712.

Holmbeck, K, Bianco, P, Caterina, J, Yamada, S, Kromer, M, Kuznetsov, SA, Mankani, M, Robey, PG, Poole, AR, Pidoux, I, Ward, JM & Birkedal-Hansen, H 1999, 'MT1-MMP-deficient mice develop dwarfism, osteopenia, arthritis, and connective tissue disease due to inadequate collagen turnover', *Cell*, vol. 99, no. 1, Oct 1, pp. 81-92.

Horovitz, DD, Magalhaes, TS, Acosta, A, Ribeiro, EM, Giuliani, LR, Palhares, DB, Kim, CA, de Paula, AC, Kerstenestzy, M, Pianovski, MA, Costa, MI, Santos, FC, Martins, AM, Aranda, CS, Correa Neto, J, Holanda, GB, Cardoso, L, Jr., da Silva, CA, Bonatti, RC, Ribeiro, BF, Rodrigues Mdo, C & Llerena, JC, Jr. 2013, 'Enzyme replacement therapy with galsulfase in 34 children younger than five years of age with MPS VI', *Mol Genet Metab*, vol. 109, no. 1, May, pp. 62-69.

Hosui, A & Hennighausen, L 2008, 'Genomic dissection of the cytokine-controlled STAT5 signaling network in liver', *Physiol Genomics*, vol. 34, no. 2, p. 135.

Huang, L, Tan, HY, Fogarty, MJ, Andrews, ZB, Veldhuis, JD, Herzog, H, Steyn, FJ & Chen, C 2014, 'Actions of NPY, and its Y1 and Y2 receptors on pulsatile growth hormone secretion during the fed and fasted state', *J Neurosci*, vol. 34, no. 49, Dec 3, pp. 16309-16319.

Huang, W, Chung, UI, Kronenberg, HM & de Crombrugghe, B 2001, 'The chondrogenic transcription factor Sox9 is a target of signaling by the parathyroid hormone-related peptide in the growth plate of endochondral bones', *Proc Natl Acad Sci U S A*, vol. 98, no. 1, Jan 2, pp. 160-165.

Huma, Z, Boulad, F, Black, P, Heller, G & Sklar, C 1995, 'Growth in children after bone marrow transplantation for acute leukemia', *Blood*, vol. 86, no. 2, Jul 15, pp. 819-824.

Hung, DT, Jamison, TF & Schreiber, SL 1996, 'Understanding and controlling the cell cycle with natural products', *Chem Biol*, vol. 3, no. 8, Aug, pp. 623-639.

Hunziker, EB 1994, 'Mechanism of longitudinal bone growth and its regulation by growth plate chondrocytes', *Microsc Res Tech*, vol. 28, no. 6, Aug 15, pp. 505-519.

Hunziker, EB, Wagner, J & Zapf, J 1994, 'Differential effects of insulin-like growth factor I and growth hormone on developmental stages of rat growth plate chondrocytes in vivo', *J Clin Invest*, vol. 93, no. 3, Mar, pp. 1078-1086.

Hurskainen, TL, Hirohata, S, Seldin, MF & Apte, SS 1999, 'ADAM-TS5, ADAM-TS6, and ADAM-TS7, novel members of a new family of zinc metalloproteases. General features and genomic distribution of the ADAM-TS family', *Journal of Biological Chemistry*, vol. 274, no. 36, Sep 3, pp. 25555-25563.

Imundo, L, Leduc, CA, Guha, S, Brown, M, Perino, G, Gushulak, L, Triggs-Raine, B & Chung, WK 2011, 'A complete deficiency of Hyaluronoglucosaminidase 1 (HYAL1) presenting as familial juvenile idiopathic arthritis', *J Inherit Metab Dis*, vol. 34, no. 5, Oct, pp. 1013-1022.

Inada, M, Wang, Y, Byrne, MH, Rahman, MU, Miyaura, C, López-Otín, C & Krane, SM 2004, 'Critical roles for collagenase-3 (Mmp13) in development of growth plate cartilage and in endochondral ossification', *Proceedings of the National Academy of Sciences of the United States of America*, vol. 101, no. 49, 11/24
07/13/received, pp. 17192-17197.

Ingham, PW & McMahon, AP 2001, 'Hedgehog signaling in animal development: paradigms and principles', *Genes Dev*, vol. 15, no. 23, Dec 01, pp. 3059-3087.

Isaksson, OG, Jansson, JO & Gause, IA 1982, 'Growth hormone stimulates longitudinal bone growth directly', *Science*, vol. 216, no. 4551, Jun 11, pp. 1237-1239.

Isaksson, OG, Lindahl, A, Nilsson, A & Isgaard, J 1987, 'Mechanism of the stimulatory effect of growth hormone on longitudinal bone growth', *Endocr Rev*, vol. 8, no. 4, Nov, pp. 426-438.

Isaksson, OG, Nilsson, A, Isgaard, J & Lindahl, A 1990, 'Cartilage as a target tissue for growth hormone and insulin-like growth factor I', *Acta Paediatr Scand Suppl*, vol. 367, pp. 137-141.

Isgaard, J, Moller, C, Isaksson, OG, Nilsson, A, Mathews, LS & Norstedt, G 1988, 'Regulation of insulin-like growth factor messenger ribonucleic acid in rat growth plate by growth hormone', *Endocrinology*, vol. 122, no. 4, Apr, pp. 1515-1520.

Ito, K, Maruyama, Z, Sakai, A, Izumi, S, Moriishi, T, Yoshida, CA, Miyazaki, T, Komori, H, Takada, K, Kawaguchi, H & Komori, T 2014, 'Overexpression of Cdk6 and Ccnd1 in chondrocytes inhibited chondrocyte maturation and caused p53-dependent apoptosis without enhancing proliferation', *Oncogene*, vol. 33, no. 14, Apr 3, pp. 1862-1871.

Ivkovic, S, Yoon, BS, Popoff, SN, Safadi, FF, Libuda, DE, Stephenson, RC, Daluiski, A & Lyons, KM 2003, 'Connective tissue growth factor coordinates chondrogenesis and angiogenesis during skeletal development', *Development*, vol. 130, no. 12, Jun, pp. 2779-2791.

Iwasaki, M, Jikko, A & Le, AX 1999, 'Age-dependent effects of hedgehog protein on chondrocytes', *J Bone Joint Surg Br*, vol. 81, no. 6, Nov, pp. 1076-1082.

Iwasaki, T, Shinkai, K, Mukai, M, Yoshioka, K, Fujii, Y, Nakahara, K, Matsuda, H & Akedo, H 1995, 'Cell-cycle-dependent invasion in vitro by rat ascites hepatoma cells', *Int J Cancer*, vol. 63, no. 2, Oct 9, pp. 282-287.

Jackson, M, Derrick Roberts, A, Martin, E, Rout-Pitt, N, Gronthos, S & Byers, S 2015, 'Mucopolysaccharidosis enzyme production by bone marrow and dental pulp derived human mesenchymal stem cells', *Mol Genet Metab*, vol. 114, no. 4, Apr, pp. 584-593.

Jones, KL, Villela, JF & Lewis, UJ 1986, 'The growth of cultured rabbit articular chondrocytes is stimulated by pituitary growth factors but not by purified human growth hormone or ovine prolactin', *Endocrinology*, vol. 118, no. 6, Jun, pp. 2588-2593.

Jones, SA, Parini, R, Harmatz, P, Giugliani, R, Fang, J & Mendelsohn, NJ 2013, 'The effect of idursulfase on growth in patients with Hunter syndrome: data from the Hunter Outcome Survey (HOS)', *Mol Genet Metab*, vol. 109, no. 1, May, pp. 41-48.

Ju, ST, Panka, DJ, Cui, H, Ettinger, R, el-Khatib, M, Sherr, DH, Stanger, BZ & Marshak-Rothstein, A 1995, 'Fas(CD95)/FasL interactions required for programmed cell death after T-cell activation', *Nature*, vol. 373, no. 6513, Feb 2, pp. 444-448.

Kakkis, ED, Muenzer, J, Tiller, GE, Waber, L, Belmont, J, Passage, M, Izykowski, B, Phillips, J, Doroshow, R, Walot, I, Hoft, R & Neufeld, EF 2001, 'Enzyme-replacement therapy in mucopolysaccharidosis I', *N Engl J Med*, vol. 344, no. 3, Jan 18, pp. 182-188.

Kaneshige, M, Suzuki, H, Kaneshige, K, Cheng, J, Wimbrow, H, Barlow, C, Willingham, MC & Cheng, S 2001, 'A targeted dominant negative mutation of the thyroid hormone alpha 1 receptor causes increased mortality, infertility, and dwarfism in mice', *Proc Natl Acad Sci U S A*, vol. 98, no. 26, Dec 18, pp. 15095-15100.

Kapelari, K, Kirchlechner, C, Hogler, W, Schweitzer, K, Virgolini, I & Moncayo, R 2008, 'Pediatric reference intervals for thyroid hormone levels from birth to adulthood: a retrospective study', *BMC Endocr Disord*, vol. 8, p. 15.

Kawashima-Ohya, Y, Satakeda, H, Kuruta, Y, Kawamoto, T, Yan, W, Akagawa, Y, Hayakawa, T, Noshiro, M, Okada, Y, Nakamura, S & Kato, Y 1998, 'Effects of Parathyroid Hormone (PTH) and PTH-Related Peptide on Expressions of Matrix Metalloproteinase- 2, -3, and -9 in Growth Plate Chondrocyte Cultures*', *Endocrinology*, vol. 139, no. 4, pp. 2120-2127.

Kim, SO, Park, JG & Lee, YI 1996, 'Increased expression of the insulin-like growth factor I (IGF-I) receptor gene in hepatocellular carcinoma cell lines: implications of IGF-I receptor gene activation by hepatitis B virus X gene product', *Cancer Research*, vol. 56, no. 16, Aug 15, pp. 3831-3836.

Kiyokawa, H, Kineman, RD, Manova-Todorova, KO, Soares, VC, Hoffman, ES, Ono, M, Khanam, D, Hayday, AC, Frohman, LA & Koff, A 1996, 'Enhanced growth of mice lacking the cyclin-dependent kinase inhibitor function of p27(Kip1)', *Cell*, vol. 85, no. 5, May 31, pp. 721-732.

Koepp, DM, Schaefer, LK, Ye, X, Keyomarsi, K, Chu, C, Harper, JW & Elledge, SJ 2001, 'Phosphorylation-dependent ubiquitination of cyclin E by the SCFFbw7 ubiquitin ligase', *Science*, vol. 294, no. 5540, Oct 5, pp. 173-177.

Kojima, M, Hosoda, H, Date, Y, Nakazato, M, Matsuo, H & Kangawa, K 1999, 'Ghrelin is a growth-hormone-releasing acylated peptide from stomach', *Nature*, vol. 402, no. 6762, Dec 09, pp. 656-660.

Kopecki, Z, Arkell, R, Powell, BC & Cowin, AJ 2009, 'Flightless I Regulates Hemidesmosome Formation and Integrin-Mediated Cellular Adhesion and Migration during Wound Repair', *Journal of Investigative Dermatology*, vol. 129, no. 8, 2009/08/01/, pp. 2031-2045.

Koyama, E, Leatherman, JL, Noji, S & Pacifici, M 1996, 'Early chick limb cartilaginous elements possess polarizing activity and express hedgehog-related morphogenetic factors', *Dev Dyn*, vol. 207, no. 3, Nov, pp. 344-354.

Koziel, L, Wuelling, M, Schneider, S & Vortkamp, A 2005, 'Gli3 acts as a repressor downstream of Ihh in regulating two distinct steps of chondrocyte differentiation', *Development*, vol. 132, no. 23, Dec, pp. 5249-5260.

Kronenberg, HM 2003, 'Developmental regulation of the growth plate', *Nature*, vol. 423, no. 6937, May 15, pp. 332-336.

Kubaski, F, Kecskemethy, HH, Harcke, HT & Tomatsu, S 2016, 'Bone mineral density in mucopolysaccharidosis IVB', *Molecular Genetics and Metabolism Reports*, vol. 8, 2016/09/01/, pp. 80-84.

Lakatos, P, Caplice, MD, Khanna, V & Stern, PH 1993, 'Thyroid hormones increase insulin-like growth factor I content in the medium of rat bone tissue', *J Bone Miner Res*, vol. 8, no. 12, Dec, pp. 1475-1481.

Lee, K, Lanske, B, Karaplis, AC, Deeds, JD, Kohno, H, Nissenson, RA, Kronenberg, HM & Segre, GV 1996, 'Parathyroid hormone-related peptide delays terminal differentiation of chondrocytes during endochondral bone development', *Endocrinology*, vol. 137, no. 11, Nov, pp. 5109-5118.

Lee, MH, Williams, BO, Mulligan, G, Mukai, S, Bronson, RT, Dyson, N, Harlow, E & Jacks, T 1996, 'Targeted disruption of p107: functional overlap between p107 and Rb', *Genes Dev*, vol. 10, no. 13, Jul 01, pp. 1621-1632.

Legault, L & Bonny, Y 1999, 'Endocrine complications of bone marrow transplantation in children', *Pediatr Transplant*, vol. 3, no. 1, Feb, pp. 60-66.

Leger, J & Czernichow, P 1989, 'Congenital hypothyroidism: decreased growth velocity in the first weeks of life', *Biol Neonate*, vol. 55, no. 4-5, pp. 218-223.

Lewinson, D & Silbermann, M 1992, 'Chondroclasts and endothelial cells collaborate in the process of cartilage resorption', *Anat Rec*, vol. 233, no. 4, Aug, pp. 504-514.

Lim, A, Shin, K, Zhao, C, Kawano, S & Beachy, PA 2014, 'Spatially restricted Hedgehog signalling regulates HGF-induced branching of the adult prostate', *Nat Cell Biol*, vol. 16, 11/02/online, p. 1135.

Lin, DI, Barbash, O, Kumar, KG, Weber, JD, Harper, JW, Klein-Szanto, AJ, Rustgi, A, Fuchs, SY & Diehl, JA 2006, 'Phosphorylation-dependent ubiquitination of cyclin D1 by the SCF(FBX4-alphaB crystallin) complex', *Mol Cell*, vol. 24, no. 3, Nov 3, pp. 355-366.

Lin, X 2004, 'Functions of heparan sulfate proteoglycans in cell signaling during development', *Development*, vol. 131, no. 24, Dec, pp. 6009-6021.

Lindeman, GJ, Gaubatz, S, Livingston, DM & Ginsberg, D 1997, 'The subcellular localization of E2F-4 is cell-cycle dependent', *Proceedings of the National Academy of Sciences*, vol. 94, no. 10, May 13, 1997, pp. 5095-5100.

Lindqvist, A, Rodríguez-Bravo, V & Medema, RH 2009, 'The decision to enter mitosis: feedback and redundancy in the mitotic entry network', *J Cell Biol*, vol. 185, no. 2, pp. 193-202.

Liu, C, Peng, J, Matzuk, MM & Yao, HHC 2015, 'Lineage specification of ovarian theca cells requires multicellular interactions via oocyte and granulosa cells', *Nature Communications*, vol. 6, 04/28/online, p. 6934.

Liu, JP, Baker, J, Perkins, AS, Robertson, EJ & Efstratiadis, A 1993, 'Mice carrying null mutations of the genes encoding insulin-like growth factor I (Igf-1) and type 1 IGF receptor (Igf1r)', *Cell*, vol. 75, no. 1, Oct 08, pp. 59-72.

Liu, Y, Xu, L, Hennig, AK, Kovacs, A, Fu, A, Chung, S, Lee, D, Wang, B, Herati, RS, Mosinger Ogilvie, J, Cai, SR & Parker Ponder, K 2005, 'Liver-directed neonatal gene therapy prevents cardiac, bone, ear, and eye disease in mucopolysaccharidosis I mice', *Mol Ther*, vol. 11, no. 1, Jan, pp. 35-47.

Livak, KJ & Schmittgen, TD 2001, 'Analysis of relative gene expression data using real-time quantitative PCR and the 2(-Delta Delta C(T)) Method', *Methods*, vol. 25, no. 4, Dec, pp. 402-408.

Lobie, PE, Ronsin, B, Silvennoinen, O, Haldosen, LA, Norstedt, G & Morel, G 1996, 'Constitutive nuclear localization of Janus kinases 1 and 2', *Endocrinology*, vol. 137, no. 9, Sep, pp. 4037-4045.

Long, F 2012, 'Building strong bones: molecular regulation of the osteoblast lineage', *Nat Rev Mol Cell Biol*, vol. 13, no. 1, Jan, pp. 27-38.

Long, F, Joeng, KS, Xuan, S, Efstratiadis, A & McMahon, AP 2006, 'Independent regulation of skeletal growth by Ihh and IGF signaling', *Dev Biol*, vol. 298, no. 1, Oct 1, pp. 327-333.

Long, F & Ornitz, DM 2013, 'Development of the endochondral skeleton', *Cold Spring Harb Perspect Biol*, vol. 5, no. 1, Jan 01, p. a008334.

Long, F, Schipani, E, Asahara, H, Kronenberg, H & Montminy, M 2001, 'The CREB family of activators is required for endochondral bone development', *Development*, vol. 128, no. 4, Feb, pp. 541-550.

Long, F, Zhang, XM, Karp, S, Yang, Y & McMahon, AP 2001, 'Genetic manipulation of hedgehog signaling in the endochondral skeleton reveals a direct role in the regulation of chondrocyte proliferation', *Development*, vol. 128, no. 24, Dec, pp. 5099-5108.

Lorincz, AE 1964, 'Hurler's syndrome in man and snorter dwarfism in cattle: heritable disorders of connective tissue acid mucopolysaccharide metabolism', *Clin Orthop Relat Res*, vol. 33, Mar-Apr, pp. 104-118.

Lupu, F, Terwilliger, JD, Lee, K, Segre, GV & Efstratiadis, A 2001, 'Roles of Growth Hormone and Insulin-like Growth Factor 1 in Mouse Postnatal Growth', *Developmental Biology*, vol. 229, no. 1, pp. 141-162.

LuValle, P & Beier, F 2000, 'Cell cycle control in growth plate chondrocytes', *Front Biosci*, vol. 5, May 1, pp. D493-503.

Mackie, EJ, Ahmed, YA, Tatarczuch, L, Chen, KS & Mirams, M 2008, 'Endochondral ossification: how cartilage is converted into bone in the developing skeleton', *Int J Biochem Cell Biol*, vol. 40, no. 1, pp. 46-62.

Mackie, EJ, Tatarczuch, L & Mirams, M 2011, 'The skeleton: a multi-functional complex organ: the growth plate chondrocyte and endochondral ossification', *J Endocrinol*, vol. 211, no. 2, Nov, pp. 109-121.

MacLean, HE, Guo, J, Knight, MC, Zhang, P, Cobrinik, D & Kronenberg, HM 2004, 'The cyclin-dependent kinase inhibitor p57(Kip2) mediates proliferative actions of PTHrP in chondrocytes', *J Clin Invest*, vol. 113, no. 9, May, pp. 1334-1343.

Macsai, CE, Derrick-Roberts, AL, Ding, X, Zarrinkalam, KH, McIntyre, C, Anderson, PH, Anson, DS & Byers, S 2012, 'Skeletal response to lentiviral mediated gene therapy in a mouse model of MPS VII', *Mol Genet Metab*, vol. 106, no. 2, Jun, pp. 202-213.

Madsen, K, Friberg, U, Roos, P, Eden, S & Isaksson, O 1983, 'Growth hormone stimulates the proliferation of cultured chondrocytes from rabbit ear and rat rib growth cartilage', *Nature*, vol. 304, no. 5926, Aug 11-17, pp. 545-547.

Maeda, Y, Nakamura, E, Nguyen, MT, Suva, LJ, Swain, FL, Razzaque, MS, Mackem, S & Lanske, B 2007, 'Indian Hedgehog produced by postnatal chondrocytes is essential for maintaining a growth plate and trabecular bone', *Proc Natl Acad Sci U S A*, vol. 104, no. 15, Apr 10, pp. 6382-6387.

Maes, C 2017, 'Signaling pathways effecting crosstalk between cartilage and adjacent tissues: Seminars in cell and developmental biology: The biology and pathology of cartilage', *Semin Cell Dev Biol*, vol. 62, Feb, pp. 16-33.

Maes, C & Kronenberg, HM 2016, 'Chapter 60 - Bone Development and Remodeling A2 - Jameson, J. Larry', in LJD Groot, DMd Kretser, LC Giudice, AB Grossman, S Melmed, JT Potts & GC Weir (eds), *Endocrinology: Adult and Pediatric (Seventh Edition)*, W.B. Saunders, Philadelphia, pp. 1038-1062.e1038.

Maes, C, Stockmans, I, Moermans, K, Van Looveren, R, Smets, N, Carmeliet, P, Bouillon, R & Carmeliet, G 2004, 'Soluble VEGF isoforms are essential for establishing epiphyseal vascularization and regulating chondrocyte development and survival', *J Clin Invest*, vol. 113, no. 2, Jan, pp. 188-199.

Mairet-Coello, G, Tury, A & DiCicco-Bloom, E 2009, 'Insulin-like growth factor-1 promotes G(1)/S cell cycle progression through bidirectional regulation of cyclins and cyclin-dependent kinase inhibitors via the phosphatidylinositol 3-kinase/Akt pathway in developing rat cerebral cortex', *J Neurosci*, vol. 29, no. 3, Jan 21, pp. 775-788.

Makihira, S, Yan, W, Murakami, H, Furukawa, M, Kawai, T, Nikawa, H, Yoshida, E, Hamada, T, Okada, Y & Kato, Y 2003, 'Thyroid hormone enhances aggrecanase-2/ADAM-TS5 expression and proteoglycan degradation in growth plate cartilage', *Endocrinology*, vol. 144, no. 6, Jun, pp. 2480-2488.

Mango, RL, Xu, L, Sands, MS, Vogler, C, Seiler, G, Schwarz, T, Haskins, ME & Ponder, KP 2004, 'Neonatal retroviral vector-mediated hepatic gene therapy reduces bone, joint, and cartilage disease in mucopolysaccharidosis VII mice and dogs', *Mol Genet Metab*, vol. 82, no. 1, May, pp. 4-19.

Manton, KJ, Leong, DF, Cool, SM & Nurcombe, V 2007, 'Disruption of heparan and chondroitin sulfate signaling enhances mesenchymal stem cell-derived osteogenic differentiation via bone morphogenetic protein signaling pathways', *Stem Cells*, vol. 25, no. 11, Nov, pp. 2845-2854.

Marti, A, Wirbelauer, C, Scheffner, M & Krek, W 1999, 'Interaction between ubiquitin-protein ligase SCFSKP2 and E2F-1 underlies the regulation of E2F-1 degradation', *Nat Cell Biol*, vol. 1, no. 1, May, pp. 14-19.

Martin, DC, Atmuri, V, Hemming, RJ, Farley, J, Mort, JS, Byers, S, Hombach-Klonisch, S, Csoka, AB, Stern, R & Triggs-Raine, BL 2008, 'A mouse model of human mucopolysaccharidosis IX exhibits osteoarthritis', *Hum Mol Genet*, vol. 17, no. 13, Jul 1, pp. 1904-1915.

Matsuo, M, Nishida, K, Yoshida, A, Murakami, T & Inoue, H 2001, 'Expression of caspase-3 and -9 relevant to cartilage destruction and chondrocyte apoptosis in human osteoarthritic cartilage', *Acta Med Okayama*, vol. 55, no. 6, Dec, pp. 333-340.

Matz-Soja, M, Aleithe, S, Marbach, E, Böttger, J, Arnold, K, Schmidt-Heck, W, Kratzsch, J & Gebhardt, R 2014, 'Hepatic Hedgehog signaling contributes to the regulation of IGF1 and IGFBP1 serum levels', *Cell Communication and Signaling*, vol. 12, no. 1, February 18, p. 11.

McClure, J, Smith, PS, Sorby-Adams, G & Hopwood, J 1986, 'The histological and ultrastructural features of the epiphyseal plate in Morquio type A syndrome (mucopolysaccharidosis type IVA)', *Pathology*, vol. 18, no. 2, Apr, pp. 217-221.

McGill, JJ, Inwood, AC, Coman, DJ, Lipke, ML, De Lore, D, Swiedler, SJ & Hopwood, JJ 2010, 'Enzyme replacement therapy for mucopolysaccharidosis VI from 8 weeks of age–a sibling control study', *Clinical Genetics*, vol. 77, no. 5, pp. 492-498.

McMahon, AP, Ingham, PW & Tabin, CJ 2003, '1 Developmental roles and clinical significance of Hedgehog signaling', in *Current Topics in Developmental Biology*, vol. 53, Academic Press, pp. 1-114.

Melbouci, M, Mason, RW, Suzuki, Y, Fukao, T, Orii, T & Tomatsu, S 2018, 'Growth impairment in mucopolysaccharidoses', *Mol Genet Metab*, 2018/03/16/.

Metcalf, JA, Zhang, Y, Hilton, MJ, Long, F & Ponder, KP 2009, 'Mechanism of shortened bones in mucopolysaccharidosis VII', *Mol Genet Metab*, vol. 97, no. 3, Jul, pp. 202-211.

Minina, E, Kreschel, C, Naski, MC, Ornitz, DM & Vortkamp, A 2002, 'Interaction of FGF, Ihh/Pthlh, and BMP signaling integrates chondrocyte proliferation and hypertrophic differentiation', *Dev Cell*, vol. 3, no. 3, Sep, pp. 439-449.

Minina, E, Wenzel, HM, Kreschel, C, Karp, S, Gaffield, W, McMahon, AP & Vortkamp, A 2001, 'BMP and Ihh/PTHrP signaling interact to coordinate chondrocyte proliferation and differentiation', *Development*, vol. 128, no. 22, Nov, pp. 4523-4534.

Mitchell, PG, Magna, HA, Reeves, LM, Lopresti-Morrow, LL, Yocum, SA, Rosner, PJ, Geoghegan, KF & Hambor, JE 1996, 'Cloning, expression, and type II collagenolytic activity of matrix metalloproteinase-13 from human osteoarthritic cartilage', *J Clin Invest*, vol. 97, no. 3, Feb 1, pp. 761-768.

Moberg, K, Starz, MA & Lees, JA 1996, 'E2F-4 switches from p130 to p107 and pRB in response to cell cycle reentry', *Mol Cell Biol*, vol. 16, no. 4, Apr, pp. 1436-1449.

Mochizuki, H, Hakeda, Y, Wakatsuki, N, Usui, N, Akashi, S, Sato, T, Tanaka, K & Kumegawa, M 1992, 'Insulin-like growth factor-I supports formation and activation of osteoclasts', *Endocrinology*, vol. 131, no. 3, pp. 1075-1080.

Mohan, S, Richman, C, Guo, R, Amaar, Y, Donahue, LR, Wergedal, J & Baylink, DJ 2003, 'Insulin-Like Growth Factor Regulates Peak Bone Mineral Density in Mice by Both Growth Hormone-Dependent and -Independent Mechanisms', *Endocrinology*, vol. 144, no. 3, pp. 929-936.

Mohan, S, Richman, C, Guo, R, Amaar, Y, Donahue, LR, Wergedal, J & Baylink, DJ 2003, 'Insulin-like growth factor regulates peak bone mineral density in mice by both growth hormone-dependent and -independent mechanisms', *Endocrinology*, vol. 144, no. 3, Mar, pp. 929-936.

Mohanalakshmi, P, V., M & S., M 2014, 'Hurler-Scheie syndrome with subclinical hypothyroidism: A case report', *2014*, vol. 5, no. 4, 2014-04-30, p. 3.

Montano, AM, Lock-Hock, N, Steiner, RD, Graham, BH, Szlago, M, Greenstein, R, Pineda, M, Gonzalez-Meneses, A, Coker, M, Bartholomew, D, Sands, MS, Wang, R, Giugliani, R, Macaya, A, Pastores, G, Ketko, AK, Ezgu, F, Tanaka, A, Arash, L, Beck, M, Falk, RE, Bhattacharya, K, Franco, J, White, KK, Mitchell, GA, Cimbalistiene, L, Holtz, M & Sly, WS 2016, 'Clinical course of sly syndrome (mucopolysaccharidosis type VII)', *J Med Genet*, vol. 53, no. 6, Jun, pp. 403-418.

Montaño, AM, Tomatsu, S, Brusius, A, Smith, M & Orii, T 2008, 'Growth charts for patients affected with Morquio A disease', *American Journal of Medical Genetics Part A*, vol. 146A, no. 10, pp. 1286-1295.

Moskot, M, Gabig-Ciminska, M, Jakobkiewicz-Banecka, J, Wesierska, M, Bochenska, K & Wegrzyn, G 2016, 'Cell cycle is disturbed in mucopolysaccharidosis type II fibroblasts, and can be improved by genistein', *Gene*, vol. 585, no. 1, Jul 01, pp. 100-103.

Muenzer, J 2011, 'Overview of the mucopolysaccharidoses', *Rheumatology (Oxford)*, vol. 50 Suppl 5, Dec, pp. v4-12.

Muenzer, J, Wraith, JE, Beck, M, Giugliani, R, Harmatz, P, Eng, CM, Vellodi, A, Martin, R, Ramaswami, U, Gucsavas-Calikoglu, M, Vijayaraghavan, S, Wendt, S, Puga, AC, Ulbrich, B, Shinawi, M, Cleary, M, Piper, D, Conway, AM & Kimura, A 2006, 'A phase

II/III clinical study of enzyme replacement therapy with idursulfase in mucopolysaccharidosis II (Hunter syndrome)', *Genet Med*, vol. 8, no. 8, Aug, pp. 465-473.

Murray, M, Butler, AM, Fiala-Beer, E & Su, GM 2005, 'Phospho-STAT5 accumulation in nuclear fractions from vitamin A-deficient rat liver', *FEBS Lett*, vol. 579, no. 17, Jul 4, pp. 3669-3673.

Nagashima, K, Endo, H, Sakakibara, K, Konishi, Y, Miyachi, K, Wey, JJ, Suzuki, Y & Onisawa, J 1976, 'Morphological and biochemical studies of a case of mucopolysaccharidosis II (Hunter's syndrome)', *Acta Pathol Jpn*, vol. 26, no. 1, Jan, pp. 115-132.

Naski, MC, Colvin, JS, Coffin, JD & Ornitz, DM 1998, 'Repression of hedgehog signaling and BMP4 expression in growth plate cartilage by fibroblast growth factor receptor 3', *Development*, vol. 125, no. 24, Dec, pp. 4977-4988.

Natowicz, MR, Short, MP, Wang, Y, Dickersin, GR, Gebhardt, MC, Rosenthal, DI, Sims, KB & Rosenberg, AE 1996, 'Clinical and biochemical manifestations of hyaluronidase deficiency', *N Engl J Med*, vol. 335, no. 14, Oct 3, pp. 1029-1033.

Neufeld, E & Muenzer, J 2001, 'The Mucopolysaccharidoses', in C Sciver, A Beaudet, W Sly & D Valle (eds), *The metabolic and molecular bases of inherited disease*, McGraw hill, New York, pp. 3421-3452.

Nilsson, A, Carlsson, B, Mathews, L & Isaksson, OG 1990, 'Growth hormone regulation of the growth hormone receptor mRNA in cultured rat epiphyseal chondrocytes', *Mol Cell Endocrinol*, vol. 70, no. 3, May 7, pp. 237-246.

Nilsson, O, Marino, R, De Luca, F, Phillip, M & Baron, J 2005, 'Endocrine regulation of the growth plate', *Horm Res*, vol. 64, no. 4, pp. 157-165.

Nishida, T, Kondo, S, Maeda, A, Kubota, S, Lyons, KM & Takigawa, M 2009, 'CCN family 2/connective tissue growth factor (CCN2/CTGF) regulates the expression of Vegf through Hif-1α expression in a chondrocytic cell line, HCS-2/8, under hypoxic condition', *Bone*, vol. 44, no. 1, 09/13, pp. 24-31.

Nuttall, JD, Brumfield, LK, Fazzalari, NL, Hopwood, JJ & Byers, S 1999, 'Histomorphometric analysis of the tibial growth plate in a feline model of mucopolysaccharidosis type VI', *Calcif Tissue Int*, vol. 65, no. 1, Jul, pp. 47-52.

O'Shea, PJ, Bassett, JH, Sriskantharajah, S, Ying, H, Cheng, SY & Williams, GR 2005, 'Contrasting skeletal phenotypes in mice with an identical mutation targeted to thyroid hormone receptor alpha1 or beta', *Mol Endocrinol*, vol. 19, no. 12, Dec, pp. 3045-3059.

Oberbauer, AM & Peng, R 1995, 'Growth hormone and IGF-I stimulate cell function in distinct zones of the rat epiphyseal growth plate', *Connect Tissue Res*, vol. 31, no. 3, pp. 189-195.

Oda, H, Sasaki, Y, Nakatani, Y, Maesaka, H & Suwa, S 1988, 'Hunter's syndrome. An ultrastructural study of an autopsy case', *Acta Pathol Jpn*, vol. 38, no. 9, Sep, pp. 1175-1190.

Ohlsson, C, Nilsson, A, Isaksson, O, Bentham, J & Lindahl, A 1992, 'Effects of tri-iodothyronine and insulin-like growth factor-I (IGF-I) on alkaline phosphatase activity, [3H]thymidine incorporation and IGF-I receptor mRNA in cultured rat epiphyseal chondrocytes', *J Endocrinol*, vol. 135, no. 1, Oct, pp. 115-123.

Ohlsson, C, Nilsson, A, Isaksson, OG & Lindahl, A 1992, 'Effect of growth hormone and insulin-like growth factor-I on DNA synthesis and matrix production in rat epiphyseal chondrocytes in monolayer culture', *J Endocrinol*, vol. 133, no. 2, May, pp. 291-300.

Ohtani, K, DeGregori, J & Nevins, JR 1995, 'Regulation of the cyclin E gene by transcription factor E2F1', *Proc Natl Acad Sci U S A*, vol. 92, no. 26, Dec 19, pp. 12146-12150.

Oltvai, ZN, Milliman, CL & Korsmeyer, SJ 1993, 'Bcl-2 heterodimerizes in vivo with a conserved homolog, Bax, that accelerates programmed cell death', *Cell*, vol. 74, no. 4, Aug 27, pp. 609-619.

Orkin, RW, Williams, BR, Cranley, RE, Poppke, DC & Brown, KS 1977, 'Defects in the cartilaginous growth plates of brachymorphic mice', *J Cell Biol*, vol. 73, no. 2, May, pp. 287-299.

Oussoren, E, Keulemans, J, van Diggelen, OP, Oemardien, LF, Timmermans, RG, van der Ploeg, AT & Ruijter, GJ 2013, 'Residual alpha-L-iduronidase activity in fibroblasts of mild to severe Mucopolysaccharidosis type I patients', *Mol Genet Metab*, vol. 109, no. 4, Aug, pp. 377-381.

Parker, EA, Hegde, A, Buckley, M, Barnes, KM, Baron, J & Nilsson, O 2007, 'Spatial and temporal regulation of GH-IGF-related gene expression in growth plate cartilage', *J Endocrinol*, vol. 194, no. 1, Jul, pp. 31-40.

Patel, P, Suzuki, Y, Maeda, M, Yasuda, E, Shimada, T, Orii, KE, Orii, T & Tomatsu, S 2014, 'Growth charts for patients with Hunter syndrome', *Molecular Genetics and Metabolism Reports*, vol. 1, no. 0, //, pp. 5-18.

Patel, P, Suzuki, Y, Tanaka, A, Yabe, H, Kato, S, Shimada, T, Mason, RW, Orii, KE, Fukao, T, Orii, T & Tomatsu, S 2014, 'Impact of Enzyme Replacement Therapy and Hematopoietic Stem Cell Therapy on Growth in Patients with Hunter Syndrome', *Mol Genet Metab Rep*, vol. 1, pp. 184-196.

Patton, JT & Kaufman, MH 1995, 'The timing of ossification of the limb bones, and growth rates of various long bones of the fore and hind limbs of the prenatal and early postnatal laboratory mouse', *J Anat*, vol. 186 (Pt 1), Feb, pp. 175-185.

Peck, SH, O'Donnell, PJM, Kang, JL, Malhotra, NR, Dodge, GR, Pacifici, M, Shore, EM, Haskins, ME & Smith, LJ 2015, 'Delayed hypertrophic differentiation of epiphyseal chondrocytes contributes to failed secondary ossification in mucopolysaccharidosis VII dogs', *Mol Genet Metab*, vol. 116, no. 3, 11//, pp. 195-203.

Piecewicz, SM, Pandey, A, Roy, B, Xiang, SH, Zetter, BR & Sengupta, S 2012, 'Insulin-like growth factors promote vasculogenesis in embryonic stem cells', *PLoS One*, vol. 7, no. 2, p. e32191.

Pievani, A, Azario, I, Antolini, L, Shimada, T, Patel, P, Remoli, C, Rambaldi, B, Valsecchi, MG, Riminucci, M, Biondi, A, Tomatsu, S & Serafini, M 2014, 'Neonatal bone marrow transplantation prevents bone pathology in a mouse model of mucopolysaccharidosis type I', *Blood*, Oct 8.

Pineda, M, O'Callaghan, M, Fernandez Lopez, A, Coll, MJ, Ullot, R & Garcia-Fructuoso, G 2016, 'Clinical Evolution After Enzyme Replacement Therapy in Twins with the Severe Form of Maroteaux-Lamy Syndrome', *JIMD Rep*, vol. 30, pp. 7-14.

Piwien-Pilipuk, G, Huo, JS & Schwartz, J 2002, 'Growth hormone signal transduction', *J Pediatr Endocrinol Metab*, vol. 15, no. 6, Jun, pp. 771-786.

Polgreen, LE & Miller, BS 2010, 'Growth patterns and the use of growth hormone in the mucopolysaccharidoses', *J Pediatr Rehabil Med*, vol. 3, no. 1, pp. 25-38.

Polgreen, LE, Plog, M, Schwender, JD, Tolar, J, Thomas, W, Orchard, PJ, Miller, BS & Petryk, A 2009, 'Short-term growth hormone treatment in children with Hurler syndrome after hematopoietic cell transplantation', *Bone Marrow Transplant*, vol. 44, no. 5, Sep, pp. 279-285.

Polgreen, LE, Thomas, W, Orchard, PJ, Whitley, CB & Miller, BS 2014, 'Effect of recombinant human growth hormone on changes in height, bone mineral density, and body composition over 1-2 years in children with Hurler or Hunter syndrome', *Mol Genet Metab*, vol. 111, no. 2, Feb, pp. 101-106.

Polgreen, LE, Tolar, J, Plog, M, Himes, JH, Orchard, PJ, Whitley, CB, Miller, BS & Petryk, A 2008, 'Growth and endocrine function in patients with Hurler syndrome after hematopoietic stem cell transplantation', *Bone Marrow Transplant*, vol. 41, no. 12, Jun, pp. 1005-1011.

Porter, LA & Donoghue, DJ 2003, 'Cyclin B1 and CDK1: nuclear localization and upstream regulators', *Prog Cell Cycle Res*, vol. 5, pp. 335-347.

Prasad, VK & Kurtzberg, J 2010, 'Transplant outcomes in mucopolysaccharidoses', *Semin Hematol*, vol. 47, no. 1, Jan, pp. 59-69.

Quartel, A, Hendriksz, CJ, Parini, R, Graham, S, Lin, P & Harmatz, P 2015, 'Growth Charts for Individuals with Mucopolysaccharidosis VI (Maroteaux–Lamy Syndrome)', *JIMD Rep*, vol. 18, 12/18
03/19/received
06/19/revised
07/01/accepted, pp. 1-11.

Ram, PA, Park, SH, Choi, HK & Waxman, DJ 1996, 'Growth hormone activation of Stat 1, Stat 3, and Stat 5 in rat liver. Differential kinetics of hormone desensitization and growth hormone stimulation of both tyrosine phosphorylation and serine/threonine phosphorylation', *Journal of Biological Chemistry*, vol. 271, no. 10, Mar 8, pp. 5929-5940.

Ram, PA & Waxman, DJ 1997, 'Interaction of growth hormone-activated STATs with SH2-containing phosphotyrosine phosphatase SHP-1 and nuclear JAK2 tyrosine kinase', *Journal of Biological Chemistry*, vol. 272, no. 28, Jul 11, pp. 17694-17702.

Ranke, MB, Schwarze, CP, Dopfer, R, Klingebiel, T, Scheel-Walter, HG, Lang, P & Niethammer, D 2005, 'Late effects after stem cell transplantation (SCT) in children--growth and hormones', *Bone Marrow Transplant*, vol. 35 Suppl 1, Mar, pp. S77-81.

Razzaque, MS, Soegiarto, DW, Chang, D, Long, F & Lanske, B 2005, 'Conditional deletion of Indian hedgehog from collagen type 2alpha1-expressing cells results in abnormal endochondral bone formation', *J Pathol*, vol. 207, no. 4, Dec, pp. 453-461.

Ren, B, Cam, H, Takahashi, Y, Volkert, T, Terragni, J, Young, RA & Dynlacht, BD 2002, 'E2F integrates cell cycle progression with DNA repair, replication, and G(2)/M checkpoints', *Genes Dev*, vol. 16, no. 2, Jan 15, pp. 245-256.

Roberts, AL, Howarth, GS, Liaw, WC, Moretta, S, Kritas, S, Lymn, KA, Yazbeck, R, Tran, C, Fletcher, JM, Butler, RN & Byers, S 2009, 'Gastrointestinal pathology in a mouse model of mucopolysaccharidosis type IIIA', *Journal of Cellular Physiology*, vol. 219, no. 2, May, pp. 259-264.

Robson, H, Siebler, T, Stevens, DA, Shalet, SM & Williams, GR 2000, 'Thyroid hormone acts directly on growth plate chondrocytes to promote hypertrophic differentiation and inhibit clonal expansion and cell proliferation', *Endocrinology*, vol. 141, no. 10, Oct, pp. 3887-3897.

Rosenberg, L 1971, 'Chemical basis for the histological use of safranin O in the study of articular cartilage', *J Bone Joint Surg Am*, vol. 53, no. 1, Jan, pp. 69-82.

Ross, JL, Sandberg, DE, Rose, SR, Leschek, EW, Baron, J, Chipman, JJ, Cassorla, FG, Quigley, CA, Crowe, BJ, Roberts, K & Cutler, GB, Jr. 2004, 'Psychological adaptation in children with idiopathic short stature treated with growth hormone or placebo', *J Clin Endocrinol Metab*, vol. 89, no. 10, Oct, pp. 4873-4878.

Rotwein, P 2012, 'Mapping the growth hormone--Stat5b--IGF-I transcriptional circuit', *Trends Endocrinol Metab*, vol. 23, no. 4, Apr, pp. 186-193.

Rowan, DJ, Tomatsu, S, Grubb, JH, Haupt, B, Montano, AM, Oikawa, H, Sosa, AC, Chen, A & Sly, WS 2012, 'Long circulating enzyme replacement therapy rescues bone pathology in mucopolysaccharidosis VII murine model', *Mol Genet Metab*, vol. 107, no. 1-2, Sep, pp. 161-172.

Rozdzynska-Swiatkowska, A, Jurecka, A, Cieslik, J & Tylki-Szymanska, A 2015, 'Growth patterns in children with mucopolysaccharidosis I and II', *World J Pediatr*, vol. 11, no. 3, Aug, pp. 226-231.

Rozdzynska, A, Tylki-Szymanska, A, Jurecka, A & Cieslik, J 2011, 'Growth pattern and growth prediction of body height in children with mucopolysaccharidosis type II', *Acta Paediatr*, vol. 100, no. 3, Mar, pp. 456-460.

Russell, C, Hendson, G, Jevon, G, Matlock, T, Yu, J, Aklujkar, M, Ng, KY & Clarke, LA 1998, 'Murine MPS I: insights into the pathogenesis of Hurler syndrome', *Clin Genet*, vol. 53, no. 5, May, pp. 349-361.

Sands, MS, Barker, JE, Vogler, C, Levy, B, Gwynn, B, Galvin, N, Sly, WS & Birkenmeier, E 1993, 'Treatment of murine mucopolysaccharidosis type VII by syngeneic bone marrow transplantation in neonates', *Lab Invest*, vol. 68, no. 6, Jun, pp. 676-686.

Sands, MS & Birkenmeier, EH 1993, 'A single-base-pair deletion in the beta-glucuronidase gene accounts for the phenotype of murine mucopolysaccharidosis type VII', *Proc Natl Acad Sci U S A*, vol. 90, no. 14, Jul 15, pp. 6567-6571.

Sands, MS, Vogler, C, Kyle, JW, Grubb, JH, Levy, B, Galvin, N, Sly, WS & Birkenmeier, EH 1994, 'Enzyme replacement therapy for murine mucopolysaccharidosis type VII', *J Clin Invest*, vol. 93, no. 6, Jun, pp. 2324-2331.

Scheijen, B, Bronk, M, van der Meer, T & Bernards, R 2003, 'Constitutive E2F1 overexpression delays endochondral bone formation by inhibiting chondrocyte differentiation', *Mol Cell Biol*, vol. 23, no. 10, May, pp. 3656-3668.

Schipani, E, Lanske, B, Hunzelman, J, Luz, A, Kovacs, CS, Lee, K, Pirro, A, Kronenberg, HM & Juppner, H 1997, 'Targeted expression of constitutively active receptors for parathyroid hormone and parathyroid hormone-related peptide delays endochondral bone formation and rescues mice that lack parathyroid hormone-related peptide', *Proc Natl Acad Sci U S A*, vol. 94, no. 25, Dec 9, pp. 13689-13694.

Schlegel, W, Halbauer, D, Raimann, A, Albrecht, C, Scharmer, D, Sagmeister, S, Helmreich, M, Hausler, G & Egerbacher, M 2010, 'IGF expression patterns and regulation in growth plate chondrocytes', *Mol Cell Endocrinol*, vol. 327, no. 1-2, Oct 7, pp. 65-71.

Schuchman, EH, Toroyan, TK, Haskins, ME & Desnick, RJ 1989, 'Characterization of the defective beta-glucuronidase activity in canine mucopolysaccharidosis type VII', *Enzyme*, vol. 42, no. 3, pp. 174-180.

Schulze-Frenking, G, Jones, SA, Roberts, J, Beck, M & Wraith, JE 2011, 'Effects of enzyme replacement therapy on growth in patients with mucopolysaccharidosis type II', *J Inherit Metab Dis*, vol. 34, no. 1, Feb, pp. 203-208.

Schwartz, CE, Stanislovitis, P, Phelan, MC, Klinger, K, Taylor, HA & Stevenson, RE 1991, 'Deletion mapping of plasminogen activator inhibitor, type I (PLANH1) and beta-glucuronidase (GUSB) in 7q21----q22', *Cytogenet Cell Genet*, vol. 56, no. 3-4, pp. 152-153.

Seghezzi, G, Patel, S, Ren, CJ, Gualandris, A, Pintucci, G, Robbins, ES, Shapiro, RL, Galloway, AC, Rifkin, DB & Mignatti, P 1998, 'Fibroblast growth factor-2 (FGF-2) induces vascular endothelial growth factor (VEGF) expression in the endothelial cells of forming capillaries: an autocrine mechanism contributing to angiogenesis', *J Cell Biol*, vol. 141, no. 7, Jun 29, pp. 1659-1673.

Selvamurugan, N, Pulumati, MR, Tyson, DR & Partridge, NC 2000, 'Parathyroid hormone regulation of the rat collagenase-3 promoter by protein kinase A-dependent transactivation of core binding factor alpha1', *Journal of Biological Chemistry*, vol. 275, no. 7, Feb 18, pp. 5037-5042.

Shalitin, S, Phillip, M, Stein, J, Goshen, Y, Carmi, D & Yaniv, I 2006, 'Endocrine dysfunction and parameters of the metabolic syndrome after bone marrow transplantation during childhood and adolescence', *Bone Marrow Transplant*, vol. 37, no. 12, Jun, pp. 1109-1117.

Shapiro, IM, Adams, CS, Freeman, T & Srinivas, V 2005, 'Fate of the hypertrophic chondrocyte: microenvironmental perspectives on apoptosis and survival in the epiphyseal growth plate', *Birth Defects Res C Embryo Today*, vol. 75, no. 4, Dec, pp. 330-339.

Shimo, T, Koyama, E, Ibaragi, S, Kurio, N, Yamamoto, D, Okui, T, Kishimoto, K, Mese, H & Sasaki, A 2008, 'Possible Involvement of p38 MAP Kinase in Retinoid-stimulated Expression of Indian Hedgehog in Prehypertrophic Chondrocytes', *Oral Science International*, vol. 5, no. 1, pp. 1-14.

Shimo, T, Nakanishi, T, Kimura, Y, Nishida, T, Ishizeki, K, Matsumura, T & Takigawa, M 1998, 'Inhibition of endogenous expression of connective tissue growth factor by its

antisense oligonucleotide and antisense RNA suppresses proliferation and migration of vascular endothelial cells', *J Biochem*, vol. 124, no. 1, Jul, pp. 130-140.

Sifuentes, M, Doroshow, R, Hoft, R, Mason, G, Walot, I, Diament, M, Okazaki, S, Huff, K, Cox, GF, Swiedler, SJ & Kakkis, ED 2007, 'A follow-up study of MPS I patients treated with laronidase enzyme replacement therapy for 6 years', *Mol Genet Metab*, vol. 90, no. 2, Feb, pp. 171-180.

Silveri, CP, Kaplan, FS, Fallon, MD, Bayever, E & August, CS 1991, 'Hurler syndrome with special reference to histologic abnormalities of the growth plate', *Clin Orthop Relat Res*, no. 269, Aug, pp. 305-311.

Simonaro, CM, D'Angelo, M, Haskins, ME & Schuchman, EH 2005, 'Joint and bone disease in mucopolysaccharidoses VI and VII: identification of new therapeutic targets and biomarkers using animal models', *Pediatr Res*, vol. 57, no. 5 Pt 1, May, pp. 701-707.

Simonaro, CM, Ge, Y, Eliyahu, E, He, X, Jepsen, KJ & Schuchman, EH 2010, 'Involvement of the Toll-like receptor 4 pathway and use of TNF-alpha antagonists for treatment of the mucopolysaccharidoses', *Proc Natl Acad Sci U S A*, vol. 107, no. 1, Jan 05, pp. 222-227.

Simonaro, CM, Haskins, ME & Schuchman, EH 2001, 'Articular chondrocytes from animals with a dermatan sulfate storage disease undergo a high rate of apoptosis and release nitric oxide and inflammatory cytokines: a possible mechanism underlying degenerative joint disease in the mucopolysaccharidoses', *Lab Invest*, vol. 81, no. 9, Sep, pp. 1319-1328.

Sims, NA, Clement-Lacroix, P, Da Ponte, F, Bouali, Y, Binart, N, Moriggl, R, Goffin, V, Coschigano, K, Gaillard-Kelly, M, Kopchick, J, Baron, R & Kelly, PA 2000, 'Bone homeostasis in growth hormone receptor-null mice is restored by IGF-I but independent of Stat5', *J Clin Invest*, vol. 106, no. 9, Nov, pp. 1095-1103.

Sjogren, K, Liu, JL, Blad, K, Skrtic, S, Vidal, O, Wallenius, V, LeRoith, D, Tornell, J, Isaksson, OG, Jansson, JO & Ohlsson, C 1999, 'Liver-derived insulin-like growth factor I (IGF-I) is the principal source of IGF-I in blood but is not required for postnatal body growth in mice', *Proc Natl Acad Sci U S A*, vol. 96, no. 12, Jun 8, pp. 7088-7092.

Sly, WS, Quinton, BA, McAlister, WH & Rimoin, DL 1973, 'Beta glucuronidase deficiency: report of clinical, radiologic, and biochemical features of a new mucopolysaccharidosis', *J Pediatr*, vol. 82, no. 2, Feb, pp. 249-257.

Smith, Kuniyoshi, J & Talamantes, F 1989, 'Mouse serum growth hormone (GH) binding protein has GH receptor extracellular and substituted transmembrane domains', *Mol Endocrinol*, vol. 3, no. 6, Jun, pp. 984-990.

Smith, LJ, Martin, JT, O'Donnell, P, Wang, P, Elliott, DM, Haskins, ME & Ponder, KP 2012, 'Effect of neonatal gene therapy on lumbar spine disease in mucopolysaccharidosis VII dogs', *Mol Genet Metab*, vol. 107, no. 1-2, Sep, pp. 145-152.

Smith, RN, Taylor, SA & Massey, JC 1970, 'Controlled clinical trial of combined triiodothyronine and thyroxine in the treatment of hypothyroidism', *Br Med J*, vol. 4, no. 5728, Oct 17, pp. 145-148.

Sohn, YB, Cho, SY, Park, SW, Kim, SJ, Ko, AR, Kwon, EK, Han, SJ & Jin, DK 2013, 'Phase I/II clinical trial of enzyme replacement therapy with idursulfase beta in patients with mucopolysaccharidosis II (Hunter syndrome)', *Orphanet J Rare Dis*, vol. 8, p. 42.

Sohn, YB, Park, SW, Kim, SH, Cho, SY, Ji, ST, Kwon, EK, Han, SJ, Oh, SJ, Park, YJ, Ko, AR, Paik, KH, Lee, J, Lee, DH & Jin, DK 2012, 'Enzyme replacement therapy improves joint motion and outcome of the 12-min walk test in a mucopolysaccharidosis type VI patient previously treated with bone marrow transplantation', *Am J Med Genet A*, vol. 158a, no. 5, May, pp. 1158-1163.

Spellacy, E, Shull, RM, Constantopoulos, G & Neufeld, EF 1983, 'A canine model of human alpha-L-iduronidase deficiency', *Proc Natl Acad Sci U S A*, vol. 80, no. 19, Oct, pp. 6091-6095.

St-Jacques, B, Hammerschmidt, M & McMahon, AP 1999, 'Indian hedgehog signaling regulates proliferation and differentiation of chondrocytes and is essential for bone formation', *Genes Dev*, vol. 13, no. 16, Aug 15, pp. 2072-2086.

Stanton, H, Rogerson, FM, East, CJ, Golub, SB, Lawlor, KE, Meeker, CT, Little, CB, Last, K, Farmer, PJ, Campbell, IK, Fourie, AM & Fosang, AJ 2005, 'ADAMTS5 is the major aggrecanase in mouse cartilage in vivo and in vitro', *Nature*, vol. 434, no. 7033, Mar 31, pp. 648-652.

Stefano, JT, Correa-Giannella, ML, Ribeiro, CM, Alves, VA, Massarollo, PC, Machado, MC & Giannella-Neto, D 2006, 'Increased hepatic expression of insulin-like growth factor-I receptor in chronic hepatitis C', *World J Gastroenterol*, vol. 12, no. 24, Jun 28, pp. 3821-3828.

Stevens, DA, Hasserjian, RP, Robson, H, Siebler, T, Shalet, SM & Williams, GR 2000, 'Thyroid hormones regulate hypertrophic chondrocyte differentiation and expression of parathyroid hormone-related peptide and its receptor during endochondral bone formation', *J Bone Miner Res*, vol. 15, no. 12, Dec, pp. 2431-2442.

Sun, Y, Wang, P, Zheng, H & Smith, RG 2004, 'Ghrelin stimulation of growth hormone release and appetite is mediated through the growth hormone secretagogue receptor', *Proc Natl Acad Sci U S A*, vol. 101, no. 13, Mar 30, pp. 4679-4684.

Takahara, M, Naruse, T, Takagi, M, Orui, H & Ogino, T 2004, 'Matrix metalloproteinase-9 expression, tartrate-resistant acid phosphatase activity, and DNA fragmentation in vascular and cellular invasion into cartilage preceding primary endochondral ossification in long bones', *J Orthop Res*, vol. 22, no. 5, Sep, pp. 1050-1057.

Takeda, K, Sakurai, A, DeGroot, LJ & Refetoff, S 1992, 'Recessive inheritance of thyroid hormone resistance caused by complete deletion of the protein-coding region of the thyroid hormone receptor-beta gene', *J Clin Endocrinol Metab*, vol. 74, no. 1, Jan, pp. 49-55.

Tao, X, Shen, D, Ren, H, Zhang, X, Zhang, D, Ye, J & Gu, B 2000, 'Hepatitis B virus X protein activates expression of IGF-IR and VEGF in hepatocellular carcinoma cells', *Zhonghua Gan Zang Bing Za Zhi*, vol. 8, no. 3, Jun, pp. 161-163.

Tchetina, EV, Kobayashi, M, Yasuda, T, Meijers, T, Pidoux, I & Poole, AR 2007, 'Chondrocyte hypertrophy can be induced by a cryptic sequence of type II collagen and is accompanied by the induction of MMP-13 and collagenase activity: implications for development and arthritis', *Matrix Biol*, vol. 26, no. 4, May, pp. 247-258.

Teglund, S, McKay, C, Schuetz, E, van Deursen, JM, Stravopodis, D, Wang, D, Brown, M, Bodner, S, Grosveld, G & Ihle, JN 1998, 'Stat5a and Stat5b proteins have essential and nonessential, or redundant, roles in cytokine responses', *Cell*, vol. 93, no. 5, May 29, pp. 841-850.

Tessitore, A, Pirozzi, M & Auricchio, A 2009, 'Abnormal autophagy, ubiquitination, inflammation and apoptosis are dependent upon lysosomal storage and are useful biomarkers of mucopolysaccharidosis VI', *PathoGenetics*, vol. 2, 06/16
02/20/received
06/16/accepted, pp. 4-4.

Thompson, CL, Patel, R, Kelly, T-AN, Wann, AKT, Hung, CT, Chapple, JP & Knight, MM 2015, 'Hedgehog signalling does not stimulate cartilage catabolism and is inhibited by Interleukin-1β', *Arthritis Research & Therapy*, vol. 17, no. 1, December 24, p. 373.

Thompson, JN, Jones, MZ, Dawson, G & Huffman, PS 1992, 'N-acetylglucosamine 6-sulphatase deficiency in a Nubian goat: a model of Sanfilippo syndrome type D (mucopolysaccharidosis IIID)', *J Inherit Metab Dis*, vol. 15, no. 5, pp. 760-768.

Tian, F, Wu, M, Deng, L, Zhu, G, Ma, J, Gao, B, Wang, L, Li, YP & Chen, W 2014, 'Core binding factor beta (Cbfbeta) controls the balance of chondrocyte proliferation and differentiation by upregulating Indian hedgehog (Ihh) expression and inhibiting parathyroid hormone-related protein receptor (PPR) expression in postnatal cartilage and bone formation', *J Bone Miner Res*, vol. 29, no. 7, Jul, pp. 1564-1574.

Toledo, SP, Costa, VH, Fukui, RR & Abelin, N 1991, '[Serum growth hormone levels in Hunter's syndrome]', *Rev Hosp Clin Fac Med Sao Paulo*, vol. 46, no. 1, Jan-Feb, pp. 9-13.

Tomatsu, S, Montano, AM, Oikawa, H, Dung, VC, Hashimoto, A, Oguma, T, Gutierrez, ML, Takahashi, T, Shimada, T, Orii, T & Sly, WS 2014, 'Enzyme replacement therapy in newborn mucopolysaccharidosis IVA mice: Early treatment rescues bone lesions?', *Mol Genet Metab*, Jun 4.

Tomatsu, S, Orii, KO, Vogler, C, Grubb, JH, Snella, EM, Gutierrez, MA, Dieter, T, Sukegawa, K, Orii, T, Kondo, N & Sly, WS 2002, 'Missense models [Gustm(E536A)Sly, Gustm(E536Q)Sly, and Gustm(L175F)Sly] of murine mucopolysaccharidosis type VII produced by targeted mutagenesis', *Proc Natl Acad Sci U S A*, vol. 99, no. 23, Nov 12, pp. 14982-14987.

Tomatsu, S, Orii, KO, Vogler, C, Nakayama, J, Levy, B, Grubb, JH, Gutierrez, MA, Shim, S, Yamaguchi, S, Nishioka, T, Montano, AM, Noguchi, A, Orii, T, Kondo, N & Sly, WS 2003, 'Mouse model of N-acetylgalactosamine-6-sulfate sulfatase deficiency (Galns-/-) produced by targeted disruption of the gene defective in Morquio A disease', *Hum Mol Genet*, vol. 12, no. 24, Dec 15, pp. 3349-3358.

Traas, AM, Wang, P, Ma, X, Tittiger, M, Schaller, L, O'Donnell, P, Sleeper, MM, Vite, C, Herati, R, Aguirre, GD, Haskins, M & Ponder, KP 2007, 'Correction of Clinical Manifestations of Canine Mucopolysaccharidosis I with Neonatal Retroviral Vector Gene Therapy', *Molecular Therapy*, vol. 15, no. 8, 8//, pp. 1423-1431.

Trippel, SB, Corvol, MT, Dumontier, MF, Rappaport, R, Hung, HH & Mankin, HJ 1989, 'Effect of somatomedin-C/insulin-like growth factor I and growth hormone on cultured growth plate and articular chondrocytes', *Pediatr Res*, vol. 25, no. 1, Jan, pp. 76-82.

Tylki-Szymanska, A, Rozdzynska, A, Jurecka, A, Marucha, J & Czartoryska, B 2010, 'Anthropometric data of 14 patients with mucopolysaccharidosis I: retrospective analysis and efficacy of recombinant human alpha-L-iduronidase (laronidase)', *Mol Genet Metab*, vol. 99, no. 1, Jan, pp. 10-17.

Valentini, RP, Brookhiser, WT, Park, J, Yang, T, Briggs, J, Dressler, G & Holzman, LB 1997, 'Post-translational processing and renal expression of mouse Indian hedgehog', *Journal of Biological Chemistry*, vol. 272, no. 13, Mar 28, pp. 8466-8473.

van der Eerden, BC, Karperien, M & Wit, JM 2003, 'Systemic and local regulation of the growth plate', *Endocr Rev*, vol. 24, no. 6, Dec, pp. 782-801.

Varga, F, Rumpler, M & Klaushofer, K 1994, 'Thyroid hormones increase insulin-like growth factor mRNA levels in the clonal osteoblastic cell line MC3T3-E1', *FEBS Lett*, vol. 345, no. 1, May 23, pp. 67-70.

Varghese, F, Bukhari, AB, Malhotra, R & De, A 2014, 'IHC Profiler: An Open Source Plugin for the Quantitative Evaluation and Automated Scoring of Immunohistochemistry Images of Human Tissue Samples', *PLoS One*, vol. 9, no. 5, p. e96801.

Veldhuis, JD & Bowers, CY 2003, 'Human GH pulsatility: an ensemble property regulated by age and gender', *J Endocrinol Invest*, vol. 26, no. 9, Sep, pp. 799-813.

Vellodi, A, Young, EP, Cooper, A, Wraith, JE, Winchester, B, Meaney, C, Ramaswami, U & Will, A 1997, 'Bone marrow transplantation for mucopolysaccharidosis type I: experience of two British centres', *Arch Dis Child*, vol. 76, no. 2, Feb, pp. 92-99.

Vogler, C, Birkenmeier, EH, Sly, WS, Levy, B, Pegors, C, Kyle, JW & Beamer, WG 1990, 'A murine model of mucopolysaccharidosis VII. Gross and microscopic findings in beta-glucuronidase-deficient mice', *Am J Pathol*, vol. 136, no. 1, Jan, pp. 207-217.

Vogler, C, Levy, B, Galvin, N, Lessard, M, Soper, B & Barker, J 2005, 'Early onset of lysosomal storage disease in a murine model of mucopolysaccharidosis type VII: undegraded substrate accumulates in many tissues in the fetus and very young MPS VII mouse', *Pediatr Dev Pathol*, vol. 8, no. 4, Jul-Aug, pp. 453-462.

Vogler, C, Sands, MS, Levy, B, Galvin, N, Birkenmeier, EH & Sly, WS 1996, 'Enzyme replacement with recombinant beta-glucuronidase in murine mucopolysaccharidosis type VII: impact of therapy during the first six weeks of life on subsequent lysosomal storage, growth, and survival', *Pediatr Res*, vol. 39, no. 6, Jun, pp. 1050-1054.

Vokes, SA, Ji, H, Wong, WH & McMahon, AP 2008, 'A genome-scale analysis of the cis-regulatory circuitry underlying sonic hedgehog-mediated patterning of the mammalian limb', *Genes Dev*, vol. 22, no. 19, Oct 1, pp. 2651-2663.

Vortkamp, A, Lee, K, Lanske, B, Segre, GV, Kronenberg, HM & Tabin, CJ 1996, 'Regulation of rate of cartilage differentiation by Indian hedgehog and PTH-related protein', *Science*, vol. 273, no. 5275, Aug 2, pp. 613-622.

Vu, TH, Shipley, JM, Bergers, G, Berger, JE, Helms, JA, Hanahan, D, Shapiro, SD, Senior, RM & Werb, Z 1998, 'MMP-9/gelatinase B is a key regulator of growth plate angiogenesis and apoptosis of hypertrophic chondrocytes', *Cell*, vol. 93, no. 3, May 01, pp. 411-422.

Wang, J, Zhou, J & Bondy, CA 1999, 'Igf1 promotes longitudinal bone growth by insulin-like actions augmenting chondrocyte hypertrophy', *Faseb j*, vol. 13, no. 14, Nov, pp. 1985-1990.

Wang, J, Zhou, J, Cheng, CM, Kopchick, JJ & Bondy, CA 2004, 'Evidence supporting dual, IGF-I-independent and IGF-I-dependent, roles for GH in promoting longitudinal bone growth', *J Endocrinol*, vol. 180, no. 2, Feb, pp. 247-255.

Wang, L, Shao, YY & Ballock, RT 2010, 'Thyroid hormone-mediated growth and differentiation of growth plate chondrocytes involves IGF-1 modulation of beta-catenin signaling', *J Bone Miner Res*, vol. 25, no. 5, May, pp. 1138-1146.

Wang, P, Sorenson, J, Strickland, S, Mingus, C, Haskins, ME & Giger, U 2015, 'Mucopolysaccharidosis VII in a Cat Caused by 2 Adjacent Missense Mutations in the GUSB Gene', *J Vet Intern Med*, vol. 29, no. 4, Jul-Aug, pp. 1022-1028.

Wang, W, Lian, N, Li, L, Moss, HE, Perrien, DS, Elefteriou, F & Yang, X 2009, 'Atf4 regulates chondrocyte proliferation and differentiation during endochondral ossification by activating Ihh transcription', *Development*, vol. 136, no. 24, Dec, pp. 4143-4153.

Wang, Y, Cheng, Z, Elalieh, HZ, Nakamura, E, Nguyen, MT, Mackem, S, Clemens, TL, Bikle, DD & Chang, W 2011, 'IGF-1R signaling in chondrocytes modulates growth plate development by interacting with the PTHrP/Ihh pathway', *J Bone Miner Res*, vol. 26, no. 7, Jul, pp. 1437-1446.

Wang, Y, Menendez, A, Fong, C, ElAlieh, HZ, Kubota, T, Long, R & Bikle, DD 2015, 'IGF-I Signaling in Osterix-Expressing Cells Regulates Secondary Ossification Center Formation, Growth Plate Maturation, and Metaphyseal Formation During Postnatal Bone Development', *J Bone Miner Res*, vol. 30, no. 12, Dec, pp. 2239-2248.

Wang, Y, Nishida, S, Sakata, T, Elalieh, HZ, Chang, W, Halloran, BP, Doty, SB & Bikle, DD 2006, 'Insulin-like growth factor-I is essential for embryonic bone development', *Endocrinology*, vol. 147, no. 10, Oct, pp. 4753-4761.

Waxman, DJ, Ram, PA, Park, SH & Choi, HK 1995, 'Intermittent plasma growth hormone triggers tyrosine phosphorylation and nuclear translocation of a liver-expressed, Stat 5-related DNA binding protein. Proposed role as an intracellular regulator of male-specific liver gene transcription', *Journal of Biological Chemistry*, vol. 270, no. 22, Jun 02, pp. 13262-13270.

Wei, F, Zhou, J, Wei, X, Zhang, J, Fleming, BC, Terek, R, Pei, M, Chen, Q, Liu, T & Wei, L 2012, 'Activation of Indian hedgehog promotes chondrocyte hypertrophy and upregulation of MMP-13 in human osteoarthritic cartilage', *Osteoarthritis and Cartilage*, vol. 20, no. 7, 2012/07/01/, pp. 755-763.

Weir, EC, Philbrick, WM, Amling, M, Neff, LA, Baron, R & Broadus, AE 1996, 'Targeted overexpression of parathyroid hormone-related peptide in chondrocytes causes chondrodysplasia and delayed endochondral bone formation', *Proc Natl Acad Sci U S A*, vol. 93, no. 19, Sep 17, pp. 10240-10245.

Williams, GR 2013, 'Thyroid Hormone Actions in Cartilage and Bone', *European Thyroid Journal*, vol. 2, no. 1, 12/19
10/04/received
11/01/revised, pp. 3-13.

Wilsman, NJ, Farnum, CE, Green, EM, Lieferman, EM & Clayton, MK 1996, 'Cell cycle analysis of proliferative zone chondrocytes in growth plates elongating at different rates', *J Orthop Res*, vol. 14, no. 4, Jul, pp. 562-572.

Wilson, R, Diseberg, AF, Gordon, L, Zivkovic, S, Tatarczuch, L, Mackie, EJ, Gorman, JJ & Bateman, JF 2010, 'Comprehensive profiling of cartilage extracellular matrix formation and maturation using sequential extraction and label-free quantitative proteomics', *Mol Cell Proteomics*, vol. 9, no. 6, Jun, pp. 1296-1313.

Wilson, S, Hashamiyan, S, Clarke, L, Saftig, P, Mort, J, Dejica, VM & Brömme, D 2009, 'Glycosaminoglycan-Mediated Loss of Cathepsin K Collagenolytic Activity in MPS I Contributes to Osteoclast and Growth Plate Abnormalities', *The American Journal of Pathology*, vol. 175, no. 5, 07/14/accepted, pp. 2053-2062.

Wit, JM, Kamp, GA & Rikken, B 1996, 'Spontaneous growth and response to growth hormone treatment in children with growth hormone deficiency and idiopathic short stature', *Pediatr Res*, vol. 39, no. 2, Feb, pp. 295-302.

Woelfle, J, Billiard, J & Rotwein, P 2003, 'Acute control of insulin-like growth factor-I gene transcription by growth hormone through Stat5b', *Journal of Biological Chemistry*, vol. 278, no. 25, Jun 20, pp. 22696-22702.

Woloszynek, JC, Roberts, M, Coleman, T, Vogler, C, Sly, W, Semenkovich, CF & Sands, MS 2004, 'Numerous transcriptional alterations in liver persist after short-term enzyme-replacement therapy in a murine model of mucopolysaccharidosis type VII', *Biochem J*, vol. 379, no. Pt 2, Apr 15, pp. 461-469.

Wu, BM, Tomatsu, S, Fukuda, S, Sukegawa, K, Orii, T & Sly, WS 1994, 'Overexpression rescues the mutant phenotype of L176F mutation causing beta-glucuronidase deficiency mucopolysaccharidosis in two Mennonite siblings', *Journal of Biological Chemistry*, vol. 269, no. 38, Sep 23, pp. 23681-23688.

Wu, S, Morrison, A, Sun, H & De Luca, F 2011, 'Nuclear factor-kappaB (NF-kappaB) p65 interacts with Stat5b in growth plate chondrocytes and mediates the effects of growth hormone on chondrogenesis and on the expression of insulin-like growth factor-1 and bone morphogenetic protein-2', *Journal of Biological Chemistry*, vol. 286, no. 28, Jul 15, pp. 24726-24734.

Wu, Y, Sun, H, Basta-Pljakic, J, Cardoso, L, Kennedy, OD, Jasper, H, Domené, H, Karabatas, L, Guida, C, Schaffler, MB, Rosen, CJ & Yakar, S 2013, 'Serum IGF-1 is insufficient to restore skeletal size in the total absence of the growth hormone receptor', *J Bone Miner Res*, vol. 28, no. 7, p. 10.1002/jbmr.1920.

Xing, W, Cheng, S, Wergedal, J & Mohan, S 2014, 'Epiphyseal chondrocyte secondary ossification centers require thyroid hormone activation of Indian hedgehog and osterix signaling', *J Bone Miner Res*, vol. 29, no. 10, Oct, pp. 2262-2275.

Xing, W, Govoni, KE, Donahue, LR, Kesavan, C, Wergedal, J, Long, C, Bassett, JH, Gogakos, A, Wojcicka, A, Williams, GR & Mohan, S 2012, 'Genetic evidence that thyroid

hormone is indispensable for prepubertal insulin-like growth factor-I expression and bone acquisition in mice', *J Bone Miner Res*, vol. 27, no. 5, May, pp. 1067-1079.

Yakar, S, Liu, JL, Stannard, B, Butler, A, Accili, D, Sauer, B & LeRoith, D 1999, 'Normal growth and development in the absence of hepatic insulin-like growth factor I', *Proc Natl Acad Sci U S A*, vol. 96, no. 13, Jun 22, pp. 7324-7329.

Yakar, S, Rosen, CJ, Beamer, WG, Ackert-Bicknell, CL, Wu, Y, Liu, JL, Ooi, GT, Setser, J, Frystyk, J, Boisclair, YR & LeRoith, D 2002, 'Circulating levels of IGF-1 directly regulate bone growth and density', *J Clin Invest*, vol. 110, no. 6, Sep, pp. 771-781.

Yamada, Y, Kato, K, Sukegawa, K, Tomatsu, S, Fukuda, S, Emura, S, Kojima, S, Matsuyama, T, Sly, WS, Kondo, N & Orii, T 1998, 'Treatment of MPS VII (Sly disease) by allogeneic BMT in a female with homozygous A619V mutation', *Bone Marrow Transplant*, vol. 21, no. 6, Mar, pp. 629-634.

Yan, Y, Frisen, J, Lee, MH, Massague, J & Barbacid, M 1997, 'Ablation of the CDK inhibitor p57Kip2 results in increased apoptosis and delayed differentiation during mouse development', *Genes Dev*, vol. 11, no. 8, Apr 15, pp. 973-983.

Yang, Y 2009, 'Chapter 1. Skeletal Morphogenesis and Embryonic Development', in *Primer on the Metabolic Bone Diseases and Disorders of Mineral Metabolism*, 7th edn.

Yang, Y, Topol, L, Lee, H & Wu, J 2003, 'Wnt5a and Wnt5b exhibit distinct activities in coordinating chondrocyte proliferation and differentiation', *Development*, vol. 130, no. 5, Mar, pp. 1003-1015.

Yang, ZQ, Zhang, HL, Duan, CC, Geng, S, Wang, K, Yu, HF, Yue, ZP & Guo, B 2017, 'IGF1 regulates RUNX1 expression via IRS1/2: Implications for antler chondrocyte differentiation', *Cell Cycle*, vol. 16, no. 6, Mar 19, pp. 522-532.

Yoon, BS, Pogue, R, Ovchinnikov, DA, Yoshii, I, Mishina, Y, Behringer, RR & Lyons, KM 2006, 'BMPs regulate multiple aspects of growth-plate chondrogenesis through opposing actions on FGF pathways', *Development*, vol. 133, no. 23, Dec, pp. 4667-4678.

Yoshida, CA, Yamamoto, H, Fujita, T, Furuichi, T, Ito, K, Inoue, K, Yamana, K, Zanma, A, Takada, K, Ito, Y & Komori, T 2004, 'Runx2 and Runx3 are essential for chondrocyte maturation, and Runx2 regulates limb growth through induction of Indian hedgehog', *Genes Dev*, vol. 18, no. 8, Apr 15, pp. 952-963.

Zetterberg, A & Larsson, O 1985, 'Kinetic analysis of regulatory events in G1 leading to proliferation or quiescence of Swiss 3T3 cells', *Proceedings of the National Academy of Sciences of the United States of America*, vol. 82, no. 16, pp. 5365-5369.

Zhang, F, McLellan, JS, Ayala, AM, Leahy, DJ & Linhardt, RJ 2007, 'Kinetic and structural studies on interactions between heparin or heparan sulfate and proteins of the hedgehog signaling pathway', *Biochemistry*, vol. 46, no. 13, Apr 03, pp. 3933-3941.

Zhang, P, Liegeois, NJ, Wong, C, Finegold, M, Hou, H, Thompson, JC, Silverman, A, Harper, JW, DePinho, RA & Elledge, SJ 1997, 'Altered cell differentiation and proliferation in mice lacking p57KIP2 indicates a role in Beckwith-Wiedemann syndrome', *Nature*, vol. 387, no. 6629, May 08, pp. 151-158.

Zhang, XM, Ramalho-Santos, M & McMahon, AP 2001, 'Smoothened mutants reveal redundant roles for Shh and Ihh signaling including regulation of L/R symmetry by the mouse node', *Cell*, vol. 106, no. 2, Jul 27, pp. 781-792.

Zhou, G, Zheng, Q, Engin, F, Munivez, E, Chen, Y, Sebald, E, Krakow, D & Lee, B 2006, 'Dominance of SOX9 function over RUNX2 during skeletogenesis', *Proc Natl Acad Sci U S A*, vol. 103, no. 50, Dec 12, pp. 19004-19009.

Zhou, Y, Xu, BC, Maheshwari, HG, He, L, Reed, M, Lozykowski, M, Okada, S, Cataldo, L, Coschigamo, K, Wagner, TE, Baumann, G & Kopchick, JJ 1997, 'A mammalian model for Laron syndrome produced by targeted disruption of the mouse growth hormone receptor/binding protein gene (the Laron mouse)', *Proc Natl Acad Sci U S A*, vol. 94, no. 24, Nov 25, pp. 13215-13220.

Zimet, GD, Owens, R, Dahms, W, Cutler, M, Litvene, M & Cuttler, L 1997, 'Psychosocial outcome of children evaluated for short stature', *Arch Pediatr Adolesc Med*, vol. 151, no. 10, Oct, pp. 1017-1023.

Zuber, Z, Rozdzynska-Swiatkowska, A, Jurecka, A & Tylki-Szymanska, A 2014, 'The effect of recombinant human iduronate-2-sulfatase (Idursulfase) on growth in young patients with mucopolysaccharidosis type II', *PLoS One*, vol. 9, no. 1, p. e85074.